Fakultät Wissenschaftszentrum Weihenstephan für Ernährung,
Landnutzung und Umwelt

Professur für Ökoklimatologie

Drought quantification by multivariate indices and their validation against various environmental data

Upasana Priyambada Bhuyan-Erhardt

Vollständiger Abdruck der von der Fakultät Wissenschaftszentrum Weihenstephan für Ernährung, Landnutzung und Umwelt der Technischen Universität München zur Erlangung des akademischen Grades eines

Doktors der Naturwissenschaften

genehmigten Dissertation

Vorsitzender:

Prof. Dr. A. Göttlein

Prüfer der Dissertation:

Prof. Dr. A. Menzel
Prof. Dr. A. Bräuning (Friedrich-Alexander
Universität Erlangen-Nürnberg)

Die Dissertation wurde am 13.11.2017 bei der Technischen Universität München eingereicht und durch die Fakultät Wissenschaftszentrum Weihenstephan für Ernährung, Landnutzung und Umwelt am 19.03.2018 angenommen.

Abstract

Drought is a complex, climatic phenomenon with detrimental effects on society and usually occurs when precipitation falls below evapotranspiration for a longer period. The global surface temperature has increased significantly during the last century and will continue to escalate unless greenhouse gas emissions are considerably reduced. As a consequence of a warmer world, a much higher temperature variability is expected, which will increase the risk of droughts. It is a challenge to quantify the characteristics of drought episodes with objectivity. In several scientific disciplines, quantitative indices are the most popular approach for drought quantification. Validation of such drought indices is of crucial importance for refined drought characterization.

The thesis makes a comprehensive comparison of the established drought indices De Martonne Aridity Index (DMI), Standardized Precipitation Index (SPI), Standardized Precipitation Evapotranspiration Index (SPEI), self-calibrating Palmer Drought Severity Index (scPDSI) and the recently developed vine copula based standardized multivariate indices (here denoted as VCI). The performance of the indices was assessed by validating them against various environmental datasets: a global and European network of tree ring data, a catchment network with streamflow data spread across Europe and carbon flux data (gross primary production and net ecosystem exchange) for Germany. Vegetation dynamics are inherently linked to climate, and the latter is known to have a direct effect on the biomass and phenological patterns of vegetation. The thesis additionally explores whether phenological metrics derived from normalized difference vegetation index (NDVI) can help to refine the understanding of the existing relationship between vegetation and drought. Various statistical methods were used in this study, such as bootstrapped correlation, regression analysis, principal component analysis, random forests, various model validation statistics and forecast verification skill scores.

Results show that the appropriate drought index for detecting impacts depends on the analysed system, the application and data being used. The thesis gives detailed information on the month-wise performance of the common drought indices (in varying temporal aggregation) in different climate zones and elevations, allowing users in accordance with their objective criteria, the selection of the most suitable

index. The results of the validation of the indices with streamflow and carbon flux data shows that VCI, with advantageous attributes such as higher probability of drought detection and lower false alarm ratio, outperforms the established indices SPEI and SPI. Overall, the thesis establishes the importance of using multiple variables/indicators for drought investigations. It recommends to improve our understanding of drought impacts with application-based, user-defined drought monitoring on a high spatial resolution, using the novel class of indices (VCI) as an additional source of information. Furthermore, the thesis demonstrates the potential of phenological metrics derived from NDVI to upgrade the understanding of the existing relationship between tree growth and drought.

Zusammenfassung

Dürre ist ein komplexes, klimatisches Phänomen mit schädlichen Auswirkungen auf die Gesellschaft und tritt in der Regel dann auf, wenn der Niederschlag die Evapotranspiration für eine längere Periode unterschreitet. Die globale Oberflächentemperatur hat sich während des letzten Jahrhunderts deutlich erhöht und wird weiter steigen, wenn die Treibhausgasemissionen nicht drastisch reduziert werden. Als Folge des Klimawandels erwartet man eine viel höhere Temperaturvariabilität, was das Risiko von Dürren erhöhen wird. Es ist eine Herausforderung, die Charakteristika von Dürre-Episoden objektiv zu quantifizieren. Für verschiedene wissenschaftliche Disziplinen sind quantitative Indizes der populärste Ansatz zur Dürrequantifizierung. Die Validierung solcher Dürreindizes ist von entscheidender Bedeutung für die verfeinerte Charakterisierung von Dürre.

Diese Arbeit stellt einen umfassenden Vergleich von den etablierten Dürreindizes De Martonne Ariditätsindex (DMI), Standardisierter Niederschlagsindex (SPI), Standardisierter Niederschlags-Evapotranspirationsindex (SPEI), selbstkalibrierender Palmer Dürre-Schweregradindex (scPDSI) und den kürzlich entwickelten Vine-Kopula basierten, standardisierten, multivariaten Indizes (hier bezeichnet als VCI) an. Die Performance der Indizes wurde durch Validierung mit verschiedenen Umwelt-bezogenen Datensätzen bewertet: einem globalen und europäischen Netzwerk mit Jahrringdaten von Bäumen, einem Netzwerk von Daten zur Wasserführung für Wassereinzugsgebiete in ganz Europa sowie Kohlenstoffflussdaten für Deutschland. Die Vegetationsdynamik ist inhärent mit dem Klima verbunden, und letzteres hat bekanntermaßen einen direkten Einfluss auf die Biomasse und die phänologischen Muster der Vegetation. Die Dissertation untersucht daher zusätzlich, ob phänologische Metriken, die von dem normalisierten differenzierten Vegetationsindex (NDVI) abgeleitet wurden, dazu beitragen können, die bestehende Beziehung zwischen Vegetation und Dürre besser verstehen zu können. Verschiedenste statistische Methoden, wie Bootstrap Korrelationen, Regressionsanalyse, Hauptkomponen-tenanalyse, Random Forests, verschiedene Modellvalidierungsmetriken und Vorher-sageverifizierungsscores wurden in dieser Studie verwendet.

Die Ergebnisse zeigen, dass die Wahl eines angemessenen Dürreindex für die Bewertung von Dürre-Auswirkungen vom analysierten System, der Anwendung selbst

und den verwendeten Daten abhängt. Die Dissertation gibt detaillierte, monatliche Informationen zur Leistungsfähigkeit der gebräuchlichen Dürreindizes (für verschiedene zeitliche Aggregationen) in verschiedenen Klimazonen und Höhenlagen, so dass die Nutzer gemäß ihren eigenen objektiven Kriterien die Auswahl des am besten geeigneten Indexes vornehmen können. Die Ergebnisse der Validierung der Indizes mit Wasserführungs- und Kohlenstoffflussdaten zeigen, dass VCI mit vorteilhaften Attributen wie einer höheren Wahrscheinlichkeit von Dürreerkennung und geringerem Fehlalarmverhältnis die Resultate von den etablierten Indizes SPEI und SPI übertrifft. Alles in allem zeigt die Arbeit die Bedeutung der gleichzeitigen Verwendung mehrerer Variablen/Indikatoren für Dürreuntersuchungen auf. Des Weiteren empfiehlt sie, unser Verständnis von Dürre-Auswirkungen mit anwendungsbasiertem, benutzerdefiniertem Dürre-Monitoring auf einer hohen räumlichen Auflösung durch Verwendung der neuen Klasse von Indizes (VCI) (als zusätzliche Informationsquelle) zu verbessern. Darüber hinaus zeigt die Arbeit das Potenzial von NDVI basierten, phänologischen Metriken, das Verständnis der bestehenden Beziehung zwischen Baumwachstum und Dürre zu verfeinern.

Table of Contents

1. Introduction

1.1 Droughts and climate change

Droughts are recurring extreme climate events and the most detrimental of all 20th century natural hazards (Wilhite & Glantz, 1985; Obasi, 1994; Mishra & Singh, 2010) which could potentially lead to land degradation and forest dieback (Allen et al., 2010; IPCC, 2013). Droughts generally occur when precipitation falls below normal recorded levels (Dai, 2011). Droughts can hinder tree growth and boost their decline and mortality (Allen et al., 2010) and therefore posing a challenge for forest management practices and undermining the supply of ecosystem goods and services from forests (Anderegg et al., 2013; Elkin et al., 2013). The recent California droughts are an apt example of the detrimental effects of drought (Mann & Gleick, 2015). Global climate change and increasing rise in water demand due to population increase and expansion of agricultural, energy and industrial sectors (Mishra & Singh, 2010) have led to amplified drought impacts in the recent years (Kogan et al., 2013).

1.1.1 Drought drivers and projections

The two most critical variables influencing drought are temperature and precipitation. The SREX (Special Report on Extreme Events), published by the Intergovernmental Panel on Climate Change (see IPCC, 2012), states that "while lack of precipitation is often the primary cause of drought, increased potential evapotranspiration induced by enhanced radiation, wind speed, or vapor pressure deficit (itself linked to temperature and relative humidity), as well as pre-conditioning (pre-event soil moisture; lake, snow, and/or groundwater storage) can contribute to the emergence of soil moisture and hydrological drought". According to the IPCC (2013), as a consequence of a warmer world (a warming of 0.85°C of the mean global surface temperature over the period 1880 to 2012 has been observed), a much higher temperature variability is expected in some regions which will increase the risk of summer droughts (Kogan et al., 2013). A number of different projections are given in the IPCC (2013) report that relate to drought, such as annual mean changes in precipitation (P), evaporation (E), relative humidity, E −P, runoff and soil moisture for 2081–2100 relative to 1986–2005 under the Representative Concentration Pathway RCP8.5 (see Figure 1). Projections indicate regional to global scale decreases in soil moisture and increased agricultural drought in presently dry regions with medium confidence (IPCC, 2013). In a warmer

world, changes of average precipitation will not be uniform, with some regions experiencing increases, and others (mid-latitude and subtropical arid and semi-arid regions) with decreases or not much change at all (IPCC, 2013). While decreases in runoff are anticipated in southern Europe and the Middle East, surface drying in the Mediterranean, southwestern USA and southern African regions are likely (high confidence) for several degrees of warming.
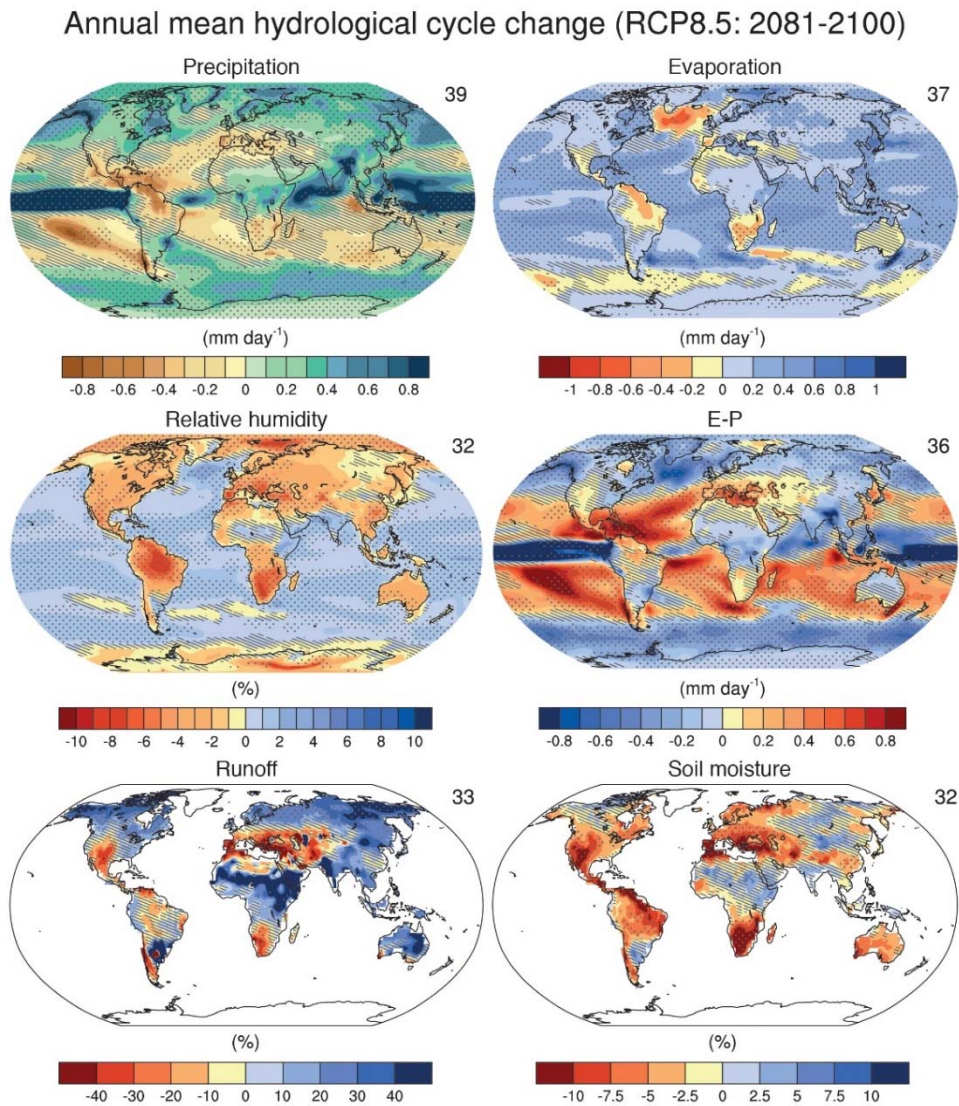
Figure 1. Annual mean changes in precipitation (P), evaporation (E), relative humidity, E –P, runoff and soil moisture for 2081–2100 relative to 1986–2005 under the Representative Concentration Pathway RCP8.5. The number of Coupled Model Intercomparison Project Phase 5 (CMIP5) models to calculate the multi-model mean is indicated in the upper right corner of each panel. Hatching indicates regions where the multi-model mean change is less than one standard deviation of internal variability. Stippling indicates regions where the multi-model mean change is greater than two standard deviations of internal variability and where 90% of models agree on the sign of change. Figure and caption are Figure TFE.1, Figure 3 (IPCC, 2013).

1.1.2   Global scale observed trend in drought

The IPCC (2007) stated with high confidence that global drought trends had increased since 1970 (see Figure 2) based on a single drought indicator, the Palmer Drought Severity Index (Palmer, 1965). In 2012 the SREX (IPCC, 2012), revised the previous finding and concluded with medium confidence that some regions of the world had experienced more intense and longer droughts.

The current assessment of the IPCC (2013) states that since the 1950s "there is low confidence in a global scale observed trend in drought or dryness (lack of rainfall), owing to lack of direct observations, dependencies of inferred trends on the index choice and geographical inconsistencies in the trends". One reason for the reduced confidence in conclusions of SREX and IPCC (2007) is that the current criteria for assessing drought does not solely rely on a single drought indicator. However, the IPCC (2013) states with high confidence that the frequency and intensity of drought since 1950 has increased in the Mediterranean and West Africa and decreased in central North America and north-west Australia.

1.1.3   Inconsistencies of drought studies

Drought is a complex phenomenon and cannot be fully explained by commonly used drought indices. Consequently discrepancies in the interpretation of results from drought studies are inevitable. While some studies found decreasing trends in the duration, intensity and severity of drought globally (Sheffield & Wood, 2008), other studies found a general global increase in drought (Dai, 2011). A solution to dealing with such inconsistencies would be to improve our understanding of drought indices. Recent years have shown a variety of drought indices and methodological developments to monitor and assess drought in a changing climate (Mishra & Singh, 2011; Zargar et al., 2011; IPCC, 2013; Keyantash & Dracup, 2004; Kao & Govindaraju, 2010; Hao & AghaKouchak, 2013; Farahmand & AghaKouchak, 2015). The quantification and prediction of drought, as well as the search for adaptation strategies, continue to remain a very challenging research topic as the future of drought continues to remain ambiguous.
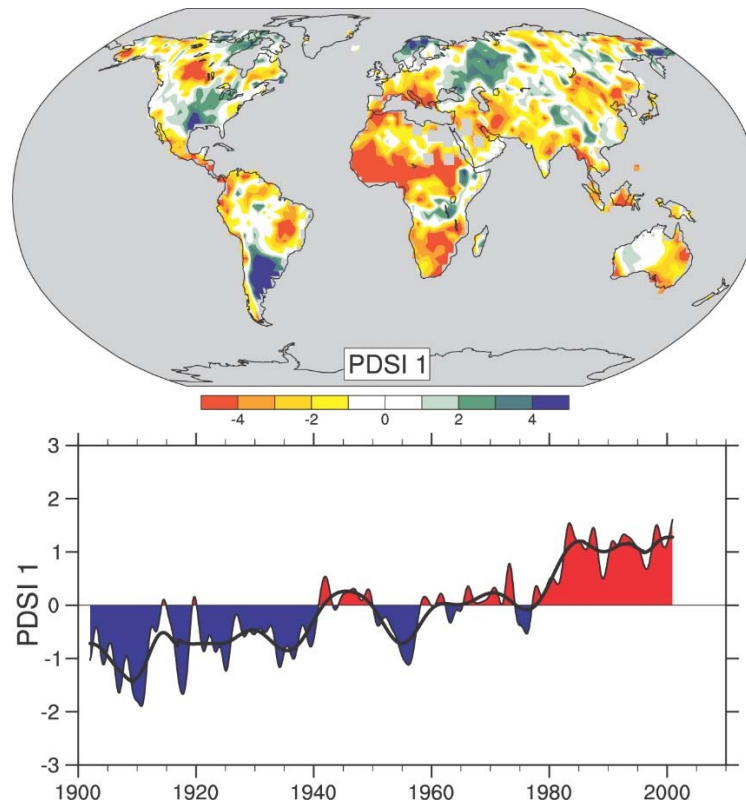
Figure 2. The most important spatial pattern (top) of the monthly Palmer Drought Severity Index (PDSI) for 1900 to 2002. The PDSI is a prominent index of drought and measures the cumulative deficit (relative to local mean conditions) in surface land moisture by incorporating previous precipitation and estimates of moisture drawn into the atmosphere (based on atmospheric temperatures) into a hydrological accounting system. The lower panel shows how the sign and strength of this pattern has changed since 1900. Red and orange areas are drier (wetter) than average and blue and green areas are wetter (drier) than average when the values shown in the lower plot are positive (negative).The smooth black curve shows decadal variations. The time series approximately corresponds to a trend, and this pattern and its variations account for 67% of the linear trend of PDSI from 1900 to 2002 over the global land area. It therefore features widespread increasing African drought, especially in the Sahel, for instance. Note also the wetter areas, especially in eastern North and South America and northern Eurasia. Adapted from Dai et al. (2004). Figure and caption are FAQ 3.2, Figure 1, in IPCC (2007).

1.2 Definition and classification

A standard universal definition of drought does not exist due to many reasons. It is difficult to determine the onset, termination and extent of drought, making it fundamentally different from other climate extremes (Wilhite & Glantz, 1985; Tate & Gustard, 2000). The impacts of drought increases slowly, often accumulate over a period of time and can even last for years after cessation. The impacts of drought spread over large geographical areas and do not have any structure (Mishra & Singh, 2010). Therefore, it becomes challenging to quantify the characteristics of drought events in terms of their severity, magnitude, duration and spatial extent (Vicente-

Serrano et al., 2010). The UN Convention to Combat Drought and Desertification (United Nations Convention to Combat Drought and Desertification in Countries Experiencing Serious Droughts and/or Desertification, 1994) defines it as "a naturally occurring phenomenon that exists when precipitation has been significantly below normal recorded levels, causing serious hydrological imbalances that adversely affect land resource production systems".

Drought can be divided into four major classes according to conventional scientific literature (Rasmussen et al., 1993; Wilhite & Glantz, 1985): (1) meteorological drought, (2) agricultural drought, (3) hydrological drought, and (4) socioeconomic drought (see Table 1). These four classes of drought are interlinked, but refer to different ways to measure and identify drought conditions. The first three categories can be seen as indicators of the environment, while the last drought type can be considered as a water resource indicator (Hisdal & Tallaksen, 2000). A meteorological drought in terms of lack of precipitation is the primary cause of a drought, which usually first leads to an agricultural drought due to lack of soil moisture. If precipitation deficiencies continue, surface water deficit develops, which leads to hydrological drought. When the water resource systems fails to meet water demands, socioeconomic drought unfolds, which incorporates attributes of meteorological, agricultural and hydrological drought (Wilhite & Glantz, 1985).

Table 1. Four drought categories, adapted from (Vose et al., 2015).

Category	Focus	General estimation method
Meteorological	Precipitation	Developing indices based on monthly precipitation data.
Agricultural	Soil moisture/Productivity of crops	Developing indices based on a combination of precipitation, temperature and soil moisture.
Hydrological	Surface and subsurface water supply	Measuring/modelling runoff and reservoir levels.
Socioeconomic	Economic impacts	Measuring/modelling financial consequences of demand of economic goods exceeding supply as a result of deficit in water supply.

1.3   Drought indices

For many scientific disciplines – dendroecology, ecology, remote sensing and agricultural sciences, quantitative indices are the one of the most widely accepted approaches for drought quantification. These (drought) indices combine information from drought related variables such as precipitation into a single number, which is more useful for the decision-makers than just the raw data (Hayes et al., 2007). One approach to validate such drought indices, which is crucial to refined drought characterization, is to analyse and compare to which degree they are able to identify drought impacts on different environmental systems (using different techniques such as forecast skill scores, linear regression etc.). In this thesis, common indices used in environmental studies are analysed, namely – De Martonne Aridity Index (DMI) (de Martonne, 1926), Standardized Precipitation Index (SPI) (Mckee et al., 1993), Standardized Precipitation Evapotranspiration Index (SPEI) (Vicente-Serrano et al., 2010) and the self-calibrating Palmer Drought Severity Index (scPDSI) (Palmer, 1965; Wells et al., 2004) (all in Chapter 4.1, scPDSI and SPEI in Chapter 4.2). The recently developed vine copula based standardized multivariate indices (VCI) (Erhardt & Czado, 2017) are used in Chapter 4.3 besides SPI and SPEI. Following is a short description of the different indices analysed in the thesis:

The **DMI** is a measure of aridity obtained by calculating mean precipitation (in mm) / (temperature (in °C) + 10) (de Martonne, 1926). It is subject to disapproval because of its empirical nature but nonetheless provides information on drought at a given location and has been used in many ecological studies (Čufar et al., 2008; Zang et al., 2014).

The **SPI** is based on long-term precipitation records that are computed on different time scales (Mckee et al., 1993). It is one of the most widely accepted index for the quantification of drought and was recommended by the Lincoln Declaration on Drought as the standard index for meteorological drought analysis (Hayes et al., 2011). SPI is computed by converting precipitation data to probabilities which are then transformed to standardized series with an average of 0 and a standard deviation of 1. A major constraint of the SPI is its lack of ability to capture the influence of increased temperatures on moisture demand (Mckee et al., 1993). Moreover, the methodology of SPI requires long-term observations (almost 30 years) and assumes a parametric

distribution to model the data. However, a suitable fit to the data, especially in the distribution tails is not certain (Farahmand & AghaKouchak, 2015; Erhardt, 2017).

The **SPEI** is an improved version of the SPI; it combines the multi-timescale aspects of the SPI with information about evapotranspiration. This makes the SPEI more reliable for studies linked to climate change (Vicente-Serrano et al., 2010). It is based on long-term climatic water balance (see e.g. Vicente-Serrano et al., 2010), which is computed as difference between precipitation and potential evapotranspiration. However, the SPEI is sensitive to the method of calculating potential evapotranspiration (PET) (Vicente-Serrano et al., 2010). Another unwanted characteristic is that by using the SPEI, temperature trends are passed on to the index (Erhardt, 2017) and like the SPI, it also requires long-term observations.

The **scPDSI** is a measure of soil moisture availability which is based on the supply and demand concepts of the water balance equation. It is calculated based on temperature, precipitation, and available water content of the soil on a monthly time scale (or other scales) (Palmer, 1965; Wells et al., 2004). For details on the calculation procedure of the PDSI, see Palmer (1965) and Alley (1984). Its disadvantages include missing multi-timescale features of the SPI and SPEI (Dai et al., 2004; Wells et al., 2004) and its autoregressive structure. "Present conditions depend on past conditions, however the time interval which influences the present varies across space but cannot be assessed from the model" (Erhardt, 2017).

Although all indices discussed above have their own advantages, yet they account only for one or two drought-relevant variables and do not taking into account their inter-dependencies (Erhardt & Czado, 2017; Erhardt, 2017). The recently developed multivariate standardized index (Erhardt & Czado, 2017) is also validated in this thesis in addition to the established indices (see Chapter 4.3). They are subsequently addressed as **VC-Index or VCI**. In the VCI inter-variable dependencies are modelled based on vine copulas (Aas et al., 2009), which facilitates flexible modelling of the full multivariate distribution of interest. This is vital for accounting the joint occurrence of extremes of different drivers of drought (Erhardt & Czado, 2017). Since a single variable based drought indicator is generally not sufficient for characterizing complex drought conditions and impacts, indices with information of multiple drought-relevant variables are required to capture different aspects of complicated

drought conditions. The VCI presents a flexible approach that allows the end-user to decide which type(s) of drought to investigate, which variables (at least three) are appropriate for her or his specific application without overlooking their inter-dependencies (for more details see Erhardt & Czado, 2017).

1.4   Proxy data for assessing performance of drought indices

In this thesis, the performance of selected drought indices was directly assessed by validating them against various natural proxies: (1) global and Europe-wide tree ring datasets (Chapter 4.2, Chapter 4.1), (2) streamflow data for Europe and carbon flux data for Germany (Chapter 4.3). Lastly, the potential of (3) phenological metrics derived from NDVI in improving the understanding of the existing relationship between drought and tree growth was studied. Following is a short description of the proxy datasets used for validation of the indices:

1.4.1   Tree rings

Trees build an ecosystem to provide habitat and food for animals, livelihood and wood for humans, facilitates purification of the atmospheric air and mitigates climate change, besides providing various other ecological, societal and climatological benefits (Anderegg et al., 2013). Nevertheless, climate is the principal driver of tree growth (Fritts, 1976) and consequently trees are vulnerable to extreme events such as drought, which makes it essential to study the response of trees to such events. Most instrumental climate records are not long enough to capture the full range of natural climate variability and studies of drought with such short records are not very statistically robust (Cook et al., 1999; Seftigen, 2014). Tree rings help to ease this problem by providing centuries-long, continuous annually resolved records of past hydroclimatic variability for regions and periods with no instrumental climate data (Cook et al., 1999). Interestingly even when instrumental climate data is available, tree rings are still very useful as they act as a unique source of validation, for instance, for drought related studies. Tree rings help to confirm the results of findings based on available instrumental or modelled satellite data.

Annual radial growth increment, also known as tree ring width is an extensively used proxy for tree vitality (Fritts et al., 1971; Dobbertin, 2005). The connection of tree ring width to climate and extreme climatic events, such as drought are well recognized as

they are known to correlate with several monthly values of temperature and precipitation during the growth year and, in some circumstances, previous years (e.g., Fritts et al., 1971; Briffa et al., 2002). In principle, most trees in seasonal climates produce one tree ring per year. At the beginning of the growing season temperature is positively correlated with ring width, as it is generally assumed that high temperature has a positive influence on growth in the beginning of the growing season (Fritts, 1976). In contrast, later in the growing season, negative correlations with ring width is observed as a consequence of high temperatures which inhibits metabolic processes of trees leading to their reduced growth (Fritts, 1976; Lévesque, 2013). As these environmental factors limit tree growth, annals of tree rings can be used as evidence of a tree's response to drought (Zang, 2010), insect outbreaks and so on. As tree species vary across biomes, it is essential to characterize drought responses of individual tree species, for comprehensive understanding of drought impacts on forest ecosystems (Bolte et al., 2009; Luyssaert et al., 2010; Zang et al., 2014). Due to abundant tree ring width data being publicly available, studies of tree growth and drought variability on local to continental scales are facilitated and at the same time tree ring data enables assessing site- and species-specific responses to drought which are important to understand, in order to derive sustainable forest management systems. The analysis of the growth response of different species to drought using tree ring width data should allow users the selection of the most appropriate index according to their application-based conditions. As the global climate continues to get warmer, understanding the responses of various tree species triggered by drought will be of escalating importance.

1.4.2   Streamflow

Hydrological drought is generally related to a period with shortage of streamflow, as well as ground-water supplies (Hao and AghaKouchak, 2013) of a given water body (Mishra & Singh, 2010). Streamflow data has been effectively used for hydrological drought analysis (Dracup et al., 1980; Mohan & Rangacharya, 1991; Clausen & Pearson, 1995) and to explore spatio-temporal properties of drought (Lorenzo-Lacruz et al., 2010; Zhai et al., 2010; Van Lanen et al., 2016). Streamflow levels are a useful indicator of drought. Hydrologists study streamflow droughts with hydrographs or charts showing river stage (height of the water above a given threshold) and streamflow (rate of flow usually measured in cubic metres per second) (Tallaksen, 2000). In general, it is assumed that the link between streamflow anomalies and

drought indices is more pronounced the more unconventional and advanced the drought index is (Haslinger et al., 2014).

1.4.3 Carbon flux

Gross primary production (GPP) is the main source of all carbon fluxes in the ecosystem (Duursma et al., 2009). It is defined as the total amount of carbon fixed by plants during the process of photosynthesis, which is measured on photosynthetic tissues, principally leaves (IPCC, 2000). The measured net ecosystem exchange (NEE) of CO_2 between the ecosystem and the atmosphere reflects the balance between GPP and ecosystem respiration (Lasslop et al., 2010). Droughts are often associated with high evaporative demand and lack of precipitation (Pereira et al., 2007), and are principal contributors to the year-to-year variability observed in terrestrial carbon sequestration (Ciais et al., 2005; Pereira et al., 2007). Both GPP and NEE serve as proxies for decline in productivity in forest ecosystems propagated by drought (Ciais et al., 2005; Luyssaert et al., 2007; Pereira et al., 2007). As the drought-NEE relationship (Ciais et al., 2005; Reichstein et al., 2005; Pereira et al., 2007) and the drought-GPP relationship (Ciais et al., 2005; Pereira et al., 2007; Vicca et al., 2016) are well recognized, in principle the performance of different drought indices can be assessed using such carbon flux variables. To date, no publication has made a performance comparison of drought indices using carbon flux data, which is studied in this thesis.

1.4.4 Phenological metrics derived from NDVI

The linkages of tree ring width to drought are well established (Fritts et al., 1971; Briffa et al., 2002; Dobbertin, 2005). However, preparing tree ring chronologies involves time-consuming, strenuous, error-prone field and laboratory work, which renders it not very beneficial to be used for monitoring real-time forest growth over large spatial scales (Camarero et al., 2015; Vicente-Serrano et al., 2016). Therefore it is important to seek alternatives for tree ring width, which can be useful for drought studies.

The remotely sensed normalized difference vegetation index (NDVI) which is based on red and near-infrared reflectance (Tucker, 1979) can be used to estimate productivity of vegetation (Myneni et al., 1997; Liang et al., 2005; Lopatin et al., 2006;

Kaufmann et al., 2008). NDVI measures photosynthetic activity at landscape-scales and although studies have linked NDVI values with tree ring growth data (Beck et al., 2013), the relationship of the latter with NDVI based phenological metrics remains to be explored.

Intra-annual changes of canopy greenness facilitates remote sensing of phenology using time series of NDVI (Liu et al., 2016). Spatio-temporal variations of vegetation phenology can act as a vital measure of photosynthetic activity (Dong et al., 2016). Consequently, important phenological metrics such as the start of the growing season (SOS) and end of the growing season (EOS) were extracted from the NDVI time series to examine their relationship with radial growth. Two NDVI products were used to explore this relationship, namely Moderate Resolution Imaging Spectroradiometer (MODIS) (Didan, 2015) and Global Inventory Modeling and Mapping Studies 3g (GIMMS3g) (Pinzon & Tucker, 2014). While MODIS has the advantage of being at a fine spatial resolution of 250m, the GIMMS3g boasts of over three decades of data as opposed to only 13 years of MODIS.

Given the lengthening of the growing season in the backdrop of global climate warming (Menzel & Fabian, 1999; Menzel et al., 2006), studying how climatic factors and phenological metrics derived from NDVI are linked to tree ring width could lead to a deeper understanding of forest response to climate change. Real-time observations based on phenological metrics derived from NDVI are not viable, however it can facilitate a thorough assessment of the past annual growth at the end of the growing season.

1.5   Previous studies

There are some publications that have reviewed the development of drought indices and compared their advantages and drawbacks (Keyantash & Dracup, 2002; Mishra & Singh, 2010, 2011; Zargar et al., 2011). However, very few studies have made a comparison of their performances, by validating them against different systems or environmental datasets, especially on a regional or global scale. Table 2 shows a list of publications comparing prominent drought indices.

Vicente-Serrano et al. (2012) compared the SPI, four versions of the PDSI and the SPEI. The study revealed that the performances of the SPEI and SPI were very similar

with only small differences. Nonetheless, SPEI was able to capture the responses of the assessed variables to summer drought most effectively. This publication represents one of the few studies that provide a global assessment of the performance of different drought indices for observing drought impacts on several hydrological, agricultural, and ecological response variables (Vicente-Serrano et al., 2012).

Keyantash and Dracup (2002) evaluated many drought indices for Willamette Valley and North Central climate divisions of Oregon. The study found that among six meteorological indices, rainfall deciles and SPI ranked first and PDSI ranked last. Amongst four hydrological drought indices, total water deficit ranked first and the Palmer hydrological drought severity index (Palmer, 1965) ranked last. Amongst four agricultural drought indices, computed soil moisture ranked first, CMI or the crop moisture index (Palmer, 1968) ranked last.

Haslinger et al. (2014) evaluated the performance of four drought indices namely the SPI and the SPEI and two indices of the Palmer family, the Z-Index, and the scPDSI, in capturing hydrological drought using an Austrian data set of 47 catchments in humid-temperate climate. The study summarized that the scPDSI gives the best performance by reaching the highest values in nearly all the different methodological approaches followed by SPEI (Haslinger et al., 2014).

Quiring and Papakryiakou (2003) compared four drought indices: PDSI, Palmer's Z-Index, SPI and NOAA Drought Index (Strommen et al., 1980) for monitoring agricultural drought and predicting Canada Western Red Spring wheat yield. It found that the Palmer's Z-Index was the most suitable index to monitor agricultural drought in Canadian prairies (Quiring & Papakryiakou, 2003).

Todisco et al. (2008) compared the performance of Palmer drought indices (PDSI, Z, CMI), SPI and a severity index (RS) in an application study based on monitoring and predicting sunflower and sorghum crop yield in Central Italy. RS was found to be more preferable to predict the agricultural drought in the region.

Additional studies that compared two prominent drought indices are: SPI and PDSI (Guttman, 1998), SPI and SPEI (Lorenzo-Lacruz et al., 2010; McEnvoy et al., 2012) SPI and standardized runoff index (Shukla & Wood, 2008). Guttman (1998) compared historical time series of the PDSI with the corresponding SPI time series for the

Table 2. List of previous studies comparing drought indices.

Reference	Drought indices	Preference	Application and study area
Vicente-Serrano et al. (2012)	SPI, four versions of the PDSI, SPEI	SPEI	Comparison of indices in capturing hydrological, agricultural, and ecological drought using global datasets of streamflow, crop yield, tree ring and soil moisture.
Keyantash and Dracup (2002)	Six meteorological indices	Rainfall deciles and SPI	Evaluation of indices in capturing meteorological, hydrological and agricultural drought in Willamette Valley and Oregon, USA, using six performance criteria. Variables such as streamflow, precipitation (station data), soil moisture etc. were used.
	Four hydrological indices	Total water deficit	
	Four agricultural indices	Computed soil moisture	
Haslinger et al. (2014)	SPI, SPEI, Palmer (Z-Index, scPDSI)	scPDSI	Comparison of indices in capturing hydrological drought in Austria, using a network of 47 catchments.
Quiring and Papakryiakou (2003)	PDSI, Palmer's Z-Index, SPI, NOAA Drought Index	Palmer's Z index	Comparison of indices in capturing and motoring agricultural drought in wheat yield in the Canadian prairies.
Todisco et al. (2008)	Palmer indices (PDSI, Z, CMI), SPI and a severity index (RS)	RS (Severity Index)	Comparison of indices in monitoring and predicting sunflower and sorghum crop yield in Central Italy.
Guttman (1998)	SPI, PDSI	SPI	Comparison of historical time series of the PDSI with the corresponding SPI time series for the contiguous USA.
Lorenzo-Lacruz et al. (2010)	SPI, SPEI	SPEI	Comparison of indices in capturing hydrological drought by analysing the headwaters of the Tagus River basin between the Iberian Range and the Plateau of Castille.
McEnvoy et al. (2012)	SPI, SPEI	SPEI	Comparison of indices in capturing hydrological drought by using standardized streamflow, lake and reservoir water surface stages at the Great Basin, USA.
Shukla & Wood (2008)	SPI, SRI (runoff index)	SRI	Comparison of indices in capturing hydrologic drought in the Feather River basin in California, USA.

contiguous USA. The study found stable results for SPI and recommended it as it was simpler, probabilistic in nature, consistent across regions and had time-scale feature (Guttman, 1998). Lorenzo-Lacruz et al. (2010) compared the performance of the SPI and SPEI by analysing the headwaters of the Tagus River basin between the Iberian Range and the Plateau of Castille. The study found a superior performance of the SPEI. Another study compared the performance of SPI and SPEI (McEnvoy et al., 2012), using standardized streamflow, lake and reservoir water surface stages at the Great Basin in the United States. Their results were similar to Lorenzo-Lacruz et al. (2010), where they found slightly higher correlations of the SPEI over SPI. Shukla and Wood (2008) compared the performance of SPI and SRI, on monthly to seasonal time scales, and reported that the SRI was a useful complement to the SPI for depicting hydrologic aspects of drought in the Feather River basin in California, United States.

The results of these previous studies are diverse. Therefore there is high uncertainty among researchers and decision makers on the selection of the appropriate drought index for their particular applications. This thesis makes an all-round assessment of established and novel drought indices by validating them against various environmental datasets on large spatial and temporal scales.

2. Aim and outline of thesis

The main objective of this thesis was to assess the performance of various drought indices. Their performance was assessed directly by comparing them to tree ring, streamflow and carbon flux data, and indirectly by assessing their NDVI mediated role in explaining tree growth–drought relationship.

The studies contribute to the following main questions:

- How do established and novel, vine copula based drought indices (VCI), perform in capturing drought signals in various environmental indicators? (Chapter 4.1, Chapter 4.3)
- Can phenological metrics derived from NDVI help to refine the understanding of the existing relationship between drought and tree growth? (Chapter 4.2)

The first publication (Chapter 4.1) "Different responses of multispecies tree ring growth to various drought indices across Europe" (Bhuyan et al., 2017a) focuses on how individual drought indices compare to each other in terms of their skill to capture drought signals in tree growth. The macroclimatic, structural, and compositional differences of forest sites at the scale of continents (Vicente-Serrano et al., 2014) lead to complexities in the study of forest vulnerability to drought. As a consequence, it is problematic to find descriptors of drought that match the temporal resolution of processes at the level of individual forests (Bhuyan et al., 2017a). In this study, an assessment of the performance of commonly used drought indices for quantifying drought impacts on forest growth is provided at a European scale, which is achieved through the study of drought impact on the radial growth of nine tree species as a function of elevation and bioclimatic zone. Chapter 4.1, upon publication, was the first study to provide detailed information on the month-wise performance of the four most commonly used drought indices: DMI, scPDSI and SPEI/SPI (in their varying temporal aggregation) in different climate zones, allowing users in accordance to their application, selection of the most appropriate index.

The second publication (Chapter 4.2) "Exploring Relationships among Tree Ring Growth, Climate Variability, and Seasonal Leaf Activity on Varying Timescales and Spatial Resolutions" (Bhuyan et al., 2017b) explores the relationship between tree ring growth, climate variability, and phenological metrics derived from NDVI. In Chapter

4.1, our results established that tree ring width is a useful proxy to assess the performance of drought indices. However, preparing tree ring chronologies can be time-consuming and prone to human errors (Camarero et al., 2015; Vicente-Serrano et al., 2016) rendering it not so useful to monitior real-time forest growth. Therefore it is important to seek proxy data for drought studies, which led to the follow-up study of Chapter 4.2. In the first section of this study (Chapter 4.2), correlation of NDVI with the radial growth of trees scattered in the Northern Hemisphere was evaluated. In the second section, the relationship between radial growth and various NDVI phenological metrics was explored. It is known that climatic conditions have a direct effect on biomass and phenological patterns of vegetation (Pettorelli et al., 2005). Hence information on drought can be provided by vegetation dynamics, as it is inherently linked to local climate (Pettorelli et al., 2005). The thesis explored whether NDVI phenological metrics can help to refine the existing relationship between vegetation and drought. Upon publication, this paper presented the first comparison of ring width index with several phenological parameters of a satellite-derived proxy of vegetation activity at multiple sites.

The third publication (Chapter 4.3) "Validation of drought indices using environmental indicators: streamflow and carbon flux data" validates the recently developed novel vine copula based drought indices (Erhardt & Czado, 2017). Validation of drought indices is an essential step in the process towards advanced drought description and assessment of their accuracy in detecting drought. Currently only a few studies have compared the relative performance of different indices to identify drought impacts on several systems (Guttman, 1998; Keyantash & Dracup, 2002; Vicente-Serrano et al., 2012; Haslinger et al., 2014). In this study, the performance of established drought indices SPI and SPEI was compared to novel index VCI, using different environmental datasets: a streamflow network of 332 catchments across Europe as well as gross primary production (GPP) and net ecosystem exchange (NEE) for Germany. The thesis contributes to the already existing question, if drought information should be based on multiple variables/indicators and if the VCI can be used as an additional source of drought information.

A schematic of the various components related to drought, studied in this thesis, is shown in Figure 3 (labelled in black).
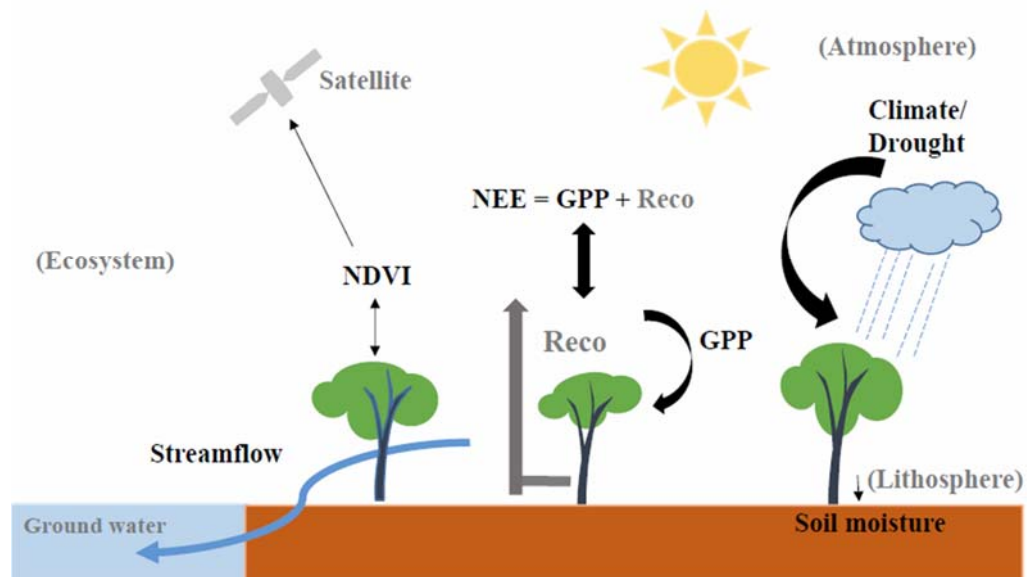
Figure 3. Major components related to drought, studied in this thesis (labelled in black). NDVI, NEE, GPP and Reco stand for normalized difference vegetation index, net ecosystem exchange, gross primary production, and ecosystem respiration respectively.

This cumulative thesis comprises three first-authored, peer-reviewed publications, two of them published (Chapter 4.1, Chapter 4.2), and one in review stage (Chapter 4.3). The chapters are shown in detail in the Appendix. The general introduction (Chapter 1) is followed by the aim of the thesis (Chapter 2) and a brief description of the data and methods (Chapter 3). Chapter 4 compiles the publication abstracts. Chapter 5 summarises the key results and includes a general discussion, Chapter 6 discusses the strengths and weaknesses of the study followed by a conclusion in Chapter 7. An outlook and the references are listed in Chapter 8 and Chapter 9, respectively.

3. Data and methods

The data and statistical methods used in this study are presented in the publications associated with each of the following chapters. An overview of the datasets used in this thesis has been summarized in Table 3.

Tree ring data and species studied: The tree ring network used in this study (Chapter 4.1) is a collection of published tree ring chronologies by Babst et al. (2013) which consists of 992 sites covering most of Europe and North Africa. The original raw tree ring width time series was detrended using a cubic smoothing spline with a frequency cut-off response of 50% at 32 years (Cook & Peters, 1997), to remove the biological trend while preserving the inter-annual to decadal variability. In the next step, temporal heteroscedasticity of the detrended series was removed using power-transformation and the series were averaged to site-wise dimensionless chronologies of ring width indices or RWI. RWI series with 56 years of data for the common period 1920–1975 was selected, after a trade-off between length of series and replication. A total of 850 sites were selected for the final analysis of the study in Chapter 4.1, as a consequence of setting a maximum period of overlap between climate data and RWI.

In Chapter 4.2, tree ring data was downloaded from the International Tree Ring Data Bank (ITRDB) (Grissino-Mayer & Fritts, 1997) which is an archive of tree ring data. "All downloaded time series from the ITRDB were filtered for three requirements (1) tree ring widths complete for the period 1982 to 2010, (2) no missing NDVI data in the time-series of each overlapping pixel, and (3) having forest cover in the corresponding remote sensing pixel" (Bhuyan et al., 2017b). Tree ring sites in the study which lay in the remote sensing pixels covering bare areas, water bodies, snow or ice and sites located in the Southern Hemisphere, were excluded (Bhuyan et al., 2017b). In total, 69 sites were reserved for analysis in Chapter 4.2. The same methodology for detrending as Chapter 4.1 was applied to tree ring data in Chapter 4.2.

The following nine species were investigated for their drought vulnerability, in Chapter 4.1, namely *Abies alba* Mill. (ABAL, silver fir), *Fagus sylvatica* L. (FASY, European beech), *Larix decidua* Mill. (LADE, European larch), *Picea abies* (L.) Karst. (PCAB, Norway spruce), *Pinus cembra* L. (PICE, stone pine), *Pinus nigra* Arn. (PINI, black pine), *Pinus sylvestris* L. (PISY, Scots pine), *Quercus petraea* (Matt.) Liebl,

(QUPE, sessile oak) and *Quercus robur* L. (QURO, common oak). The species in Chapter 4.2, were grouped into coniferous and broadleaf type for analysis, as there were not enough sites for a species-wise investigation.

Table 3. Datasets used in the thesis with the periods of analyses and sources.

Gridded Climate datasets				
Name	Period used in analysis	Resolution used at (km)	Reference	Used in chapter
CRU TS 3.21	1920-1975 (4.1), 1982-2010 (4.2), 2000-2010 (4.2)	50	Harris et al. (2014)	4.1 , 4.2
ERA-20C	1980-2010	25 50	Poli et al. (2016)	4.3
E-OBS	1950-2010	25	Haylock et al. (2008)	4.1
Environmental datasets				
Tree ring data	1920-1975	50	Babst et al. (2013), Grissino-Mayer & Fritts (1997)	4.1, 4.2
Streamflow data	1980-2010	25	GRDC (2016)	4.3
Gross primary production	1980-2010	50	Tramontana et al. (2016), FLUXCOM (2017), Jung et al. (2017)	4.3
Net ecosystem exchange	1980-2010	50	Tramontana et al. (2016), FLUXCOM (2017), Jung et al. (2017)	4.3
MODIS NDVI	2001-2010	0.25	Didan (2015)	4.2
GIMMS 3g NDVI	2001-2010, 1982-2010	8	Pinzon & Tucker (2014)	4.2
Köppen-Geiger climate classification map	1951-2000	50	Kottek et al. (2006)	4.1, 4.2
GlobCover (Forest Cover Map)	2010	50	Olivier et al. (2009)	4.2

NDVI data: Two NDVI datasets were used in Chapter 4.2, (1) Moderate Resolution Imaging Spectroradiometer (MODIS) (Didan, 2015) at a spatial resolution of 250m and (2) Global Inventory Modeling and Mapping Studies 3g (GIMMS3g) (Pinzon & Tucker, 2014) at spatial resolution of 8km. This enabled to study the effects of spatial resolution on the RWI-NDVI relationship. For MODIS, the MOD13Q1 product which is the MODIS/Terra vegetation index was used. It is provided as a 16-day composite or 23 observations per year, where quality information was used to discard possible

snow and cloud values. The MODIS NDVI data from 2001 (the first complete year of NDVI data) until 2010, the last year of our assembled tree ring dataset, was analysed (Bhuyan et al., 2017b). The third-generation Global Inventory Modeling and Mapping Studies, GIMMS3g is based on the Advanced Very High Resolution Radiometer (AVHRR), which is provided at a temporal resolution of 15 days resulting in two maximum-value composites per month or 24 observations per year. The GIMMS3g NDVI data from 1982 (the first complete year of NDVI data) to the end of 2010 was investigated to maximize the overlap with the tree ring dataset (Bhuyan et al, 2017b).

CRU TS 3.21: For Chapter 4.1 and Chapter 4.2, mean temperature, precipitation sum, and potential evapotranspiration (PET) monthly datasets from the observational CRU TS 3.21 (Climatic Research Unit) worldwide dataset available on a 0.5° grid (Harris et al., 2014) was used. The dataset contains monthly time series of precipitation, frost, water vapour, daily maximum and minimum temperatures, cloud cover, and other variables for the period 1901-2012. The data set uses more than 4000 individual weather station records in its computation.

ERA 20C Reanalysis: To validate the different drought indices used in Chapter 4.3, the publicly available ECMWF Atmospheric Reanalysis of the 20th Century (ERA-20C) data (European Centre for Medium-Range Weather Forecasts, 2014; Poli et al., 2016) was employed. The ERA 20C data set is a reanalysis of the weather observed on the earth's surface for the period 1900–2010. "The ERA-20C assimilates surface pressure and marine wind observations" (Poli et al., 2016). For Chapter 4.3, time series of total precipitation, volumetric soil water content and potential evapotranspiration at a 0.25° grid were used for validation against streamflow data. Similarly, climatic water balance, volumetric soil water content and temperature data was used for validation against carbon flux data, at a 0.50° grid. Using the method proposed by Thornthwaite (1948), the variable potential evapotranspiration was computed based on temperature and latitude information. The called climatic water balance (see e.g. Vicente-Serrano et al., 2010) was computed as a difference between precipitation and potential evapotranspiration.

E-OBS: In order to validate the findings of Chapter 4.1 using CRU TS 3.21 data, station data from E-OBS was used. The data set is a gridded data set derived/interpolated from station observations (Haylock et al., 2008). It covers the

European continent and is available for different grids and spatial resolutions. The version 13.1 of the data set was used, which provides daily values of all the variables used in Chapter 4.1.

Climate classification data: Data on climate classification used in Chapter 4.1 and Chapter 4.2, was obtained from the world Köppen-Geiger climate classification map (Kottek et al., 2006).

Forest Cover map: For Chapter 4.2, the world forest-cover map (GlobCover) from the European Space Agency was used to filter pixels with forest cover. The GlobCover map is based on Envisat Medium Resolution Imaging Spectrometer (MERIS) data between December 2004 and June 2006 (Olivier et al., 2009).

Streamflow data: The streamflow data used in Chapter 4.3 was obtained from the Global Runoff Data Centre (GRDC, 2016) which is a repository for the world's river discharge data and associated metadata hosted by The German Federal Institute of Hydrology. In the archive, there are streamflow time series from 1315 European catchments. "In this study, we selected 332 catchments for the period 1980-2010, which have a size less than 500 km^2, as smaller catchments are more likely to contain drought signals less affected by external processes. For each catchment, we derived the catchment boundary using data from Catchment Characterisation and Modelling database (de Jager and Vogt, 2010)" (Bhuyan-Erhardt et al., 2017).

Carbon flux data: Data on monthly carbon flux variables, gross primary production and net ecosystem exchange for Germany used in Chapter 4.3, were obtained from RS+METEO product of FLUXCOM (Tramontana et al., 2016; FLUXCOM, 2017; Jung et al., 2017). The carbon flux data was available at 0.50° spatial resolution for the period 1980-2013. Monthly ensemble means of six variants (three machine learning algorithms and two observed flux variants from two partitioning methods) (Reichstein et al., 2005; Lasslop et al., 2010) were used to generate time series of GPP and NEE (Bhuyan-Erhardt et al., 2017). For validation of drought indices against carbon flux data, the period of 1980-2010 and the drought year 2003 in Germany were taken as a case study.

Statistical Analyses

Statistical methods used in this thesis were mainly but not restricted to: correlation function analyses (Fritts et al., 1971), correlation, bootstrapped correlation, linear regression techniques, principal component analysis, Procrustes tests, random forest analysis, various model validation statistics and calculation of forecast verification skill scores such as probability of detection (POD) and false alarm ratio (FAR).

In Chapter 4.1, in order to assess the species-specific growth-drought relationships, correlation function analyses (Fritts et al., 1971) were calculated between RWI and the selected four drought indices. The correlation coefficients calculated for the year of ring formation (March to September), were introduced into a "Q" mode principal component analysis (PCA) to find persistent drought patterns in space (Machado-Machado et al., 2011). To calculate the influence of each variable on the formation of the reduced space, an equilibrium circle of descriptors, with radius $\sqrt{(d/p)}$ (with p total and d reduced dimension in ordination), was drawn as reference (Legendre & Legendre, 1998). "R package bootRes (Zang & Biondi, 2013) was used for calculating bootstrapped correlations between RWI and drought indices; and package ggplot2 was used for visualizations (Wickham, 2009)" (Bhuyan et al., 2017b).

In Chapter 4.2, random forest (RF) analysis was used to rank the importance of NDVI phenological metrics in explaining tree growth. RF is a multivariate non-parametric regression method, which is an ensemble learning technique developed by Breiman (2001). The RF model was fitted using all tree ring sites. 70% of the data was randomly sampled to train the RF and the remaining 30% were retained for RF prediction-error testing. "The proportion of explained variance in the outcome of the training data and the normalized root mean square error (NRMSE) were used to quantify the association between RWI and NDVI/climate" (Bhuyan et al., 2017b). RF models were calculated using R package randomForest package (Liaw & Wiener, 2002).

In Chapter 4.3, for comparison of the drought indices with streamflow time series, daily data was converted to monthly values and then standardized using long-term monthly mean and standard deviation. The performance of the drought indices to detect low-flow events focusing on the low-flow season (August to Nov) was assessed using verification skill scores. Such scores facilitate the process of comparing forecasts to relevant observations and hence enabling measurement of the quality of different

forecasts. In this thesis the metrics: probability of detection (POD) or hit rate and false alarm ratio (FAR) were the point of focus. "POD is a verification measure of categorical forecast performance that measures the total number of correct event forecasts (hits) divided by the total number of events observed. FAR is the number of false alarms divided by the total number of event forecasts. While POD is only sensitive to hits and ignores false alarms, the opposite holds for the FAR. Hence, it is always recommended to use these two verification skills together (WWRP/WGNE Joint Working Group on Forecast Verification Research, 2015)" (Bhuyan-Erhardt et al., 2017). Verification skill scores were calculated using R package Verification (Pocernich, 2012). For validation of drought indices with carbon flux data, regression technique was used. For visualizing pixel-wise linear regression of carbon flux data and drought indices, R package rasterVis was used (Lamigueiro & Hijmans, 2016).

For reading and writing spatial data which was used throughout the study, the following R packages were used: maps, mapdata, maptools, ncdf4, rgdal, sp, raster. All statistical analyses were performed with different versions of the statistical software R (R Core Team, 2017).

4. Abstracts of individual publications

4.1 Different responses of multispecies tree ring growth to various drought indices across Europe.

Increasing frequency and intensity of drought extremes associated with global change are a key challenge for forest ecosystems. Consequently, the quantification of drought effects on tree growth as a measure of vitality is of highest concern from the perspectives of both science and management. To date, a multitude of drought indices have been used to accompany or replace primary climatic variables in the analysis of drought-related growth responses. However, it remains unclear how individual drought metrics compare to each other in terms of their ability to capture drought signals in tree growth. In our study, we employ a European multispecies tree ring network at the continental scale and a set of four commonly used drought indices (De Martonne Aridity Index, self-calibrating Palmer Drought Severity Index, Standardized Precipitation Index and Standardized Precipitation Evapotranspiration Index, the latter two on varying temporal scales) to derive species-specific growth responses to drought conditions. For nine common European tree species, we demonstrate spatio-temporal matches and mismatches of tree growth with drought indices subject to species, elevation and bioclimatic zone. Forests located in the temperate and Mediterranean climate were drought sensitive and tended to respond to short- and intermediate-term drought (<1 year). In continental climates, forests were comparably more drought resistant and responded to long-term drought. For the same species, stands were less drought sensitive at higher elevations compared to lower elevations. We provide detailed information on the month-wise performance of the four drought indices in different climate zones allowing users the selection of the most appropriate index according to their objective criteria. Our results showed that species-specific differences in responses to multiple stressors result in complex, yet coherent patterns of tree growth.

Contributions: Lead by Annette Menzel and Christian Zang, I conceptualized the design of the study. I carried out the data processing and wrote the manuscript. All

authors contributed to the interpretation of results and editing of the manuscript, with contributions of Annette Menzel to writing. Christian Zang assisted in the choice of analytical methods and gave leads on what packages to be used for the tree ring data analysis. About 70% of the work was done by myself.

4.2 Exploring relationships among tree ring growth, climate variability, and seasonal leaf activity on varying timescales and spatial resolutions.

In the first section of this study, we explored the relationship between ring width index (RWI) and normalized difference vegetation index (NDVI) time series on varying timescales and spatial resolutions, hypothesizing positive associations between RWI and current and previous- year NDVI at 69 forest sites scattered across the Northern Hemisphere. We noted that the relationship between RWI and NDVI varies over space and between tree types (deciduous versus coniferous), bioclimatic zones, cumulative NDVI periods, and spatial resolutions. The high-spatial-resolution NDVI (MODIS) reflected stronger growth patterns than those with coarse-spatial-resolution NDVI (GIMMS3g). In the second section, we explored the link between RWI, climate and NDVI phenological metrics (in place of NDVI) for the same forest sites using random forest models to assess the complicated and nonlinear relationships among them. The results were as following (a) The model using high-spatial-resolution NDVI time series explained a higher proportion of the variance in RWI than that of the model using coarse-spatial-resolution NDVI time series. (b) Amongst all NDVI phenological metrics, summer NDVI sum could best explain RWI followed by the previous year's summer NDVI sum and the previous year's spring NDVI sum. (c) We demonstrated the potential of NDVI metrics derived from phenology to improve the existing RWI-climate relationships. However, further research is required to investigate the robustness of the relationship between NDVI and RWI, particularly when more tree-ring data and longer records of the high-spatial-resolution NDVI become available.

Contributions: Together with Annette Menzel, Sergio M. Vicente-Serrano and Christian Zang, I conceptualized the design of the study. I carried out the data processing and wrote the manuscript with contributions of Annette Menzel. All authors contributed to the interpretation of results and editing of the manuscript.

Christian Zang assisted in the choice of analytical methods. About 70 % of the work was done by myself.

4.3 Validation of drought indices using environmental indicators: streamflow and carbon flux data.

Bhuyan-Erhardt Upasana, Erhardt Tobias Michael, Laaha Gregor, Zang Christian, Parajka Juraj, Menzel Annette (2017)

In several scientific disciplines, quantitative indices are the most popular approach for drought quantification. Aiming for refined drought characterization, the validation of such drought indices is of vital importance. It allows assessing the indices' accuracy in detecting drought. In this study, we compared the performance of established drought indices – the SPI (Standardized Precipitation Index) and the SPEI (Standardized Precipitation Evapotranspiration Index) – with standardized drought indices computed using a recently developed, vine copula based method for the computation of multivariate drought indices (here addressed as VC-Index or VCI). For our validation study, we used several environmental drought indicators: streamflow time series from a network of 332 catchments across Europe, as well as gross primary production (GPP) and net ecosystem exchange (NEE) for Germany. The novel multivariate VC-Indices can combine two or more user-selected, drought relevant variables to model different drought types, depending on the user-application. This approach utilizes the flexibility of vine copulas in modeling multivariate non-Gaussian dependencies and allows for stable indices using much shorter observation periods. The results of the validation showed that the VC-Indices outperform the established drought indices SPI and SPEI. For the streamflow data, the VCI was found to have advantageous attributes such as higher probability of drought detection and lower false alarm ratio compared to SPEI and SPI. Regression of the drought indices against NEE and GPP showed that the VCI captured the drought-impact relationship on carbon flux data best. Overall, our results emphasize that the major key to improving our understanding of drought impacts on ecosystem conditions could be a user-defined, application-based drought monitoring on a high spatial resolution, using a method such as vine copulas. We recommend using the VCI as an additional source of information, in order to allow better understanding of drought characterization.

Contributions: I conceptualized the design of the study with substantial inputs from Annette Menzel, Gregor Laaha, Tobias Michael Erhardt and Christian Zang. Tobias Michael Erhardt provided software to calculate the novel drought index. Christian Zang and Juraj Parajka provided data and key information. I carried out the data processing and wrote the manuscript. All authors contributed to the interpretation of results and editing of the manuscript. About 80% of the work was done by myself.

5. Discussion

"This drought emergency is over, but the next drought could be around the corner. Conservation must remain a way of life." - Jerry Brown, California Governor

The thesis and the publications coupled to it aim at a better understanding of drought quantification using drought indices, mainly from an ecological perspective. How individual drought metrics compare to each other in terms of their ability to capture drought signals was assessed using various environmental datasets. In addition to a short summary of the discussions presented in the individual publications, this chapter constitutes a general discussion of the results. The diversity of environmental indicators evaluated in the thesis allows us to make a comprehensive comparison of the different indices. Our findings provide evidence that the patterns of growth, streamflow and carbon flux responses to drought do not follow any general geographical structure (Vicente-Serrano et al., 2014). Depending on the type of indicator, these patterns can be driven by various factors such as climatic and biogeographical conditions, elevation of the site, time of the year when studied etc. In the first section, responses of various environmental indicators to different drought indices are discussed and in the second section, performance of drought indices in relation to NDVI phenological metrics and tree rings, are examined. Table 4 summarizes the performance of the indices based on the different environmental indicators.

5.1 Responses of various environmental indicators to different drought indices

Key findings:

- Tree rings: Spatio-temporal matches and mismatches of tree growth with drought indices are subject to species, elevation and bioclimatic zone. scPDSI, SPEI/SPI at longer time-scales best captured drought in tree ring width data.
- Streamflow: The multivariate vine copula based index (VCI) was able to capture drought information in streamflow data most effectively, as per forecast verification skill scores.
- Carbon flux: The multivariate vine copula based index (VCI) was able to capture drought information in carbon flux data most effectively, as per regression analysis.

Table 4. General performance of drought indices based on different environmental indicators. "x","✓" and "✓✓" summarize the results as "drought information not captured", "drought information captured" and "drought information captured effectively", respectively.

Period	Data and Method	Index	Result
Tree rings			
1920-1975	1st Principal component	DMI	✓
		SPEI	✓✓ (scale>12)
		SPI	✓✓ (scale>12)
		scPDSI	✓✓
Streamflow			
1980-2010	Forecast verification score (POD and FAR)	SPEI	✓
		SPI	✓
		VCI	✓✓
Gross primary production			
1980-2010	Pixel-wise linear regression	SPEI	x
		SPI	x
		VCI	✓✓
Net ecosystem exchange			
1980-2010	Pixel-wise linear regression	SPEI	✓
		SPI	x
		VCI	✓✓
NDVI phenological metrics			
2001-2010	Random forest	scPDSI	✓✓
		SPEI	✓

Tree rings: The findings of our study in contrasting bioclimatic zones and elevations, stress the importance of considering different drought indices, time-scales and study periods for a better understanding of how tree species respond to drought.

Shifts in vegetation growth rates and distributions during the twenty-first century are anticipated due to climate change (Williams et al., 2010). In terms of general growth-drought index relationship, strongest correlations with growth (RWI) were found for scPDSI and SPI/SPEI at longer time scales (in Chapter 4.1). This finding was similar to the study of Vicente-Serrano et al. (2012), which found closer growth–drought correlations for SPI and SPEI (at time scale of 1 month) compared to PDSI. Similar behaviour of scPDSI to SPI and SPEI at longer time scales was observed, which could be explained by the fact that scPDSI has significant lagged autocorrelation, as it takes into account temperature and precipitation for the specific and the preceding months (Palmer, 1965; Dai et al., 2004).

In Chapter 4.1, a group of four commonly used drought indices DMI, scPDSI, SPEI and SPI (the latter two on varying temporal scales) was used to derive species-specific

growth responses to drought for nine European tree species. In general, it was found that forests located in the temperate/Mediterranean and continental climates were relatively drought sensitive and resistant, respectively. While forests located in the temperate and Mediterranean climate, were more inclined to respond to short- and intermediate-term drought (less than a year), forests in continental climates responded to long-term drought.

Recommended drought index for different species

For each species of the study, the different months and drought indices with maximum correlation with RWI are reported in Chapter 4.1. "In general, scPDSI showed maximum correlations with the deciduous species beech, and the two oak species, as well as coniferous species black pine. DMI had maximum correlations with beech, sessile oak and black pine but as well silver fir. SPEI and SPI at varying degrees captured the drought signal of all species" (Bhuyan et al., 2017a). Studies based on observation (Pichler & Oberhuber, 2007; Lebourgeois et al., 2010; Schuster & Oberhuber, 2013; van der Maaten-Theunissen et al., 2013; Boden et al., 2014; Pretzsch et al., 2014) and expert assessment (Niinemets & Valladares, 2006) confirm the classification for Norway spruce, silver fir and European beech as drought-sensitive species as found in results of Chapter 4.1. Effect of long-term drought was observed in high elevation stands of Norway spruce which showed greater drought resistance similar to several studies (van der Maaten-Theunissen et al., 2013; Zang et al., 2014). For temperate beech forests, scPDSI, SPI and SPEI during the main summer months, were most suitable. All drought indices DMI, scPDSI, SPI, SPEI were able to capture drought impacts on oak species, during summer. Confirming pervious findings (Friedrichs et al., 2008; Zang et al., 2011), the sessile and common oak were found to be drought sensitive and were particularly affected by short-term drought. For Scots pine in general and European larch and stone pine in the alpine zone, the performances of all drought indices were quite similar. Species of the genus Pinus showed a diverse range of responses from being drought sensitive such as the Black and Scots pine (Martin-Benito et al., 2013; Pichler & Oberhuber, 2007; Camarero et al., 2015; Thabeet et al., 2009) to drought resistant such as Stone pine. The effect of elevation was more pronounced for some species like European larch, beech and common oak (Bhuyan et al., 2017a). Detailed information on the recommended index for all the species in different climate zones and elevations can be found in Bhuyan et al. (2017a).

In general our results established that RWI is a useful proxy to assess the performance of drought indices, however it is not always practical. Therefore it is important to seek potential alternatives for the RWI or proxy data for drought studies, which led to the follow-up study of Chapter 4.2.

Streamflow data: The climate-based indices SPI and SPEI describe only the climate anomalies in isolation from their hydrological context (Shukla & Wood, 2008), while the VCI offers an adept method for jointly characterizing the effects of climate anomalies and hydrologic conditions.

Depending on the capacity of the catchment to store and release water, which can boost or amplify atmospheric drought signals, hydrological events can differ from meteorological ones (Van Lanen et al., 2016; Laaha et al., 2017). Amongst SPEI, SPI and VCI, the streamflow drought relationship was most prominent with VCI. It had maximum values in fall and had a higher mean correlation value for all months. SPI and SPEI had low correlations during the period March-June, which can be attributed to the fact that at around this time of the year, rainfall deficit and snow melt influence streamflow (Haslinger et al., 2014; Staudinger et al., 2014). This effect is not accounted for by SPEI and SPI, since a time lag with streamflow drought has previously been observed for SPI and SPEI (Shukla & Wood, 2008; Haslinger et al., 2014). The effect due to snowmelt processes is however not as evident in case of VCI, as it is a hydro-metorological drought index, and not purely meteorological. In general, the results of Chapter 4.3 confirm the hypotheses that the relationship between streamflow anomalies and drought indices is more striking the more complex the drought index is, as shown in Haslinger et al. (2014). Using the forecast verification skill scores probability of detection and false alarm rate, VCI outperformed the other indices with the highest POD and lowest FAR scores. This result was similar to studies where a multivariate drought index resulted in a higher probability of drought detection compared to single parameter based index (Hao & AghaKouchak, 2013; Hao & AghaKouchak, 2014; AghaKouchak, 2014). The superior performance of VCI could be a consequence of including volumetric soil water content, besides precipitation and potential evapotranspiration into the computation, and secondly due to the fact that it uses vine copulas to explain for inter-variable dependencies in an adjustable fashion (Aas et al., 2009). It was observed that catchment area (upto 500 km^2) had no consequence on the responses of the drought indices, however elevation of the

catchment resulted in variable performance of the indices. Streamflow data showed that for low, medium and high elevations of a catchment, VCI was the best performing index when considering POD and FAR scores in conjunction.

Carbon Flux: Similar to the results with the streamflow data, it was observed that the VCI skillfully captured drought information when validated against carbon flux variables, whereas the climate-based indices described the climate anomalies in isolation from their carbon balance context.

In biogeosciences, an ongoing objective is to accurately account terrestrial carbon (Schimel, 1995). The pixel-wise regression analysis of the drought indices and carbon fluxes in Chapter 4.3, showed a varying strength of the correlation depending on the drought index, the period of analysis (1980-2010, 2003) and the carbon flux variable under consideration. The average R^2 values of the pixel-wise regression of NEE and GPP with the drought indices were highest for drought index VCI, followed by SPEI and SPI, when considering the long period of 1980-2010 (Bhuyan-Erhardt et al., 2017). In general, the indices confirmed the relationship of drought with carbon flux variables: GPP and NEE (Ciais et al., 2005; Reichstein et al., 2005; Pereira et al., 2007; Vicca et al., 2016). This drough-flux relationship was most reflected in case of both GPP and NEE by VCI with all statistically significant values, which enables us to interpret with confidence the superiority of the methodology of drought index VCI in depicting drought events of the past. Similar to results of the period 1980-2010, the average R^2 values of linear regression of NEE and GPP for the drought year 2003, with the drought indices were highest for drought index VCI.

> "MODIS greatly improves scientists' ability to measure plant growth on a global scale." – NASA Earth Observatory

5.2   Performance of drought indices in relation to phenological metrics derived from NDVI and tree rings

   Key findings:
- Understanding of the existing tree growth–drought relationship can be refined using NDVI phenological metrics.
- scPDSI better highlighted tree growth-NDVI relationship compared to SPEI.

- Summer NDVI sum best explained RWI followed by the previous year's summer NDVI sum and the previous year's spring NDVI sum.

- The NDVI-growth relationship was more striking with the high-resolution NDVI (MODIS).

In Chapter 4.2, it was seen that drought index scPDSI in conjunction with phenological metrics derived from NDVI and other climatic parameters, best described tree growth. SPEI also revealed this relationship, however the proportion of variance of tree growth explained by SPEI was lower than scPDSI. This could be attributed to the fact the climate-only index such as the SPEI does not integrate soil properties like the scPDSI, which enables capturing tree growth information more effectively. In general, results established that spatio-temporal variations of vegetation phenology can help to refine the relationship between drought and tree-growth.

In Chapter 4.2, both GIMMS3g and MODIS NDVI were used, which were at significantly different spatial resolutions. In general, a positive relationship between NDVI in the growing season and RWI was seen for many forests (at the local level) (Kaufmann et al., 2004; Vicente-Serrano et al., 2016) with MODIS NDVI generally reflecting stronger growth patterns than GIMMS3g NDVI. For instance, for conifers in a continental climate, growth was strongly linked to a MODIS NDVI signal during summer (similar to studies by Lopatin et al., 2006, Bunn et al., 2013; Beck & Goetz, 2011; Brehaut 2015; Berner et al., 2013) upto 10–15 cumulative NDVI observations, in contrast to almost a non-existent GIMMS3g NDVI signal. Details of the results for deciduous and conifer trees in three different climate types: semiarid, temperate and continental, can be found in Bhuyan et al. (2017b). A negative relationship between NDVI and RWI was also observed for some forests, which could be due to site-level factors and changing environmental conditions (Wilmking et al., 2005).

Our results showed that MODIS NDVI based phenological information improved the RWI modelling noticeably compared to GIMMS3g (Kern et al., 2016), since the high-spatial-resolution data was able to capture local climatic or other information reflecting the changes in RWI better than the coarse-spatial-resolution data. Amongst NDVI phenological metrics, RF models identified that summer NDVIs of current and previous years, best reflected RWI (Kaufmann et al., 2008). Other important parameters found in our study were the spring and growing season NDVIs of previous

and current years. They had a higher score than precipitation in the RF model, which demonstrates the potential of NDVI metrics to improve the relationship between tree-growth and drought (Bhuyan et al., 2017b).

5.3   Synopsis of discussion

The diversity of environmental indicators evaluated in the thesis allows us to make a wide-ranging comparison of the different indices. Although some drought indices such as SPI are popularly accepted, the variety of drought indices that exist reflects a fundamental lack of a unique definition and functioning requirement. Nevertheless, our results point to the advantage of having multiple variables in the calculation of a drought index, as the VCI.

The magnitudes of the correlations between various variables and the compared drought indices clearly showed that the multiscalar, climate based indices SPI and SPEI are comparable to each other in their ability to capture drought conditions in different systems (Vicente-Serrano et al., 2014, Bhuyan et al., 2017a). The results clearly demonstrate that, although precipitation (SPI) is the main driver of drought severity, adding the influence of the atmospheric evaporative demand (SPEI) improves drought detection in case of several variables such as river discharges and reservoir storages (Lorenzo-Lacruz et al., 2010), tree ring width (Vicente-Serrano et al., 2014, Bhuyan et al., 2017a), atmospheric circulation (Tan et al., 2015) and net ecosystem exchange (Bhuyan-Erhardt et al., 2017). Although some studies recommended SPI over scPDSI (Guttman, 1998; Keyantash & Dracup, 2002) there were also studies that reported the contrary (Haslinger et al., 2014). scPDSI is found to be generally more suited to test water availability in tree growth or agricultural crops as seen in many studies (Orwig & Abrams, 1997; Akinremi et al. 1996; Quiring and Papakryiakou 2003; Scian and Donnari 1997; Mavromatis 2007, Bhuyan et al., 2017a; Bhuyan et al., 2017b). scPDSI can be qualified as a mid and long time scale index owing to the strong lagged autocorrelation whereas the SPI/SPEI can suitably monitor short and long-term drought using selected timescales (Bhuyan et al., 2017a; Zhao et al., 2015). Nevertheless, when data is available, combining multiple data sets can be considered more advantageous as reflected by the results of Chapter 4.3.

Results of this thesis, which links phenological metrics derived from NDVI to radial growth of trees, are encouraging. NDVI phenological metrics hold the potential to

refine the understanding of the existing relationship between drought and tree growth. Yet, there is a large gap in knowledge to be filled, before such inferences can be made at longer time scales and across larger spatial extents. Also, our current understanding between phenological metrics derived from NDVI and field-based measures of production has been limited to correlation analyses which is very simplistic or one-dimensional from an ecological perspective. An important start would be to improve the statistical models between tree growth and NDVI metrics, in order to better understand changes in tree growth under current climate change scenarios.

6. Strengths and shortcomings of the studies

Gridded climate/environmental data products

The thesis employs different spatially coarse gridded climate/environmental data products (CRU, ERA-20C, E-OBS, GIMMS3g, MODIS and FLUXCOM) which have many advantages in situations where station data is not available, especially with good temporal coverage, or unavailability of the desired data from other sources. Chapter 4.1 and Chapter 4.2 use the CRU TS 3.21 dataset which covers all land masses between 60°S and 80°N for the period of 1900-2012. This is especially useful for global studies or continental studies (Chapter 4.1 - 4.2) where a long time period over large spatial scales is desirable for analysis. For instance, for tree ring studies large temporal coverage is necessary since tree ring data is available from as early as 1800s. For validation of the results of Chapter 4.1, the E-OBS data set was used, which is usually the only available dataset for studies such as comparison of regional climate model (RCM) outputs for the whole of Europe (Hofstra et al., 2009) and for validation of results obtained with other climate data products (Chapter 4.1). In Chapter 4.3, the ERA-20C reanalysis product was used to calculate the drought indices including the novel multivariate drought index VCI, as it contains long, gap-free gridded records of many climate variables like the volumetric soil water content, which is otherwise not available from a different source on a global scale for a long time period. The carbon flux data from FLUXCOM was used as a dataset to assess the performance of drought indices in Chapter 4.3, and is generally very preferable because it combines the strengths of multiple global satellite-based observations with site-level observations using several methods (Koirala et al., 2017). Chapter 4.2 uses MODIS and GIMM3g NDVI datasets. The GIMMS3g NDVI dataset spans over three decades, which is very useful as it fulfils the high demand for a continuous and consistent long-term NDVI dataset. The MODIS dataset is at a relatively fine resolution of 250m and is well recognized for its wide range of applications, and has the highest quality due to its quality control, cutting-edge sensor characteristics, advanced calibration and data processing algorithms (Didan et al., 2015; Kern et al., 2016).

However, the weakness of such gridded data sets is that they are known to contain product-specific biases (Zhao et al., 2012; Garnaud et al., 2014) which adds to uncertainty. The CRU dataset, which is used in Chapter 4.1 and Chapter 4.2, is not

specifically homogeneous (Harris et al., 2014). It has been recommended that analysis with the CRU dataset should be complemented by comparison with other datasets (Harris et al., 2014) as done in Chapter 4.1. Some shortcomings of the ERA-20C include the slight negative impact of the data assimilation on trends and low-frequency variability (Poli et al., 2016). The E-OBS dataset derived through interpolation of station data also contains errors introduced by the station data (Haylock et al., 2008). The MODIS NDVI dataset has short temporal coverage of 13 years and as a consequence results of statistical analyses with MODIS NDVI are not as robust. GIMM3g NDVI on the other hand is at a coarse resolution making it not very suitable for correlating with forests, which do not lie within the NDVI pixel by default. An imperfect applicability of GIMMS3g has also been found for Central Europe (Kern et al., 2016). In the FLUXCOM dataset, it has been observed that the information content of the driving input variables may not be sufficient to capture the variability of the fluxes in all conditions (Tramontana et al., 2015). Moreover it uses remote sensing and meteorological gridded data sets which are affected by uncertainties themselves (Tramontana et al., 2016).

Tree ring data and species studied

Chapter 4.1 and Chapter 4.2 analyses tree ring data. The greatest advantage of tree ring width data is that it provides centuries-long, continuous annual records of past hydroclimatic variability for regions and periods with no station climate data (Cook et al., 1999) and therefore is very useful for studying the past climate. However, tree ring sample collections may represent variable sample homogeneity and hence different growth-forcing signals. Moreover, additional drivers of growth could add noise to the climate signals extracted from tree ring data. A limitation of the study (Chapter 4.1) is that recommendations for drought indices were provided based on some European species, therefore, studying a restricted number of species under a restricted set of conditions, many questions remain. Also, the interpretation of NDVI and its relation to ring widths is challenging (Chapter 4.2), since it is constrained by the assumption that the forests being analysed dominate the NDVI pixel.

Random forest models

Random forest models (Breiman, 2001) are used in Chapter 4.2 to assess the performance of different NDVI phenological metrics, climatic and auxiliary

parameters. Compared to other statistical models, it is relatively less prone to over fitting, hence preferred. However it can have unstable results, because a different aggregate model is observed at each run as it takes different bootstrap samples (Liaw & Wiener, 2002) and the ranks of variables depend on number of included variables (Breiman, 2001).

Challenges of using multivariate indices

In section 5, the advantages and the superiority of using multivariate drought indices was established. However, the results of a multivariate index such as the VCI depends on the choice of variables used in its computation. The selection of the most appropriate drought-relevant variables is not necessarily an easy task for all end-users. Another challenge associated with using/developing a multivariate index like the VCI is that ground-based observations of many drought-related variables (e.g., soil moisture, snowmelt, and water vapour) are not readily available or easy to assess compared to variables such as precipitation (used in SPI) and potential evapotranspiration (used in SPEI). Even when data of drought-related variables such as soil moisture is available they are many times restricted to certain regions of the world. This prohibits the development of multi-index indicators (Hao & AghaKouchak, 2014). Moreover, for many satellite data, length of the climate records are limited to a decade or have very coarse resolution which limits the methodology of indices to be utilized to their maximum capabilities (Bhuyan-Erhardt et al., 2017).

7. Conclusions

Overall, the studies compiled in this thesis delivered new insights in several areas revolving around drought indices from different ecological perspectives. The studies utilized proper scores, methods and various environmental datasets in order to provide an all-rounded assessment of different drought indices. Our results are particularly relevant within the changing climate framework, because the degree to which ecosystems respond to water deficiency can show how responsive they could be to future climate change.

It was seen that the appropriate drought index for detecting impacts depends on the analysed system, the application and data being used. For nine tree species of the study, located in different bioclimatic zones and elevations, the month wise performance of drought indices DMI, scPDSI and SPEI/SPI (in their varying temporal aggregation) are provided to facilitate users the selection of the most suitable index depending on their application. Results of the RF models established that NDVI phenological metrics have the potential to refine the understanding of the existing relationship between drought and tree growth, especially when NDVI is at a fine spatial resolution such as MODIS. Validation of drought indices using streamflow and carbon flux data showed varying performance of the drought indices with one stable result: the novel multivariate drought indices (VCI) outperformed the established indices in all investigations, with attributes such as higher probability of detection and lower false alarm rates.

Given the observed impacts of global warming processes on water availability and the results obtained in this thesis using various environmental datasets at the global and regional scale, it is advocated to use multiple variables/indicators for drought characterization. VCI is recommended to be used as an added source of drought information and possibly to improve the accuracy of projections under global change scenarios.

8. Outlook

The IPCC AR5 (2013) stressed low confidence in a global scale observed trend in drought. Also, studies have suggested that drought may become so widespread and severe in the coming decades that current drought indices might no longer be able to quantify future drought episodes effectively (Dai, 2011).

One obvious future directions for drought indices research could be understanding of drought impacts on ecosystem conditions using high spatial resolution, application-based user-defined drought monitoring. Progress needs to be made in the field of exploiting novel remote sensing information, as longer temporal records of existing sensors such as MODIS become available. Due to the complexity and time-dependency of these processes, current studies cannot yet deliver concluding answers. While there is clearly a need for targeted drought indices, their validation is equally important and at the same time testing of their boundary conditions and limitations.

It is suggested that scientists from different disciplines study patterns of responses to drought using different environmental indicators such as drought-sensitive plant species, streamflow and carbon flux data, and by taking advantage of droughts while they are still headway. This would result in more robust models to understand the effects of climate change on the ecosystem.

9. References

Aas K, Czado C, Frigessi A, Bakken H (2009) Pair-copula constructions of multiple dependence. *Insurance: Mathematics and Economics*, **44**, 182–198.

AghaKouchak A (2014) A baseline probabilistic drought forecasting framework using standardized soil moisture index: Application to the 2012 United States drought. *Hydrology and Earth System Sciences*, **18**, 2485–2492.

AghaKouchak A (2015) A multivariate approach for persistence-based drought prediction: Application to the 2010-2011 East Africa drought. *Journal of Hydrology*, **526**, 127–135.

AghaKouchak A, Farahmand A, Melton FS, Teixeira J, Anderson MC, Wardlow BD, Hain CR (2015) Remote sensing of drought: Progress, challenges and opportunities. *Reviews of Geophysics*, **53**, 1–29.

Akinremi OO, Mcginn SM, Barr AG (1996) Evaluation of the Palmer drought index on the Canadian prairies. *Journal of Climate*, **9**, 897–905.

Allen CD, Macalady AK, Chenchouni H et al. (2010) A global overview of drought and heat-induced tree mortality reveals emerging climate change risks for forests. *Forest Ecology and Management*, **259**, 660–684.

Alley WM (1984) The Palmer Drought Severity Index: Limitations and assumptions. *Journal of Applied Meteorology and Climatology*, **23**, 1100–1109.

Anderegg WRL, Kane JM, Anderegg LDL (2013) Consequences of widespread tree mortality triggered by drought and temperature stress. *Nature Climate Change*, **3**, 30–36.

Babst F, Poulter B, Trouet V et al. (2013) Site- and species-specific responses of forest growth to climate across the European continent. *Global Ecology and Biogeography*, **22**, 706–717.

Beck PSA, Goetz SJ (2011) Satellite observations of high northern latitude vegetation productivity changes between 1982 and 2008: ecological variability and regional differences. *Environmental Research Letters*, **6**, 45501.

Beck PSA , Andreu-Hayles L, D'Arrigo R, Anchukaitis KJ, Tucker CJ, Pinzón JE, Goetz SJ (2013) A large-scale coherent signal of canopy status in maximum latewood density of tree rings at arctic treeline in North America. *Global and Planetary Change*, **100**, 109–118.

Berner LT, Beck PSA, Bunn AG, Goetz SJ (2013) Plant response to climate change along the forest-tundra ecotone in northeastern Siberia. *Global Change Biology*, **19**, 3449–3462.

Bhuyan U, Zang C, Menzel A (2017a) Different responses of multispecies tree ring growth to various drought indices across Europe. *Dendrochronologia*, **44**, 1–8.

References

Bhuyan U, Zang C, Vicente-Serrano SM, Menzel A (2017b) Exploring relationships among tree-ring growth, climate variability, and seasonal leaf activity on varying timescales and spatial resolutions. Remote Sensing, **9**, 1–13.

Bhuyan-Erhardt U, Erhardt TM, Laaha G, Zang C, Parajka J, Menzel A (2017) Validation of drought indices using environmental indicators: streamflow and carbon flux. In review at Science of the Total Environment.

Boden S, Kahle H-P, Wilpert K von, Spiecker H (2014) Resilience of Norway spruce (*Picea abies* (L.) Karst) growth to changing climatic conditions in Southwest Germany. *Forest Ecology and Management*, **315**, 12–21.

Bolte A, Ammer C, Löf M et al. (2009) Adaptive forest management in central Europe: Climate change impacts, strategies and integrative concept. *Scandinavian Journal of Forest Research*, **24**, 473–482.

Brehaut LD (2015) The Use of NDVI and Tree Ring-Widths to Evaluate Changes in Vegetation Production in a Mountainous Boreal Landscape. Master's Thesis, Queen's University, Kingston, ON, Canada, 2015.

Breiman L (2001) Random Forests. *Machince Learning*, **45**, 5–32.

Briffa K, Cook E (2008) What are the sources of uncertainty in the tree-ring data: how can they be quantified and represented? White Paper Presented as Part of Paleoclimatic Meeting on Proxy Uncertainties, Held in Trieste, Italy, June 9–11.

Briffa KR, Osborn TJ, Schweingruber FH, Jones PD, Shiyatov SG, Vaganov EA (2002) Tree-ring width and density data around the Northern Hemisphere: Part 1, local and regional climate signals. *The Holocene*, **12**, 737–757.

Bunn AG, Hughes MK, Kirdyanov AV et al. (2013) Comparing forest measurements from tree rings and a space-based index of vegetation activity in Siberia. *Environmental Research Letters*, **8**, 35034.

Camarero JJ, Franquesa M, Sangüesa-Barreda G (2015) Timing of Drought Triggers Distinct Growth Responses in Holm Oak: Implications to Predict Warming-Induced Forest Defoliation and Growth Decline. *Forests*, **6**, 1576–1597.

Ciais P, Reichstein M, Viovy N et al. (2005) Europe-wide reduction in primary productivity caused by the heat and drought in 2003. *Nature*, **437**, 529–533.

Clausen B, Pearson CP (1995) Regional frequency analysis of annual maximum streamflow drought. *Journal of Hydrology*, **173**, 111–130.

Cook ER, Peters K (1997) Calculating unbiased tree-ring indices for the study of climatic and environmental change. *The Holocene*, **7**, 361–370.

Cook ER, Meko DM, Stahle DW, Cleaveland MK (1999) Drought reconstructions for the continental United States. *Journal of Climate*, **12**, 1145–1163.

Čufar K, De Luis M, Eckstein D, Kajfež-Bogataj L (2008) Reconstructing dry and wet summers in SE Slovenia from oak tree-ring series. *International Journal of Biometeorology*, **52**, 607–615.

Dai A (2011) Drought under global warming: A review. *Wiley Interdisciplinary Reviews: Climate Change*, **2**, 45–65.

Dai A, Trenberth KE, Qian T (2004) A Global Dataset of Palmer Drought Severity Index for 1870 – 2002 : Relationship with Soil Moisture and Effects of Surface Warming. *Journal of Hydrometeorology*, **5**, 1117–1130.

Didan K (2015) MOD13Q1 MODIS/Terra Vegetation Indices 16-Day L3 Global 250m SIN Grid V006. NASA EOSDIS Land Processes DAAC. https://doi.org/10.5067/modis/mod13q1.006.

Dobbertin M (2005) Tree growth as indicator of tree vitality and of tree reaction to environmental stress: A review. *European Journal of Forest Research*, **124**, 319–333.

Dong T, Liu J, Shang J et al. (2016) Assessing the impact of climate variability on cropland productivity in the Canadian prairies using time series MODIS FAPAR. *Remote Sensing*, **8**, 1–18.

Dracup JA, Lee KS, Paulson Jr EG (1980) On the statistical characteristics of drought events. *Water Resources Research*, **16**, 289–296.

Duursma RA, Kolari P, Permki M et al. (2009) Contributions of climate, leaf area index and leaf physiology to variation in gross primary production of six coniferous forests across Europe: A model-based analysis. *Tree Physiology*, **29**, 621–639.

Elkin C, Gutiérrez AG, Leuzinger S, Manusch C, Temperli C, Rasche L, Bugmann H (2013) A 2 °C warmer world is not safe for ecosystem services in the European Alps. *Global Change Biology*, **19**, 1827–1840.

Erhardt TM (2017) Development of Vine Copula based Drought Indices and Model Evaluation under the Presence of Non-Stationarity. Doctoral Dissertation, Technische Universität München.

Erhardt TM, Czado C (2017) Standardized drought indices: A novel uni- and multivariate approach. *Journal of the Royal Statistical Society*: Series C (Applied Statistics). DOI:10.1111/rssc.12242. Accepted manuscript.

European Centre for Medium-Range Weather Forecasts (2014) ERA-20C Project (ECMWF Atmospheric Reanalysis of the 20th Century).

Farahmand A, AghaKouchak A (2015) A generalized framework for deriving nonparametric standardized drought indicators. *Advances in Water Resources*, **76**, 140–145.

FLUXCOM (2017) FLUXCOM Global Energy and Carbon Fluxes, Max Planck Institute for Biogeochemistry, Jena, Germany.

Friedrichs DA, Büntgen U, Frank DC, Esper J, Neuwirth B, Löffler J (2008) Complex climate controls on 20th century oak growth in Central-West Germany. *Tree Physiology*, **29**, 39–51.

References

Fritts HC (1976) Tree rings and climate. Academic Press, London, 567 pp.

Fritts HC, Blasing TJ, Hayden BP, Kutzbach JE (1971) Multivariate Techniques for Specifying Tree-Growth and Climate Relationships and for Reconstructing Anomalies in Paleoclimate. *Journal of Applied Meteorology*, **10**, 845–864.

Garnaud C, Sushama L, Arora VK (2014) The effect of driving climate data on the simulated terrestrial carbon pools and fluxes over North America. *International Journal of Climatology*, **34**, 1098–1110.

GRDC (2016) Global Runoff Data Centre-Dataset of river discharge time series. Koblenz, Germany.

Grissino-Mayer HD, Fritts HC (1997) The International Tree-Ring Data Bank: an enhanced global database serving the global scientific community. *The Holocene*, **7**, 235–238.

Guttman NB (1998) Comparing the Palmer Drought Index and the Standardized Precipitation Index. *Journal of the American Water Resources Association*, **34**, 113–121.

Hao Z, AghaKouchak A (2013) Multivariate Standardized Drought Index: A parametric multi-index model. *Advances in Water Resources*, **57**, 12–18.

Hao Z, AghaKouchak A (2014) A Nonparametric Multivariate Multi-Index Drought Monitoring Framework. *Journal of Hydrometeorology*, **15**, 89–101.

Harris I, Jones PD, Osborn TJ, Lister DH (2014) Updated high-resolution grids of monthly climatic observations - the CRU TS3.10 Dataset. *International Journal of Climatology*, **34**, 623–642.

Haslinger K, Koffler D, Schöner W, Laaga G (2014) Exploring the link between meteorological drought and streamflow: Effects of climate-catchment interaction. *Water Resources Research*, **50**, 2468–2487.

Hayes MJ, Alvord C, Lowrey J (2007) Drought Indices. *Intermountain West Climate Summary*, **3**, 2–6.

Hayes M, Svoboda M, Wall N, Widhalm M (2011) The Lincoln declaration on drought indices: Universal meteorological drought index recommended. *Bulletin of the American Meteorological Society*, **92**, 485–488.

Haylock MR, Hofstra N, Klein Tank AMG, Klok EJ, Jones PD, New M (2008) A European daily high-resolution gridded data set of surface temperature and precipitation for 1950-2006. *Journal of Geophysical Research Atmospheres*, **113**, D20119, doi:10.1029/2008JD010201.

Hisdal H, Tallaksen LM (2000) Drought event definition, Assessment of the Regional Impact of Droughts in Europe Technical Report No. 6, University of Oslo, Oslo, Norway.

Hofstra N, Haylock M, New M, Jones PD (2009) Testing E-OBS European high-resolution gridded data set of daily precipitation and surface temperature. *Journal of Geophysical Research Atmospheres*, **114**, 1–16.

IPCC (2000) Summary for policymakers. Special Report on Land Use, Land-Use Change, and Forestry. [Robert T. Watson, Ian R. Noble, Bert Bolin, N. H. Ravindranath, David J. Verardo and David J. Dokken (eds.)]. Cambridge University Press, UK, 375 pp.

IPCC (2007) Climate Change 2007: The Physical Science Basis. Contribution of Working Group I to the Fourth Assessment Report of the Intergovernmental Panel on Climate Change [Solomon, S., D. Qin, M. Manning, Z. Chen, M. Marquis, K.B. Averyt, M. Tignor and H.L. Miller (eds.)].Cambridge University Press, Cambridge, United Kingdom and New York, NY, USA, 996 pp.

IPCC (2012) Summary for Policymakers. Managing the Risks of Extreme Events and Disasters to Advance Climate Change Adaptation. A Special Report of Working Groups I and II of the Intergovernmental Panel on Climate Change (IPCC) [C.B. Field, V. Barros, T.F. Stocker, D. Qin, D.J. Dokken, K.L. Ebi, M.D. Mastrandrea, K.J. Mach, G-K. Plattner, S.K. Allen, M. Tignor, and P.M. Midgley (eds.)]. Cambridge, UK, and New York, NY, USA: Cambridge University Press, 3–21.

IPCC (2013) Summary for policymakers. Climate Change 2013: The Physical Science Basis. Contribution of Working Group I to the Fifth Assessment Report of the Intergovernmental Panel on Climate Change [Stocker, T.F., D. Qin, G.-K. Plattner, M. Tignor, S. K. Allen, J. Boschung, A. Nauels, Y. Xia, V. Bex and P.M. Midgley (eds.)] Cambridge University Press, Cambridge, UK and New York, NY, USA, 3–39.

de Jager AL, Vogt JV (2010) Development and demonstration of a structured hydrological feature coding system for Europe. *Hydrological Sciences Journal*, **55**, 661–675.

Jung M, Reichstein M, Schwalm CR et al. (2017) Compensatory water effects link yearly global land CO_2 sink changes to temperature. *Nature*, **541**, 516–520.

Kao SC, Govindaraju RS (2010) A copula-based joint deficit index for droughts. *Journal of Hydrology*, **380**, 121–134.

Kaufmann RK, D'Arrigo RD, Laskowski C, Myneni RB, Zhou L, Davi NK (2004) The effect of growing season and summer greenness on northern forests. *Geophysical Research Letters*, **31**, 3–6.

Kaufmann RK, D'Arrigo RD, Paletta LF, Tian HQ, Jolly WM, Myneni RB (2008) Identifying climatic controls on ring width: The timing of correlations between tree rings and NDVI. *Earth Interactions*, **12**, 1–14.

Kern A, Marjanović H, Barcza Z (2016) Evaluation of the Quality of NDVI3g Dataset against Collection 6 MODIS NDVI in Central Europe between 2000 and 2013. *Remote Sensing*, **8**, 1–30.

References

Keyantash J, Dracup JA (2002) The quantification of drought: An evaluation of drought indices. *Bulletin of the American Meteorological Society*, **83**, 1167–1180.

Kogan F, Adamenko T, Guo W (2013) Global and regional drought dynamics in the climate warming era. *Remote Sensing Letters*, **4**, 364–372.

Koirala S, Jung M, Reichstein M et al. (2017) Global distribution of groundwater-vegetation spatial covariation. *Geophysical Research Letters*, **44**, 4134–4142.

Kottek M, Grieser J, Beck C, Rudolf B, Rubel F (2006) World map of the Köppen-Geiger climate classification updated. *Meteorologische Zeitschrift*, **15**, 259–263.

Lamigueiro PO, Hijmans R (2016) meteoForecast. R package version 0.40. Available from http://oscarperpinan.github.io/rastervis/.

Van Lanen HAJ, Laaha G, Kingston DG et al. (2016) Hydrology needed to manage droughts: the 2015 European case. *Hydrological Processes*, **30**, 3097–3104.

Lasslop G, Reichstein M, Papale D et al. (2010) Separation of net ecosystem exchange into assimilation and respiration using a light response curve approach: Critical issues and global evaluation. *Global Change Biology*, **16**, 187–208.

Lebourgeois F, Rathgeber CBK, Ulrich E (2010) Sensitivity of French temperate coniferous forests to climate variability and extreme events (*Abies alba, Picea abies* and *Pinus sylvestris*). *Journal of Vegetation Science*, **21**, 364–376.

Legendre P, Legendre L (1998) Numerical ecology, Vol. 20. 870 pp.

Lévesque M (2013) Drought response of five conifers along an ecological gradient in Central Europe : A multiproxy dendroecological analysis. Doctoral Dissertation, ETH-Zürich.

Liang EY, Shao XM, He JC (2005) Relationships between tree growth and NDVI of grassland in the semi-arid grassland of north China. *International Journal of Remote Sensing*, **26**, 2901–2908.

Liu Y, Wu C, Peng D et al. (2016) Improved modeling of land surface phenology using MODIS land surface reflectance and temperature at evergreen needleleaf forests of central North America. *Remote Sensing of Environment,* **176**, 152–162.

Liaw A, Wiener M (2002) Classification and Regression by randomForest. *R news*, **2**, 18–22.

Van Loon AF, Laaha G (2015) Hydrological drought severity explained by climate and catchment characteristics. *Journal of Hydrology*, **526**, 3–14.

Lopatin E, Kolström T, Spiecker H (2006) Determination of forest growth trends in Komi Republic (northwestern Russia): Combination of tree-ring analysis and remote sensing data. *Boreal Environment Research,* **11**, 341–353.

Lorenzo-Lacruz J, Vicente-Serrano SM, López-Moreno JI, Beguería S, García-Ruiz JM, Cuadrat JM (2010) The impact of droughts and water management on various

hydrological systems in the headwaters of the Tagus River (central Spain). *Journal of Hydrology*, **386**, 13–26.

Luyssaert S, Inglima I, Jung M et al. (2007) CO2 balance of boreal, temperate, and tropical forests derived from a global database. *Global Change Biology*, **13**, 2509–2537.

Luyssaert S, Ciais P, Piao SL et al. (2010) The European carbon balance. Part 3: Forests. *Global Change Biology*, **16**, 1429–1450.

van der Maaten-Theunissen M, Kahle HP, Van Der Maaten E (2013) Drought sensitivity of Norway spruce is higher than that of silver fir along an altitudinal gradient in southwestern Germany. *Annals of Forest Science*, **70**, 185–193.

Machado-Machado EA, Neeti N, Eastman RJ, Chen H (2011) Implications of space-time orientation for Principal Components Analysis of Earth observation image time series. *Earth Science Informatics*, **4**, 117–124.

Mann ME, Gleick PH (2015) Climate change and California drought in the 21st century. *Proceedings of the National Academy of Sciences*, **112**, 3858–3859.

Martin-Benito D, Beeckman H, Cañellas I (2013) Influence of drought on tree rings and tracheid features of *Pinus nigra* and *Pinus sylvestris* in a mesic Mediterranean forest. *European Journal of Forest Research*, **132**, 33–45.

de Martonne E (1926) Une nouvelle fonction climatologique: L'indice d'aridité. *La Meteorologie*, 449-458.

Mavromatis T (2007) Drought index evaluation for assessing future wheat production in Greece. *International Journal of Climatology*, **27**, 911–924.

McEvoy DJ, Huntington JL, Abatzoglou JT, Edwards LM (2012) An evaluation of multiscalar drought indices in Nevada and Eastern California. *Earth Interactions*, **16**, 1–18.

Mckee TB, Doesken NJ, Kleist J (1993) The relationship of drought frequency and duration to time scales. *Water*, **179**, 17–22.

Menzel A, Fabian P (1999) Growing season extended in Europe. *Nature*, **397**, 659.

Menzel A, Sparks TH, Estrella N, Koch E, Aasa A et al. (2006) European phenological response to climate change matches the warming pattern. *Global Change Biology*, **12**, 1969–1976.

Mishra AK, Singh VP (2010) A review of drought concepts. *Journal of Hydrology*, **391**, 202–216.

Mishra AK, Singh VP (2011) Drought modeling - A review. *Journal of Hydrology*, **403**, 157–175.

Mohan S, Rangacharya NCV (1991) A modified method for drought identification. *Hydrological Sciences Journal*, **36**, 11–21.

References

Myneni RB, Keeling CD, Tucker CJ, Asrar G, Nemani RR (1997) Increased plant growth in the northern high latitudes from 1981 to 1991. *Nature*, **386**, 698–702.

Niinemets Ü, Valladares F (2006) Tolerance to shade, drought, and waterlogging of temperate northern hemisphere trees and shrubs. *Ecological Monographs*, **76**, 521–547.

Obasi GOP (1994) WMO's Role in the International Decade for Natural Disaster Reduction. *Bulletin of the American Meteorological Society*, **75**, 1655–1661.

Olivier A, Jose Julio RP, Vasileios K, Bontemps S, Defourny P, Van Bogaert E (2009) Global Land Cover Map for 2009 (GlobCover 2009). Available online: https://doi.pangaea.de/10.1594/PANGAEA.787668.

Orwig DA, Abrams MD (1997) Variation in radial growth responses to drought among species, site, and canopy strata. *Trees*, **11**, 474–484.

Palmer WC (1965) Meteorological drought. Research Paper No. 45. U.S. Dept of Commerce, 55.

Palmer WC (1968) Keeping track of crop moisture conditions, nationwide: The new Crop Moisture Index. *Weatherwise*, **21**, 156–161.

Pereira JS, Mateus JA, Aires LM et al. (2007) Effects of drought - altered seasonality and low rainfall - in net ecosystem carbon exchange of three contrasting Mediterranean ecosystems. *Biogeosciences Discussions*, **4**, 1703–1736.

Pettorelli N, Vik JO, Mysterud A, Gaillard JM, Tucker CJ, Stenseth NC (2005) Using the satellite-derived NDVI to assess ecological responses to environmental change. *Trends in Ecology and Evolution*, **20**, 503–510.

Pichler P, Oberhuber W (2007) Radial growth response of coniferous forest trees in an inner Alpine environment to heat-wave in 2003. *Forest Ecology and Management*, **242**, 688–699.

Pinzon JE, Tucker CJ (2014) A Non-Stationary 1981–2012 AVHRR NDVI3g Time Series. *Remote Sensing*, **6**, 6929–6960.

Pocernich M (2012) Verification Package : examples using weather forecasts. *Forecast*, 1–9.

Poli P, Hersbach H, Dee DP et al. (2016) ERA-20C: An atmospheric reanalysis of the twentieth century. *Journal of Climate*, **29**, 4083–4097.

Pretzsch H, Rötzer T, Matyssek R et al. (2014) Mixed Norway spruce (*Picea abies* [L.] Karst) and European beech (*Fagus sylvatica* [L.]) stands under drought: from reaction pattern to mechanism. *Trees, 28,* 1305 –1321.

Quiring SM, Papakryiakou TN (2003) An evaluation of agricultural drought indices for the Canadian prairies. *Agricultural and Forest Meteorology*, **118**, 49–62.

R Core Team (2017) R: A Language and Environment for Statistical Computing. R Foundation for Statistical Computing, Vienna Austria https://www.R-project.org/.

Rasmussen EM, Dickinson RE, Kutzbach JE, Cleaveland MK (1993) Climatology. *Handbook of Hydrology*, D. R. Maidment, Ed., McGraw-Hill, 2.1– 2.44.

Reichstein M, Falge E, Baldocchi D et al. (2005) On the separation of net ecosystem exchange into assimilation and ecosystem respiration: Review and improved algorithm. *Global Change Biology*, **11**, 1424–1439.

Schimel DS (1995) Terrestrial ecosystems and the carbon cycle. *Global Change Biology*, **1**, 77–91.

Schuster R, Oberhuber W (2013) Age-dependent climate–growth relationships and regeneration of *Picea abies* in a drought-prone mixed-coniferous forest in the Alps. *Canadian Journal of Forest Research*, **43**, 609–618.

Scian B, Donnari M (1997) Retrospective analysis of the palmer drought severity index in the semi-arid Pampas region, Argentina. *International Journal of Climatology*, **17**, 313–322.

Seftigen K (2014) Late Holocene spatiotemporal hydroclimatic variability over Fennoscandia inferred from tree-rings. Doctoral Dissertation, University of Gothenburg.

Sheffield J & Wood EF (2008) Global trends and variability in soil moisture and drought characteristics, 1950–2000, from observation-driven simulations of the terrestrial hydrologic cycle. *Journal of Climate*, **21**, 432–458.

Shukla S, Wood AW (2008) Use of a standardized runoff index for characterizing hydrologic drought. *Geophysical Research Letters*, **35**, 1–7.

Staudinger M, Stahl K, Seibert J (2014) A drought index accounting for snow. *Water Resources Research*, **50**, 7861–7872.

Strommen N, Krumpe P, Reid M, Steyaert L (1980) Early warning assessments of droughts used by the US agency for international development. *Climate and Risk*, 8–37.

Tallaksen LM (2000) Streamflow Drought Frequency Analysis. Vogt JV, Somma F (eds) Drought and Drought Mitigation in Europe. *Advances in Natural and Technological Hazards Research*, **14,** Springer, Dordrecht.

Tan C, Yang J, Li M (2015) Temporal-Spatial Variation of Drought Indicated by SPI and SPEI in Ningxia Hui Autonomous Region, China. *Atmosphere*, **6**, 1399–1421.

Tate EL, Gustard A (2000) Drought definition: a hydrological perspective (ed F.Somma JVV and). Kluwer Academic Publishers, Netherlands, 23-48.

References

Thabeet A, Vennetier M, Gadbin-Henry C, Denelle N, Roux M, Caraglio Y, Vila B (2009) Response of *Pinus sylvestris* L. to recent climatic events in the French Mediterranean region. *Trees*, **23**, 843–853.

Thornthwaite CW (1948) An approach toward a rational classification of climate. *Geographical Review*, **38**, 55–94.

Todisco F, Vergni L, Mannocchi F (2008) An evaluation of some drought indices in the monitoring and prediction of agricultural drought impact in central Italy. Santini A. (ed.), Lamaddalena N. (ed.), Severino G. (ed.), Palladino M. (ed.). Irrigation in Mediterranean agriculture: challenges and innovation for the next decades. *Bari: CIHEAM,* 203–211.

Tramontana G, Ichii K, Camps-Valls G, Tomelleri E, Papale D (2015) Uncertainty analysis of gross primary production upscaling using Random Forests, remote sensing and eddy covariance data. Remote Sensing of Environment, **168**, 360–373.

Tramontana G, Jung M, Schwalm CR et al. (2016) Predicting carbon dioxide and energy fluxes across global FLUXNET sites with regression algorithms. *Biogeosciences*, **13**, 4291–4313.

Tucker CJ (1979) Red and photographic infrared linear combinations for monitoring vegetation. *Remote Sensing of Environment*, **8**, 127–150.

United Nations Convention to Combat Drought and Desertification in Countries Experiencing Serious Droughts and/or Desertification, Particularly in Africa (1994) UN Secretariat General. Paris.

Vose JM, Clark JS, Luce CH, Patel-Weynand T (2015) Effects of drought on forests and rangelands in the United States: a comprehensive science synthesis. GTR WO-93b. *U.S. Dept of Agriculture General Technical Report*, **WO-93a**, 302.

Vicca S, Balzarolo M, Filella I et al. (2016) Remotely-sensed detection of effects of extreme droughts on gross primary production. *Scientific Reports*, **6**, 1–13.

Vicente-Serrano SM, Beguería S, López-Moreno JI (2010) A multiscalar drought index sensitive to global warming: The standardized precipitation evapotranspiration index. *Journal of Climate*, **23**, 1696–1718.

Vicente-Serrano SM, Beguería S, Lorenzo-Lacruz J et al. (2012) Performance of drought indices for ecological, agricultural, and hydrological applications. *Earth Interactions*, **16**, 1–27.

Vicente-Serrano SM, Camarero JJ, Azorin-Molina C (2014) Diverse responses of forest growth to drought time-scales in the Northern Hemisphere. *Global Ecology and Biogeography*, **23**, 1019–1030.

Vicente-Serrano SM, Camarero JJ, Olano JM et al. (2016) Diverse relationships between forest growth and the Normalized Difference Vegetation Index at a global scale. *Remote Sensing of Environment*, **187**, 14–29.

Wells N, Goddard S, Hayes MJ (2004) A self-calibrating Palmer Drought Severity Index. *Journal of Climate*, **17**, 2335–2351.

Wickham H (2009) ggplot2: elegant graphics for data analysis. Springer New York.

Wilhite DA, Glantz MH (1985) Understanding: the Drought Phenomenon: The Role of Definitions. *Water International*, **10**, 111–120.

Williams AP, Michaelsen J, Leavitt SW, Still CJ (2010) Using Tree Rings to Predict the Response of Tree Growth to Climate Change in the Continental United States during the Twenty-First Century. *Earth Interactions*, **14**, 1–20.

Wilmking M, D'Arrigo R, Jacoby GC, Juday GP (2005) Increased temperature sensitivity and divergent growth trends in circumpolar boreal forests. *Geophysical Research Letters*, **32**, 2–5.

WWRP/WGNE Joint Working Group on Forecast Verification Research (2015) WWRP/WGNE Joint Working Group on Forecast Verification Research.

Zang C (2010) Growth reaction of temperate forest trees to summer drought - a multispecies tree-ring network approach. Doctoral Dissertation, Technische Universität München.

Zang C, Biondi F (2013) Dendroclimatic calibration in R: The bootRes package for response and correlation function analysis. *Dendrochronologia*, **31**, 68–74.

Zang C, Rothe A, Weis W, Pretzsch H (2011) Zur Baumarteneignung bei Klimawandel: Ableitung der Trockenstress-Anfälligkeit wichtiger Waldbaumarten aus Jahrringbreiten. *Allgemeine Forst- und Jagdzeitung,* **182**, 98–112.

Zang C, Hartl-Meier C, Dittmar C, Rothe A, Menzel A (2014) Patterns of drought tolerance in major European temperate forest trees: Climatic drivers and levels of variability. *Global Change Biology*, **20**, 3767–3779.

Zargar A, Sadiq R, Naser B, Khan FI (2011) A review of drought indices. *Environmental Reviews*, **19**, 333–349.

Zhai J, Su B, Krysanova V, Vetter T, Gao C, Jiang T (2010) Spatial variation and trends in PDSI and SPI indices and their relation to streamflow in 10 large regions of china. *Journal of Climate*, **23**, 649–663.

Zhao H, Gao G, An W, Zou X, Li H, Hou M (2015) Timescale differences between SC-PDSI and SPEI for drought monitoring in China. *Physics and Chemistry of the Earth, Parts A/B/C*, http://dx.doi.org/10.1016/j.pce.2015.10.022, in press.

Zhao Y, Ciais P, Peylin P et al. (2012) How errors on meteorological variables impact simulated ecosystem fluxes: A case study for six French sites. *Biogeosciences*, **9**, 2537–2564.

10. List of tables and figures

11. Acknowledgements

From the inception of my journey as a doctoral researcher, many people have guided and supported me.

Last but not the least, I would also like to acknowledge the immense love and support of my parents and my very loving husband, for always supporting and believing in me.

12. Appendix

12.1 Academic CV

Upasana Priyambada Bhuyan-Erhardt

* 1. September 1987 in Assam, India

Hollerner Straße 3

85386 Eching

Tel.: +49 176 71964880

E-Mail: upasanabhuyan@gmail.com

Scientific Career

	Research associate
12/2013-–10/2017	Department of Ecoclimatology Technical University of Munich (TUM), Germany
	Interdisciplinary project on drought modeling
	Two research stays of six weeks each: Instituto Pirenaico de Ecología, Zaragoza, Spain Institute of Hydrology and Water Resource Management, TU Wien, Austria

Education

	PhD Candidate
Since 12/2013	Department of Ecoclimatology Technical University of Munich (TUM), Germany International Graduate School of Science and Engineering (IGSSE) PhD thesis on Drought quantification by multivariate indices and their validation against various environmental data
	Master's in Environmental Science
10/2010 –12/2012	University of Cologne, Germany Master's thesis in the area of Environmental Management Degree: Master of Science (M.Sc.) with overall score 1.8
	Bachelor's in Electronics and Communication Engineering
06/2006 –06/2010	Sikkim Manipal Institute of Technology, Sikkim, India Bachelor's thesis on image processing using MATLAB Degree: Bachelor of Technology (B.Tech.) with overall score 7.7 (out of 10)

Publications

2017	Bhuyan-Erhardt, Upasana, Erhardt, Tobias Michael, Laaha, Gregor, Zang, Christian, Parajka, Juraj, Menzel, Annette. 2017. "Validation of drought indices using environmental indicators: streamflow and carbon flux data." In review at Science of the Total Environment.*
2017	Bhuyan, Upasana, Christian Zang, and Annette Menzel. 2017. "Different Responses of Multispecies Tree Ring Growth to Various Drought Indices across Europe." Dendrochronologia 44. Elsevier GmbH: 1–8. doi:10.1016/j.dendro.2017.02.002. *
2017	Bhuyan, Upasana, Christian Zang, Sergio M. Vicente-Serrano, and Annette Menzel. 2017. "Exploring Relationships among Tree-Ring Growth, Climate Variability, and Seasonal Leaf Activity on Varying Timescales and Spatial Resolutions." Remote Sensing 9 (6). doi:10.3390/rs9060526.*
2017	Sánchez-Salguero, Raúl, Andrea Hevia, J. Julio Camarero, Kerstin Treydte, Dave Frank, Alan Crivellaro, Marta Domínguez-Delmás, et al. 2017. "An Intensive Tree-Ring Experience: Connecting Education and Research during the 25th European Dendroecological Fieldweek (Asturias, Spain)." Dendrochronologia 42: 80–93. doi:10.1016/j.dendro.2016.12.005.
2016	Vicente-Serrano, Sergio M., J. Julio Camarero, José M. Olano, Natalia Martín-Hernández, Marina Peña-Gallardo, Miquel Tomás-Burguera, Antonio Gazol, Cesar Azorin-Molina, Upasana Bhuyan, and Ahmed El Kenawy. 2016. "Diverse Relationships between Forest Growth and the Normalized Difference Vegetation Index at a Global Scale." Remote Sensing of Environment 187. Elsevier Inc.: 14–29. doi:10.1016/j.rse.2016.10.001.
	(Publications marked with *, are part of this thesis)

Research stays abroad

2016	Institute of Hydrology and Water Resource Management, Technische Universität Wien, Karlsplatz 13/222, A-1040 Wien. Host: Dr. Günter Blöschl (6 weeks stay)
2015	Instituto Pirenaico de Ecología, Consejo Superior de Investigaciones Científicas (IPE–CSIC), Zaragoza 50059. Spain. Host: Dr. Sergio M. Vicente-Serrano (6 weeks stay)

Scientific workshops

2015	Advanced strategies for ecological data analysis, Freising, Germany.
2015	The Stats Doctor is in the House. Summer Semester, Freising, Germany.
2015	Remediating the Human Water Footprint. Institute of Advanced Studies, Garching, Germany.
2014	Spatial Copula workshop, Münster Germany.
2014	Using R for Statistical Data Analysis I & II, Garching, Germany.

| 2014 | European Dendrological Fieldweek in Oviedo, Spain. |

Conference and symposium

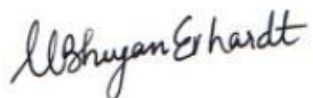| 2016 | Upasana Bhuyan, Claudia Czado, Tobias Erhardt, Michael Matiu, Annette Menzel, Christian Zang: Drought modeling and monitoring by novel statistical and analytical methods. International Graduate School of Science and Engineering (IGSSE), Focus Area Water Midterm Meeting. Weihenstephan/Munich) |
| 2014, 2015, 2016 | Upasana Bhuyan, Claudia Czado, Tobias Erhardt, Michael Matiu, Annette Menzel, Christian Zang: Drought modeling and monitoring by novel statistical and analytical methods. IGSSE Annual Forum and Workshops. Raitenhaslach, Germany. |
| 2014 | Upasana Bhuyan, Christian Zang and Annette Menzel (2014): Drought Metrics and tree growth: matches, mismatches, and some implications for modelling continental-scale drought. Eurodendro. Lugo, Spain. |

Software skills

Statistics software R	advanced
SPSS	basic
GIS	basic
C	basic
MATLAB	basic
Linux	basic
Windows	advanced
Microsoft Office	advanced

Language skills

Assamese	mother tongue
Hindi	fluent
English	fluent
German	basic

Eching, November 6th, 2017

12.2   Publication reprints

The next pages show reprints of the publications used in this thesis (see Section 4).

No restrictions to reprint apply, since:

(i) The publisher (Elsevier) grants access to use in dissertations, without further permission seeking. Refer to subpoint "Can I include/use my article in my thesis/ dissertation?" under https://www.elsevier.com/about/our-business/policies/copyright/permissions and author user rights under https://www.elsevier.com/__data/assets/pdf_file/0007/55654/AuthorUserRights.pdf (accessed on 1st Nov 2017).

(ii) Open access

(iii) Same as (i)

Different responses of multispecies tree ring growth to various drought indices across Europe

Upasana Bhuyan [a,*], Christian Zang [b], Annette Menzel [a,c]

[a] *Ecoclimatology, Department of Ecology and Ecosystem Management, Technische Universität München, Hans-Carl-von-Carlowitz-Platz 2, 85354 Freising, Germany*
[b] *Land Surface-Atmosphere Interactions, Department of Ecology and Ecosystem Management, Technische Universität München, Hans-Carl-von-Carlowitz-Platz 2, 85354 Freising, Germany*
[c] *Institute for Advanced Study, Technische Universität München, Lichtenbergstr 2a, 85748 Garching, Germany*

ARTICLE INFO

ABSTRACT

Increasing frequency and intensity of drought extremes associated with global change are a key challenge for forest ecosystems. Consequently, the quantification of drought effects on tree growth as a measure of vitality is of highest concern from the perspectives of both science and management. To date, a multitude of drought indices have been used to accompany or replace primary climatic variables in the analysis of drought-related growth responses. However, it remains unclear how individual drought metrics compare to each other in terms of their ability to capture drought signals in tree growth.

In our study, we employ a European multispecies tree ring network at the continental scale and a set of four commonly used drought indices (De Martonne Aridity Index, self-calibrating Palmer Drought Severity Index, Standardized Precipitation Index and Standardized Precipitation Evapotranspiration Index, the latter two on varying temporal scales) to derive species-specific growth responses to drought conditions. For nine common European tree species, we demonstrate spatio-temporal matches and mismatches of tree growth with drought indices subject to species, elevation and bioclimatic zone. Forests located in the temperate and Mediterranean climate were drought sensitive and tended to respond to short- and intermediate-term drought (<1 year). In continental climates, forests were comparably more drought resistant and responded to long-term drought. For the same species, stands were less drought sensitive at higher elevations compared to lower elevations. We provide detailed information on the month-wise performance of the four drought indices in different climate zones allowing users the selection of the most appropriate index according to their objective criteria. Our results show that species-specific differences in responses to multiple stressors result in complex, yet coherent patterns of tree growth.

1. Introduction

Droughts are complex multi-dimensional climatic phenomena with detrimental effects on social and natural systems (Wilhite and Glantz, 1985; Obasi, 1994; Mishra and Singh, 2010). The impacts of drought have been aggravated in the recent years by the increasing rise in water demand due to global climate change, the latter being signified by the increase in mean global air temperature by 0.85 °C during the period 1880–2012 (IPCC, 2013).

The frequency and their duration is likely to increase by factors of two and six, respectively, due to anthropogenic climate change (Kogan et al., 2013). Important natural systems challenged by this

intensification of (especially summer) drought events are forest ecosystems (Bolte et al., 2009). Forests are characterized by large carbon stocks and flows, both sensitive to climatic extremes, most importantly drought, resulting in large (and potentially lagged, Anderegg et al., 2015) effects on the carbon cycle (Frank et al., 2015). The impairment of tree vitality by drought is therefore one of the key processes controlling drought impact on forests. Tree species differ across biomes, rendering the comprehensive characterization of drought response of individual species a pivotal component of understanding drought impact on forest ecosystems (Bolte et al., 2009; Luyssaert et al., 2010; Zang et al., 2014).

Tree ring width or annual radial growth increment is a widely used proxy for tree vitality (Fritts et al., 1971; Dobbertin, 2005) and its connection to climate and extreme climatic events, such as drought. The high abundance of tree ring data allows tree growth and drought variability to be studied on local to continental scales.

Yet, the study of forest vulnerability to climatic extremes, particularly drought events, is complicated by macroclimatic, structural, and compositional differences of forest sites at continental scales (Vicente-Serrano et al., 2014; Gazol et al., 2016). These differences explain the difficulty to find generalized descriptors of drought that match the temporal resolution of processes at the scale of individual forests. A typical example for a commonly used drought index that does not allow for varying temporal resolutions is the Palmer Drought Severity Index, PDSI (Dai et al., 2004). Since site-specific macroclimatic and species-specific physiological response characteristics mediate the differential drought response at the level of sites (Babst et al., 2013) and individual trees (Dittmar et al., 2012; Zang et al., 2014), the PDSI and other drought metrics with fixed time scales are not able to capture the ecologically meaningful temporal offset between onset of drought conditions and growth response of forests (Vicente-Serrano et al., 2012).

Acknowledging this shortcoming of traditional drought metrics, Vicente-Serrano et al. (2010) proposed the Standardized Potential Evapotranspiration Index SPEI as a novel drought index. It is available for varying time scales like the older Standardized Precipitation Index, SPI (Mckee et al., 1993), but in contrast to the SPI it incorporates the effect of temperature. Vicente-Serrano et al. (2012) provided a global assessment of the performance of different drought indices including the ones discussed in the paper for monitoring drought impacts on streamflows, soil moisture, forest growth, and crop yields. The study detected small differences in the comparative performance of the SPI and the SPEI indices, but SPEI best captured the responses of hydrological, agricultural and ecological variables. It has been recommended for use when the responses of the variables of interest to drought are not known. On the other hand PDSI has been widely used for decades particularly in the United States, and also in climate change analyses (Seneviratne et al., 2012). In a hemispherical assessment of drought response of forests using tree ring data, Vicente-Serrano et al. (2014) identified characteristic differences in response time, with a clear gradient in drought response in the northern hemisphere: response to long-term drought conditions in xeric environments, and a response to increasingly shorter time scales of drought with increasingly humid conditions. This pattern confirmed earlier findings based on multiple data streams for vegetation activity on large scales (Maherali and Pockman, 2004; Vicente-Serrano et al., 2012) and tree ring parameters for small scale intensive case studies (Lévesque et al., 2013). However, many recent tree ring studies employ drought indices other than SPEI (Babst et al., 2013; Hogg et al., 2013; Zang et al., 2014). Moreover, the hemispherical approach of Vicente-Serrano et al. (2014) is focused on SPEI solely. Consequently, a direct comparison of potentially macroclimatic and species-specific differences in response to different commonly used drought indices and their varying temporal aggregation is currently not available.

In this study, we use a large data set of tree ring widths (Babst et al., 2013) to assess the connection between drought and tree growth and to provide a continental assessment of the performance of commonly used drought indices for quantifying drought impacts on forest growth. This is achieved through the study of drought impact on the radial growth of nine tree species as a function of elevation and bioclimatic zone. For this purpose, we compare tree growth with four of the most widely used drought indices – SPI (Mckee et al., 1993), self-calibrating Palmer Drought Severity Index, scPDSI (Palmer, 1965; Wells et al., 2004), SPEI (Vicente-Serrano et al., 2010) and De Martonne Aridity Index, DMI (de Martonne, 1926). For the SPI and SPEI time scales from 1 to 36 months have been applied. Considering the different vulnerabilities of different tree species to drought and a lack of appropriate descriptors of drought, the study aims to assess the connection between existing drought indices and the response of different tree species to a drought event. With our study we try to answer which indices best represent drought impacts for the species studied.

2. Material and methods

2.1. Tree ring data

The tree ring network used in this study is a compilation of published tree ring chronologies by Babst et al. (2013) which consists of 992 sites covering most of Europe and North Africa (30–70° N/10° W–40° E) (including information on elevation). A 32 year spline with 50% frequency cutoff response was used to remove the biological trend present in the original raw tree ring width time series while preserving the inter-annual to decadal variability at the same time. The resulting detrended series were power-transformed to remove temporal heteroscedasticity and then robustly averaged to site-wise dimensionless chronologies of ring width indices (RWI). Optimizing the trade-off between series length and replication, we selected RWI series with 56 years of data for the common period 1920–1975. When considering the nine most common species of the network and allowing a maximum period of overlap between climate data and RWI, a total of 850 sites were retained for the final analysis of the study. The following nine species were investigated for their drought vulnerability, namely *Abies alba* Mill. (ABAL, silver fir), *Fagus sylvatica* L. (FASY, European beech), *Larix decidua* Mill. (LADE, European larch), *Picea abies* (L.) Karst. (PCAB, Norway spruce), *Pinus cembra* L. (PICE, stone pine), *Pinus nigra* Arn. (PINI, black pine), *Pinus sylvestris* L. (PISY, Scots pine), *Quercus petraea* (Matt.) Liebl. (QUPE, sessile oak) and *Quercus robur* L. (QURO, common oak). All species' abbreviations are used subsequently in the figures and tables.

2.2. Climate data

We used mean temperature (TMP), precipitation sum (PRE), and potential evapotranspiration (PET) monthly datasets from the observational CRU TS 3.21 worldwide dataset available on a 0.5° grid (Harris et al., 2014; http://badc.nerc.ac.uk/). Data on climate classification was obtained from the world Köppen-Geiger climate classification map (Kottek et al., 2006). The climate classification data is based on recent data sets from the CRU and the Global Precipitation Climatology Centre (GPCC) at the German Meteorological Service. In the study, climate zone Cf, Cs and D denote temperate climate without dry season, temperate climate with dry summer (Mediterranean) and continental climate respectively. Taking into account the uncertainties involved with spatially coarse and interpolated gridded data, we have validated the results of the study using station data from E-OBS (Haylock et al., 2008). The details of the analysis can be found in Appendix B in Supplementary material.

2.3. Drought indices

The drought indices SPI and SPEI were calculated using the R package SPEI (Vicente-Serrano et al., 2010) for time scales of 1, 6, 12, 24 and 36 months based on input data from CRU. The DMI was also calculated using PRE and TMP data from CRU. The scPDSI, which is based on climatic data from the CRU, was downloaded from the KNMI Climate Explorer web page (available at http://climexp.knmi.nl/). The DMI is a measure of aridity obtained by calculating mean precipitation (in mm)/(temperature (in °C) + 10). It is subject to criticism because of its empirical nature but nevertheless provides information on the drought level at a given site. SPI is based on long-term precipitation records that are computed on different time scales. To calculate the SPI, precipitation data is converted to probabilities which are then transformed to standardized series
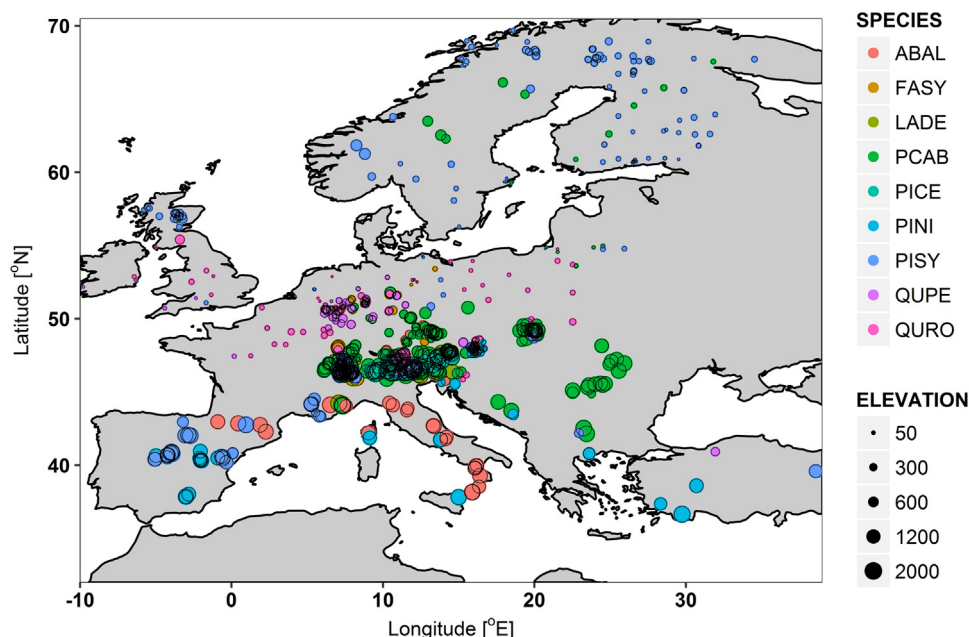
Fig. 1. Spatial distribution of the 850 tree ring sites and their elevation (m a.s.l) across Europe. ABAL silver fir, FASY European beech, LADE European larch, PCAB Norway spruce, PICE stone pine, PINI black pine, PISY Scots pine, QUPE sessile oak, and QURO common oak.

with an average of 0 and a standard deviation of 1. A key limitation of the SPI is its inability to capture the effect of increased temperatures on moisture demand (Mckee et al., 1993). The SPEI is an extension of the SPI; it combines the multi-timescales aspects of the SPI with information about evapotranspiration, making it more reliable for climate change studies. A limitation of the SPEI is its sensitivity to the method of calculating potential evapotranspiration (PET) (Vicente-Serrano et al., 2010). The scPDSI is based on the supply and demand concepts of the water balance equation. It is calculated based on precipitation and temperature data, as well as on the water content of the soil. Its disadvantages include non-comparability across regions and missing multi-timescale features (Dai et al., 2004; Wells et al., 2004).

2.4. Statistical analyses

To assess the species-specific growth-drought relationships, correlation function analyses (Fritts et al., 1971) were calculated between RWI and the selected four drought indices: SPI/SPEI (time scale = 1, 6, 12, 24, 36 months), DMI and scPDSI for the period of 1920–1975. Since the different time scales of the indices already captured the effect of previous year conditions, the correlation coefficients were calculated only for the year of ring formation (March to September). These correlations were then introduced into a principal component analysis (PCA). The first few components encompass the bulk of the variability in the original variables enabling it to identify and summarize the spatial and temporal variability across the study area (Seftigen, 2014). A 'Q' mode PCA was used since we aimed to find persistent drought patterns in space (Machado-Machado et al., 2011). An equilibrium circle of descriptors, with radius $\sqrt{\frac{d}{p}}$ (with p total and d reduced dimension in ordination), was drawn as reference to assess the contribution of each descriptor to the formation of the reduced space (Legendre and Legendre, 1998). This aids to identify meaningful scores and loadings in reduced space (Legendre and Legendre, 1998). R package *bootRes* (Zang and Biondi, 2013) was used for calculating bootstrapped correlations between RWI and drought indices; and package *ggplot2* was used for visualizations (Wickham, 2009). All

statistical procedures were performed using R 3.2.0 (R Core Team, 2015).

2.5. Modelling tree growth by drought indices

We used linear models to predict tree growth at each site by monthly drought indices from March to September. For these linear models, we divided the dataset into training and test datasets, with the earlier years of the RWI time series for testing (1920–1947) and the most recent years for training the model (1948–1975). Using external validation, i.e. the test dataset, the performance of these models was quantified by the normalized root-mean-square deviation (NRMSE). Since our dataset is based on tree ring sites with different species in different elevations and climate zones, we chose to standardize all estimates of the root mean square error (RMSE) and to relate the RMSE to the observed range of the variables.

3. Results

3.1. Tree growth – drought relationship: summarizing growth response to drought

The spatial distribution and elevation of the sites of nine species analyzed in the study can be seen in Fig. 1. The tree-growth responses to the drought indices DMI, scPDSI, SPI/SPEI (time scale = 1, 6, 12, 24, 36 months) was summarized by conducting a PCA on the correlation matrix and by analyzing the first two principal components (PCs). These components accounted for 75% of the variance, showing which drought indices were more influential in terms of tree response to drought given as variables outside the equilibrium circle (Fig. 2). The behavior of SPEI (Appendix A, Fig. 1 in Supplementary material) was similar to SPI (Fig. 2), hence not displayed in Fig. 2 to foster readability. The ordination of the first two components resulted in a nearly complete separation of short- and intermediate-term drought from long-term drought effects. Based on the PC1, the major modes of tree growth responses to the different drought indices for the months of March to September can be seen in Fig. 3. The drought indices SPI and SPEI at higher time scales of 24 and 36 months revealed maximum absolute loadings to PC1,
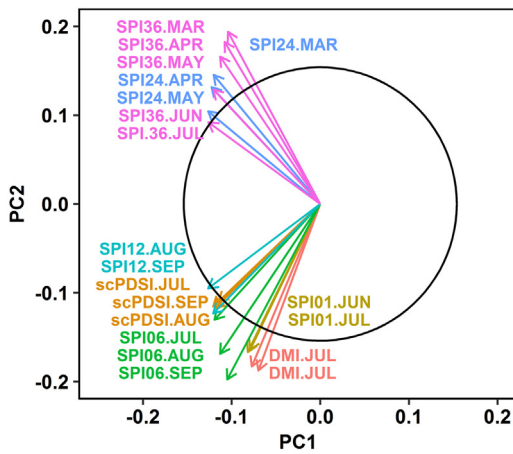
Fig. 2. Equilibrium circle and selected drought indices of the PCA. The PCA performed on the correlation coefficients calculated between 850 RWI series and the monthly scPDSI, DMI, SPI/SPEI (time scales = 1, 6, 12, 24, 36) for the period of 1920–1975. DMI, PDSI and SPI stand for De Martonne Aridity Index, self-calibrating Palmer Drought Severity Index and Standardized Precipitation Index (see text).

thus showing maximum correlations with RWI whereas DMI, SPI, and SPEI (time scale = 1) had the lowest. The behavior of scPDSI was comparable to SPI and SPEI at higher time scales (6–12).

3.2. Species-specific variation with elevation and bioclimatic zone

The PCA score plots for different species grouped by climate zone and elevation can be seen in Fig. 4. Species-specific differences were revealed in the score plots along the bioclimatic and elevation gradient and in their responses to drought duration: short- to intermediate-term drought: DMI, scPDSI, SPI/SPEI (time scale = 1, 6, 12) and long-term drought SPI/SPEI (time scale = 24, 36). The score plot was interpreted with the aid of the behavior of the variables in Fig. 2 where it was observed that species were drought sensitive in case of PC1 < 0. In case of PC1 < 0 and PC2 < 0, species were responsive to short- and intermediate-term drought. Similarly, in case of PC1 < 0 and PC2 > 0, species were responsive to long-term drought.

However, it was noted that all species responded to drought, albeit to varying degrees (Fig. 4).

For silver fir and European beech, the majority of the stands were drought sensitive and silver fir was predominantly influenced by long-term drought in all climate zones. European beech was both affected by short- and long-term drought with its high elevation sites being more responsive to long-term drought. In climate zone D, their high elevation sites showed more drought resistance compared to its stands in climate zone Cf.

European larch was affected by both short- and long-term drought with the high elevation sites showing greater drought resistance compared to lower elevation stands specifically in the climate zone Cf. Most stands of Norway spruce were drought sensitive with a majority being affected by long-term drought with similar response for both climate zones Cf and D. Stone pine was least affected by drought, if at all then by long-term drought whereas Scots pine and black pine were majorly affected by short-term drought. In climate zone Cs, for both pine species, the high elevation stands were less drought sensitive. The two *Quercus* species, sessile and common oak, were predominantly influenced by short-term drought. Common oak stands in climate zone D and at high elevation responded to long-term drought compared to the stands in low elevations. The effect of elevation was seen clearly in the case of several species where high elevation sites showed greater drought resistance compared to stands at lower elevation in the same climate zone. We also observed a clear effect of bioclimatic zonation in the species' response to drought: Stands which experienced continental climates (D) were more responsive to long-term drought whereas stands that experienced temperate (Cf) and Mediterranean (Cs) climates were more responsive to short-term drought (Fig. 4). Hence, the sites with more sensitive stands were seen to have a relatively warmer climate (Cf, Cs) compared to the sites with less drought sensitive stands.

3.3. Summarizing the performance of drought indices

The month-wise mean Pearson correlation coefficients for all drought indices were grouped into species and climate zones (Fig. 5). All groups with N < 10 were omitted and thus are displayed
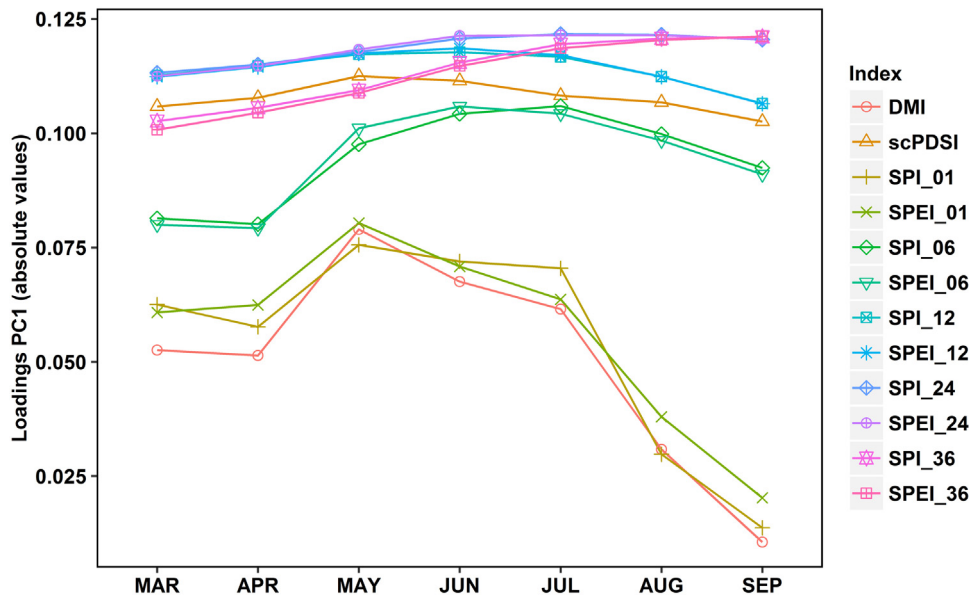

Fig. 3. Major modes of tree growth responses to 12 drought indices for the current year growing season based on the first principal component (PC1). PCA was performed on the correlation coefficients calculated between 850 RWI series and the monthly scPDSI, DMI, SPI/SPEI (time scales = 1, 6, 12, 24, 36) for the period of 1920–1975. DMI, scPDSI, SPI and SPEI stand for De Martonne Aridity Index, self-calibrating Palmer Drought Severity Index, Standardized Precipitation Index and Standardized Potential Evapotranspiration Index.
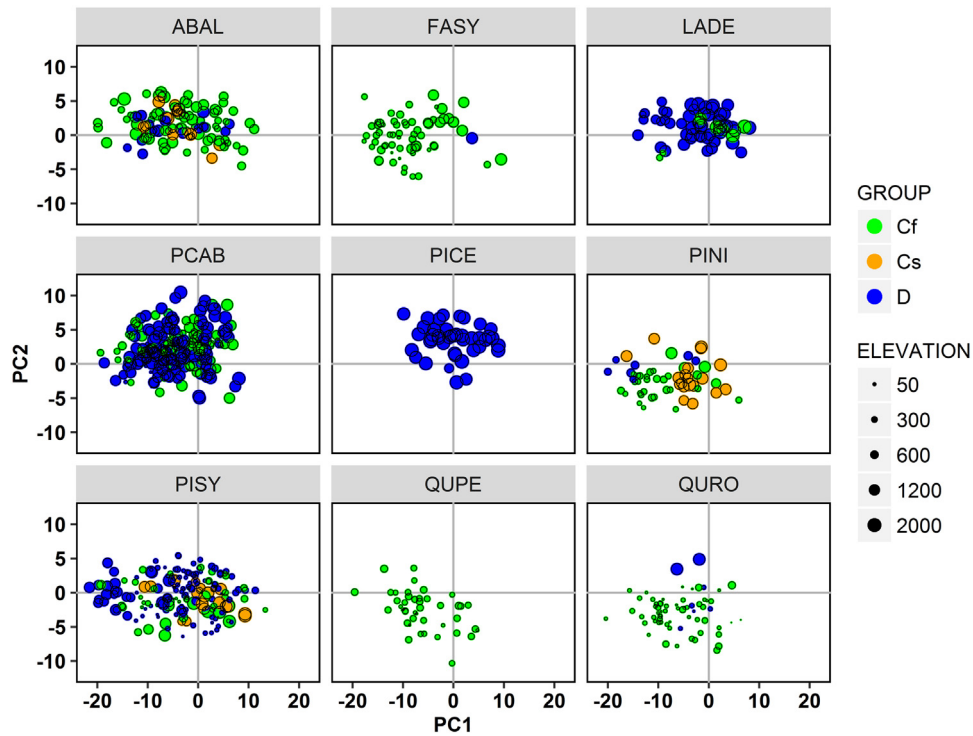
Fig. 4. PCA score plot for the nine studied species indicating climate zone (Cf, Cs, D) and elevation (m a.s.l). PCA was performed on the correlation coefficients calculated between 850 RWI series and the monthly scPDSI, DMI, SPI/SPEI (time scales = 1, 6, 12, 24, 36) for 1920–1975. DMI, scPDSI, SPI and SPEI stand for De Martonne Aridity Index, self-calibrating Palmer Drought Severity Index, Standardized Precipitation Index and Standardized Potential Evapotranspiration Index. The species analyzed are ABAL silver fir, FASY European beech, LADE European larch, PCAB Norway spruce, PICE stone pine, PINI black pine, PISY Scots pine, QUPE sessile oak, and QURO common oak. Cf, Cs and D denote temperate climate without dry season, temperate climate with dry summer (Mediterranean) and continental climate respectively as per Köppen climate classification.
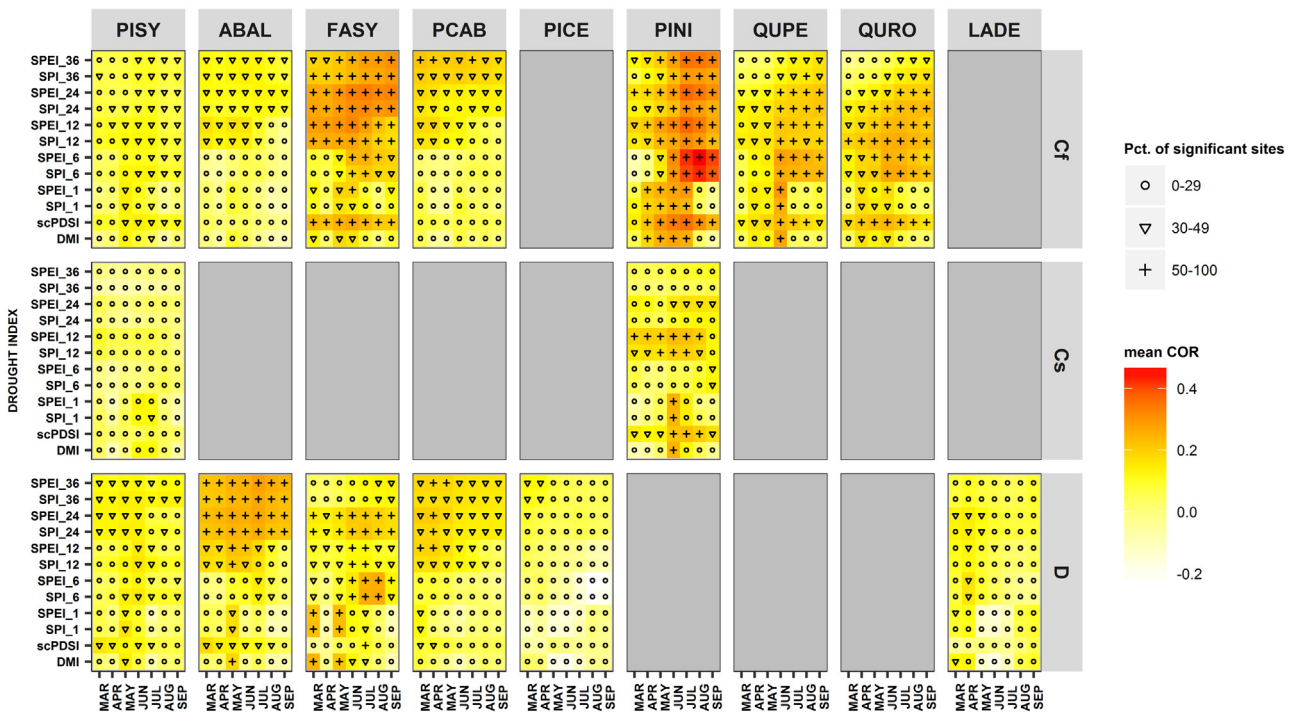

Fig. 5. Month-wise averaged Pearson correlation coefficients of different drought indices with RWI for the nine species studied in different climate zones calculated for the period of 1920–1975. The different symbols indicate the percentage of sites that were significant at the 0.05 level for each averaged correlation value. DMI, scPDSI, SPI and SPEI denote De Martonne Aridity Index, self-calibrating Palmer Drought Severity Index, Standardized Precipitation Index and Standardized Potential Evapotranspiration Index. Groups with N < 10 were omitted. The species analyzed are ABAL silver fir, FASY European beech, LADE European larch, PCAB Norway spruce, PICE stone pine, PINI black pine, PISY Scots pine, QUPE sessile oak, and QURO common oak. Cf, Cs and D denote temperate climate without dry season, temperate climate with dry summer (Mediterranean) and continental climate respectively as per Köppen climate classification.

in grey in the figure. When comparing all species, the conifers Scots pine in all climate zones as well as European larch and stone pine in climate zone D were relatively drought resistant as could be seen from their low mean correlation coefficients, consistent across indices and time scales. Stands of silver fir in climate zone Cf were less drought sensitive compared to stands in climate zone D. The indices SPEI and SPI at higher time scales best captured its drought signals in climate zone D. European beech in climate zone Cf and D was sensitive to both short- and long-term drought. In climate zone Cf, scPDSI, SPI and SPEI best captured its drought signals mostly at intermediate to longer time scales from March to September. DMI, SPI, and SPEI at shorter time scales best captured its drought signals in climate zone D. Norway spruce in climate zone Cf was best represented by long-term drought indices SPI and SPEI from March to September, whereas in climate zone D short-term drought during early growing season months (March to May) mattered. Black pine in climate zone Cf was seen to be very drought sensitive to all indices capturing the drought signals during the main summer months; however SPI and SPEI at intermediate time scales were best. In the Mediterranean climate zone Cs, drought impacts in black pine were best described by all indices during short- and intermediate-term drought. *Quercus* species in climate zone Cf were drought sensitive. Drought indices of the scale of 1 up to 12 months mostly during the growing season (June onwards) best represented growth responses of these species.

The predictive capability of the developed models in terms of NRMSE mostly reflects the long-term correlation of tree-ring growth and drought indices (Appendix A, Fig. 2 in Supplementary material), and higher long-term correlation is connected to better predictive power. There is, however, only small variation in NRMSE across individual models and groups.

4. Discussion

This study is a first step towards an increased and improved understanding of drought variability of nine tree species across Europe, including sites where climate station data is not available. It confirms that tree response to drought can vary significantly along large ecological gradients (see e.g. Pasho et al., 2012). The need to use a wider set of parameters to estimate the current and future response of trees to climate extremes is well known. This is particularly true for the continental scale, where very few studies have investigated and compared the drought tolerance of co-occurring species along wide ecological gradients using several drought metrics.

In our study we focused on various drought indices to test the impact of water availability on tree growth: e.g., scPDSI takes into account soil moisture (Wells et al., 2004) and site-specific water balance (Stephenson, 1990), whereas SPEI includes evaporative demand. We observed that the behavior of scPDSI was similar to SPI and SPEI at longer time scales (up to 12 months). This could be explained by the fact that scPDSI is a direct metric of moisture conditions taking both temperature and precipitation into account for the specific and the preceding months (Palmer, 1965; Dai et al., 2004). We found that scPDSI, SPI, and SPEI at longer time scales had the strongest correlations with RWI (Fig. 3). Similar results by Vicente-Serrano et al. (2012) indicated closer growth–drought correlations for SPI and SPEI compared to PDSI when considered for a time scale of 1 month. At this point it is worth noting that due to different calculation procedures and variables considered for the drought indices they are expected to perform differently. The timescale differences between scPDSI and SPEI for drought monitoring has been discussed by Zhao et al. (2015). This study found that scPDSI can be qualified as a mid- and long timescale drought-monitoring index owing to the strong lagged autocor-

relation whereas the SPEI can conveniently monitor short- and long-term drought using selected timescales.

The analysis of the growth response to drought indices revealed distinct species-specific patterns. Our results for the main forest tree species in Europe, Norway spruce, silver fir and European beech, confirm their classification as drought-intolerant from both expert assessment (Niinemets and Valladares, 2006), and observational studies (Pichler and Oberhuber, 2007; Lebourgeois et al., 2010; Schuster and Oberhuber, 2013; van der Maaten-Theunissen et al., 2013; Boden et al., 2014; Pretzsch et al., 2014) (Fig. 4). There was no clear separation of the response of silver fir stands between low and high elevations. This could be due to preconditioning by the high SO$_2$ concentrations in the atmosphere during the mid-20th century (Elling et al., 2009). However, lacking a Europe wide dataset of SO$_2$ deposition, this hypothesis could not be tested. High elevation stands of silver fir were more affected by long-term drought and showed greater drought resistance. This is in line with studies in which higher elevation stands were shown to be more drought resistant (van der Maaten-Theunissen et al., 2013; Zang et al., 2014). There are studies that show a reduced summer drought sensitivity of silver fir in mixed stands (Lebourgeois et al., 2013) which could also explain the less drought sensitive behavior of some stands. In climate zone Cs, silver fir responded to long-term drought. The general response of Norway spruce was similar to that of silver fir. It showed drought sensitivity at all elevations (shown similarly by van der Maaten-Theunissen et al., 2013) and was mostly affected by long-term drought in both Cs and Cf climate zones. Its shallow rooting system may have contributed to the observed pronounced drought sensitivity. European larch and beech display a variation in drought response by elevation. Beech at high elevations in climate zone D showed greater drought resistance, and in climate zone Cf, larch at high elevations was influenced by long-term drought and showed more drought resistance in comparison to stands at lower elevations. Stone pine, a typical species in alpine areas with D climates, was relatively drought resistant and responded to long-term drought only. The two oak species, sessile and common oak, were drought sensitive and were mainly affected by short-term drought, corroborating previous findings (Friedrichs et al., 2008; Zang et al., 2011). In climate zone D, high elevation stands of common oak responded to long-term drought while the low elevation stands responded to short-term drought. The effect of elevation was very pronounced here as well. Species of the genus *Pinus* were seen to show a wide range of drought responses from being drought sensitive to drought resistant. Black and Scots pine were found to be drought susceptible which confirms the reported growth reductions in black pine (Martin-Benito et al., 2013) and Scots pine in connection to extreme summer droughts for Austria (Pichler and Oberhuber, 2007; Camarero et al., 2015) and the French Mediterranean region (Thabeet et al., 2009). High elevation stands of the same two species in climate zone Cs were more drought resistant compared to stands in other climate zones. In climate zone D, stands of Scots pine at higher elevations were more drought sensitive compared to stands at low elevations. In general, forests located in the temperate and Mediterranean climate were drought sensitive and tended to respond to short- and intermediate-term drought (<1 year). In continental climates, forests were comparably more drought resistant and responded to long-term drought.

For each species of the study, the different months and drought indices with maximum correlation with RWI are reported (Fig. 5). In general, scPDSI showed maximum correlations with the deciduous species beech and the two oak species as well as coniferous species black pine; DMI with beech, sessile oak and black pine but as well silver fir. SPEI and SPI at varying degrees captured the drought signal of all species. For silver fir in cold climates, SPI and SPEI at higher time scales best represented drought impacts. For temperate beech forests, it was most suitable to use scPDSI,

SPI and SPEI during the main summer months. In cold climates, the impact of drought on growth is well described by short-term DMI, SPI and SPEI. Scots pine stands in temperate and cold climates mainly responded to long-term SPI and SPEI during early summer months. Temperate stands of black pine were very drought sensitive and their drought signal was reflected by all indices in the main and late summer months, whereas in Mediterranean climate short-term drought during June and July was decisive. All drought indices (DMI, scPDSI, SPI, SPEI) were able to capture drought impacts on oak species, preferably those of the months of June and July. For Scots pine in general and European larch and stone pine in the alpine zone, the performance of all drought indices was quite similar; no particular index outperformed the others. These results have been supported by the predictive performance of the linear models run for each site, with each drought index as a predictor for RWI (Appendix A, Fig. 2 in Supplementary material). This suggests that indices at longer scales showing higher correlation with tree-ring growth reflect high-frequency fluctuations in growth to a better extent, rendering them superior predictors for tree-ring based reconstructions. However, the predictive power of the individual drought indices needs to be further tested using independent data with longer temporal coverage and from an even wider range of growing conditions. On the other hand different approaches to quantify drought responses such as growth resilience indices seem particularly interesting (Gazol et al., 2016). These indices confirm that there are different strategies among forests depending on the biome, tree species and the prevailing climatic conditions to cope with drought.

The results of the validation performed with E-OBS data (Appendix B in Supplementary material) confirmed that ecological patterns were consistent in both datasets and the species patterns we describe reflect true variations and do not constitute any statistical artifacts.

5. Conclusion

To conclude, there are apparent matches between the spatio-temporal characteristics of tree ring network data and the employed drought descriptors. Our findings have implications for dendroclimatic calibration as well as for the relation of these drought descriptors to relevant ecosystem-level responses. However, we should consider that the present study is constrained by the fact that forest productivity is influenced by several other factors besides climate such as human activity. These additional drivers of growth could add noise to the climate signals. The use of spatially coarse gridded climate data due to lacking station data with good temporal coverage adds to the uncertainty of our findings. The CRU dataset is not specifically homogeneous, that is observations are non-necessarily homogenized before inclusion (Harris et al., 2014). This dataset should only be used for climate trend analysis. It has been recommend that such analysis should be complemented by comparison with other datasets (Harris et al., 2014) as it is done in this paper. The second factor of uncertainty refers to tree ring data. It is known that a chronology does not necessarily have a unique growth signal, but a potential mix of ecological forcings and responses at different timescales and levels within trees (Briffa and Cook, 2008). The studied tree ring network consists of data collected with different aims and sampling designs, besides being prone to human errors. Sample collections may represent varying sample homogeneity and hence different growth-forcing signals. Therefore, the sites and species cannot be considered as fully representative of all European forests (Babst et al., 2013). We encourage tree ring researchers to continue publishing their data, since an extended European-wide tree ring network would help to refine the findings from this study and allow for a more fine-grained perspective on spatio-temporal matches and mismatches of tree-growth and drought metrics.

Appendix A. Supplementary data

Supplementary data associated with this article can be found, in the online version, at http://dx.doi.org/10.1016/j.dendro.2017.02.002.

References

Anderegg, W.R.L., Schwalm, C., Biondi, F., Camarero, J.J., Koch, G., Litvak, M., et al., 2015. Pervasive drought legacies in forest ecosystems and their implications for carbon cycle models. Science 349, 528–532.

Babst, F., Poulter, B., Trouet, V., Tan, K., Neuwirth, B., Wilson, R., et al., 2013. Site-and species-specific responses of forest growth to climate across the European continent. Glob. Ecol. Biogeogr. 22, 706–717.

Boden, S., Kahle, H.-P., von, Wilpert K., Spiecker, H., 2014. Resilience of Norway spruce (*Picea abies* (L.) Karst) growth to changing climatic conditions in Southwest Germany. For. Ecol. Manage. 315, 12–21.

Bolte, A., Ammer, C., Löf, M., et al., 2009. Adaptive forest management in central Europe: climate change impacts, strategies and integrative concept. Scand. J. For. Res. 24, 473–482.

Briffa, K., Cook, E., 2008. What are the sources of uncertainty in the tree-ring data: how can they be quantified and represented? In: White Paper Presented as Part of Paleoclimatic Meeting on Proxy Uncertainties, Held in Trieste, Italy, June 9–11.

Camarero, J.J., Gazol, A., Sangüesa-Barreda, G., Oliva, J., Vicente-Serrano, S.M., 2015. To die or not to die: early-warning signals of dieback in response to a severe drought. J. Ecol. 103, 44–57.

de Martonne, E., (1926). Aréisme et indice artidite. Comptes Rendus de L'Acad Sci, Paris 182, 1395–1398.

Dai, A., Trenberth, K.E., Qian, T., 2004. A global dataset of palmer drought severity index for 1870–2002: relationship with soil moisture and effects of surface warming. J. Hydrometeorol. 5, 1117–1130.

Dittmar, C., Eißing, T., Rothe, A., 2012. Elevation-specific tree-ring chronologies of Norway spruce and silver fir in Southern Germany. Dendrochronologia 30, 73–83.

Dobbertin, M., 2005. Tree growth as indicator of tree vitality and of tree reaction to environmental stress: a review. Eur. J. For. Res. 24, 319–333.

Elling, W., Dittmar, C., Pfaffelmoser, K., Rötzer, T., 2009. Dendroecological assessment of the complex causes of decline and recovery of the growth of silver fir (*Abies alba* Mill.) in Southern Germany. For. Ecol. Manage. 257, 1175–1187.

Frank, D., Reichstein, M., Bahn, M., Thonicke, K., Frank, D., Mahecha, M.D., et al., 2015. Effects of climate extremes on the terrestrial carbon cycle: concepts, processes and potential future impacts. Glob. Change Biol. 21 (8), 2861–2880.

Friedrichs, D.A., Buentgen, U., Frank, D.C., Esper, J., Neuwirth, B., Loeffler, J., 2008. Complex climate controls on 20th century oak growth in Central-West Germany. Tree Physiol. 29, 39–51.

Fritts, H.C., Blasing, T.J., Hayden, B.P., Kutzbach, J.E., 1971. Multivariate techniques for specifying tree-growth and climate relationships and for reconstructing anomalies in paleoclimate. J. Appl. Meteorol. 10, 845–864.

Gazol, A., Camarero, J.J., Anderegg, W.R.L., Vicente-Serrano, S.M., 2016. Impacts of droughts on the growth resilience of Northern Hemisphere forests. Glob. Ecol. Biogeogr., http://dx.doi.org/10.1111/geb.12526.

Harris, I., Jones, P.D., Osborn, T.J., Lister, D.H., 2014. Updated high-resolution grids of monthly climatic observations – the CRU TS3.10 Dataset. Int. J. Climatol. 34, 623–642.

Haylock, M.R., Hofstra, N., Klein Tank, A.M.G., Klok, E.J., Jones, P.D., New, M., 2008. A European daily high-resolution gridded data set of surface temperature and

precipitation for 1950–2006. J. Geophys. Res. 113, D20119, http://dx.doi.org/10.1029/2008JD010201.

Hogg, E.H., Barr, A.G., Black, T.A., 2013. A simple soil moisture index for representing multi-year drought impacts on aspen productivity in the western Canadian interior. Agric. For. Meteorol. 178–179, 173–182.

IPCC, 2013. Summary for policymakers. Climate change 2013: the physical science basis. In: Contribution of Working Group I to the Fifth Assessment Report of the Intergovernmental Panel on Climate Change. Cambridge University Press, Cambridge, UK and New York, NY, pp. 3–39.

Kogan, F., Adamenko, T., Guo, W., 2013. Global and regional drought dynamics in the climate warming era. Remote Sens. Lett. 4, 364–372.

Kottek, M., Grieser, J., Beck, C., Rudolf, B., Rubel, F., 2006. World map of the Köppen-Geiger climate classification updated. Meteorol. Z. 15, 259–263.

Lévesque, M., Saurer, M., Siegwolf, R., Eilmann, B., Brang, P., Bugmann, H., Rigling, A., 2013. Drought response of five conifer species under contrasting water availability suggests high vulnerability of Norway spruce and European larch. Glob. Change Biol. 19, 3184–3199.

Lebourgeois, F., Rathgeber, C.B.K., Ulrich, E., 2010. Sensitivity of French temperate coniferous forests to climate variability and extreme events (*Abies alba, Picea abies* and *Pinus sylvestris*). J. Veg. Sci. 21, 364–376.

Lebourgeois, F., Gomez, N., Pinto, P., Mérian, P., 2013. Mixed stands reduc *Abies alba* tree-ring sensitivity to summer drought in the Vosges mountains, western Europe. For. Ecol. Manage. 303, 61–71.

Legendre, P., Legendre, L., 1998. Numerical Ecology. Elsevier Ltd, Amsterdam.

Luyssaert, S., Ciais, P., Piao, S.L., Schulze, E.-D., Jung, M., Zaehle, S., et al., 2010. The European carbon balance. Part 3: forests. Glob. Change Biol. 16, 1429–1450.

van der Maaten-Theunissen, M., Kahle, H.-P., van der Maaten, E., 2013. Drought sensitivity of Norway spruce is higher than that of silver fir along an altitudinal gradient in southwestern Germany. Ann. For. Sci. 70, 185–193.

Maherali, H., Pockman, W.T., 2004. Adaptive variation in the vulnerability of woody plants to xylem cavitation. Ecology 85, 2184–2199.

Machado-Machado, E.A., Neeti, N., Eastman, R.J., Chen, H., 2011. Implications of space-time orientation for Principal Components Analysis of Earth observation image time series. Earth Sci. Inform. 4, 117–124.

Martin-Benito, D., Beeckman, H., Cañellas, I., 2013. Influence of drought on tree rings and tracheid features of *Pinus nigra* and *Pinus sylvestris* in a mesic Mediterranean forest. Eur. J. For. Res. 132, 33-45.

Mckee, T.B., Doesken, N.J., Kleist, J., 1993. The relationship of drought frequency and duration to time scales. Water 179, 17–22.

Mishra, A.K., Singh, V.P., 2010. A review of drought concepts. J. Hydrol. 391, 202–216.

Niinemets, Ü., Valladares, F., 2006. Tolerance to shade, drought, and waterlogging of temperate northern hemisphere trees and shrubs. Ecol. Monogr. 76, 521–547.

Obasi, G.O.P., 1994. WMO's role in the international decade for natural disaster reduction. Bull. Am. Meteorol. Soc. 75, 1655–1661.

Palmer, W.C., 1965. Meteorological drought. In: Research Paper No. 45. U.S. Dept of Commerce, pp. 55.

Pasho, E., Camarero, J.J., de Luis, M., Vicente-Serrano, S.M., 2012. Factors driving growth responses to drought in Mediterranean forests. Eur. J. For. Res. 131, 1797–1807.

Pichler, P., Oberhuber, W., 2007. Radial growth response of coniferous forest trees in an inner Alpine environment to heat-wave in 2003. For. Ecol. Manage. 242, 688–699.

Pretzsch, H., Rötzer, T., Matyssek, R., Grams, T.E.E., Häberle, K.-H., Pritsch, K., et al., 2014. Mixed Norway spruce (*Picea abies* [L.] Karst) and European beech (*Fagus sylvatica* [L.]) stands under drought: from reaction pattern to mechanism. Trees – Struct. Funct. 28, 1305–1321.

R Core Team, 2015. R: A Language and Environment for Statistical Computing. R Foundation for Statistical Computing, Vienna Austria https://www.R-project.org/.

Schuster, R., Oberhuber, W., 2013. Age-dependent climate–growth relationships and regeneration of *Picea abies* in a drought-prone mixed-coniferous forest in the Alps. Can. J. For. Res. 43, 609–618.

Seftigen, K., 2014. Late Holocene Spatiotemporal Hydroclimatic Variability over Fennoscandia Inferred from Tree-rings Doctoral Dissertation. University of Gothenburg.

Seneviratne, S.I.N., Nicholls, D., Easterling, C.M., Goodess, S., Kanae, J., Kossin Luo, Y., et al., 2012. Managing the risks of extreme events and disasters to advance climate change adaptation. In: Field, C.B., Barros, V., Stocker, T.F., Qin, D., Dokken, D.J., Ebi, K.L., Mastrandrea, M.D., Mach, K.J., Plattner, G.-K., Allen, S.K., Tignor, M., Midgley, P.M. (Eds.), A Special Report of Working Groups I and II of the Intergovernmental Panel on Climate Change (IPCC). Cambridge University Press, Cambridge, UK, and New York, NY, USA, pp. 109–230.

Stephenson, N.L., 1990. Climatic control of vegetation distribution: the role of the water balance. Am. Nat. 135, 649–670.

Thabeet, A., Vennetier, M., Gadbin-Henry, C., Denelle, N., Roux, M., Caraglio, Y., Vila, B., 2009. Response of *Pinus sylvestris* L. to recent climatic events in the French Mediterranean region. Trees – Struct. Funct. 23, 843–853.

Vicente-Serrano, S.M., Beguería, S., López-Moreno, J.I., 2010. A multiscalar drought index sensitive to global warming: the standardized precipitation evapotranspiration index. J. Clim. 23, 1696–1718.

Vicente-Serrano, S.M., Beguería, S., Lorenzo-Lacruz, J., Camarero, J.J., López-Moreno, J.I., Azorin-Molina, C., et al., 2012. Performance of drought indices for ecological, agricultural, and hydrological applications. Earth Interact. 16, 1–27.

Vicente-Serrano, S.M., Camarero, J.J., Azorin-Molina, C., 2014. Diverse responses of forest growth to drought time-scales in the Northern Hemisphere. Glob. Ecol. Biogeogr. 23, 1019–1030.

Wells, N., Goddard, S., Hayes, M.J., 2004. A self-calibrating palmer drought severity index. J. Clim. 17, 2335–2351.

Wickham, H., 2009. Ggplot2: Elegant Graphics for Data Analysis. Springer, New York.

Wilhite, D.A., Glantz, M.H., 1985. Understanding: the drought phenomenon: the role of definitions. Water Int. 10, 111–120.

Zang, C., Biondi, F., 2013. Dendroclimatic calibration in R: the bootRes package for response and correlation function analysis. Dendrochronologia 31, 68–74.

Zang, C., Rothe, A., Weis, W., Pretzsch, H., 2011. Zur Baumarteneignung bei Klimawandel: Ableitung der Trockenstress-Anfaelligkeit wichtiger Waldbaumarten aus Jahrringbreiten. Allg. Forst Jagdztg. 182, 98–112.

Zang, C., Hartl-Meier, C., Dittmar, C., Rothe, A., Menzel, A., 2014. Patterns of drought tolerance in major European temperate forest trees: climatic drivers and levels of variability. Glob. Change Biol. 20, 3767–3779.

Zhao, H., Gao, G., An, W., Zou, X., Li, H., Hou, M., 2015. Timescale differences between SC-PDSI and SPEI for drought monitoring in China. Phys. Chem. Earth Parts A/B/C, http://dx.doi.org/10.1016/j.pce.2015.10.022, in press.
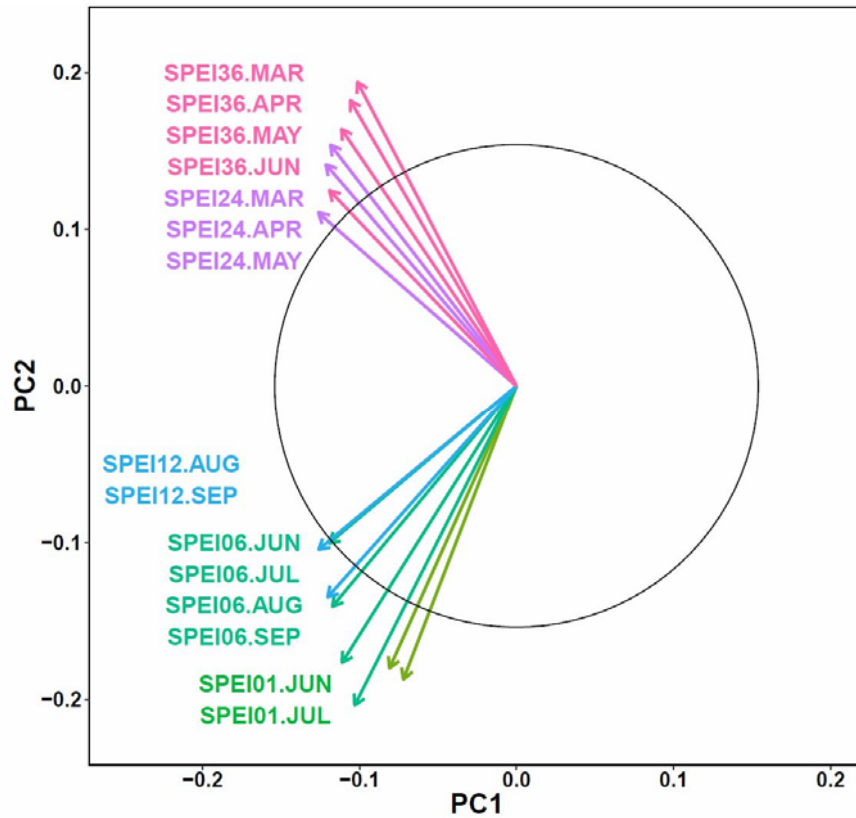
Appendix 1: Supplementary Figures

Figure 1. Equilibrium circle and selected drought indices (SPEI) of the PCA (selected). The PCA was performed on the correlation coefficients calculated between 850 RWI series and the monthly scPDSI, DMI, SPI / SPEI (time scales = 1, 6, 12, 24, 36) for the period of 1920-1975. SPEI stands for Standardized Potential Evapotranspiration Index.
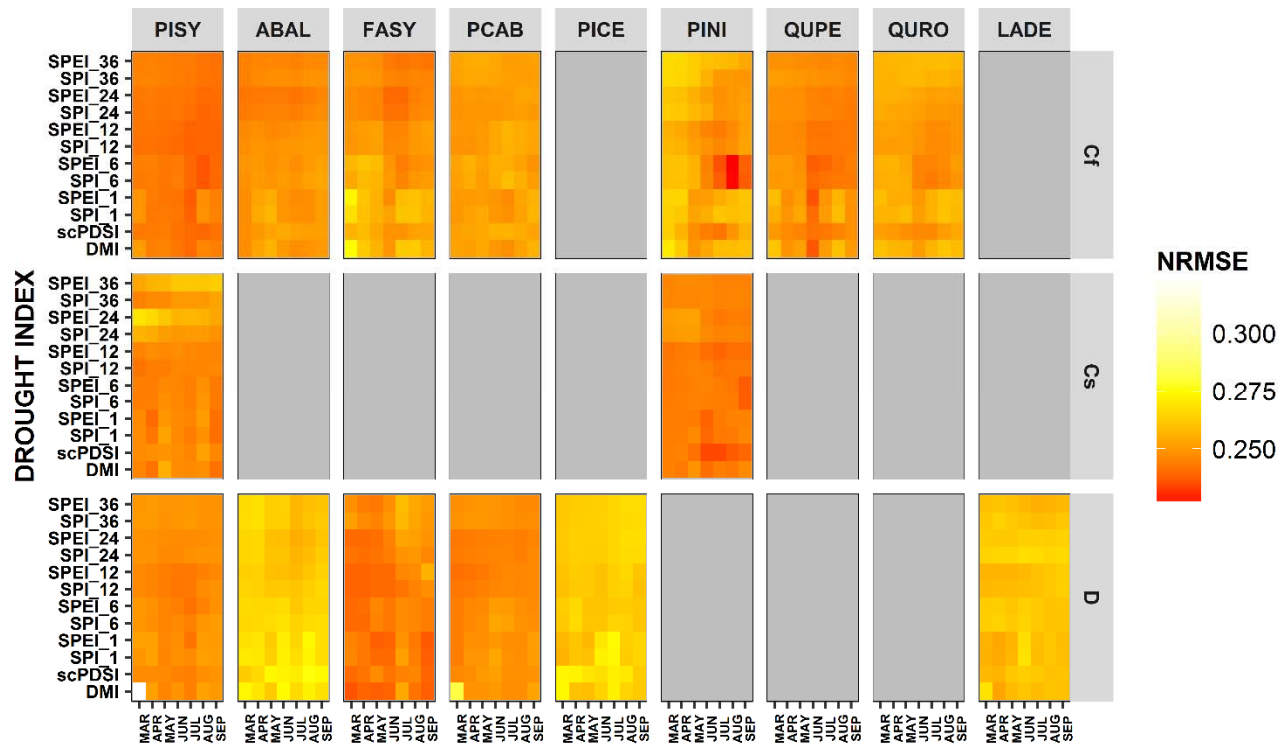
Figure 2 Plot of normalized RMSE values of the prediction of linear model (RWI~DROUGHT INDEX) calculated site-wise for each drought index for all species in different climate zones. Groups with N < 10 were omitted. The second half of the tree ring and drought time series were used for training the data (1948 to 1975), while the first half of the time series was used for testing the liner fit (1920 to 1947). Then the mean of the RMSE values were calculated for the different groups. The species analyzed are ABAL silver fir, FASY European beech, LADE European larch, PCAB Norway spruce, PICE stone pine, PINI black pine, PISY Scots pine, QUPE sessile oak, and QURO common oak. Cf, Cs and D denote temperate climate without dry season, temperate climate with dry summer (Mediterranean) and continental climate respectively as per Köppen climate classification.

Appendix 2: Validation with E-OBS data

For validating the results of the study, and estimating uncertainties, we have used station data from E-OBS (Haylock *et al.,* 2008). We have compared the PCA ordination results (1st and 2nd components) from the CRU dataset (Harris *et al.,* 2014) with the PCA ordination results (1st and 2nd components) from the E-OBS dataset using the Procrustes tests. A high correlation in a symmetric Procrustes rotation makes us confident that the species patterns we describe reflect true variations and do not constitute any statistical artifacts. The Procrustes test determines whether two ordinations are significantly correlated. Our results confirmed that ecological patterns were consistent in both datasets (Peres-Neto and Jackson, 2001; Legendre and Legendre, 1998; Ramette, 2007). The PCA for the original dataset was performed on the correlation coefficients calculated between 850 RWI series and twelve drought indices for the period of 1920-1975. The PCA for the validation dataset was performed on the correlation coefficients calculated between 850 RWI series and eleven drought indices (E-OBS) for the period of 1950-1975. The validation was performed for all the drought indices except scPDSI due to unavailability of soil data.
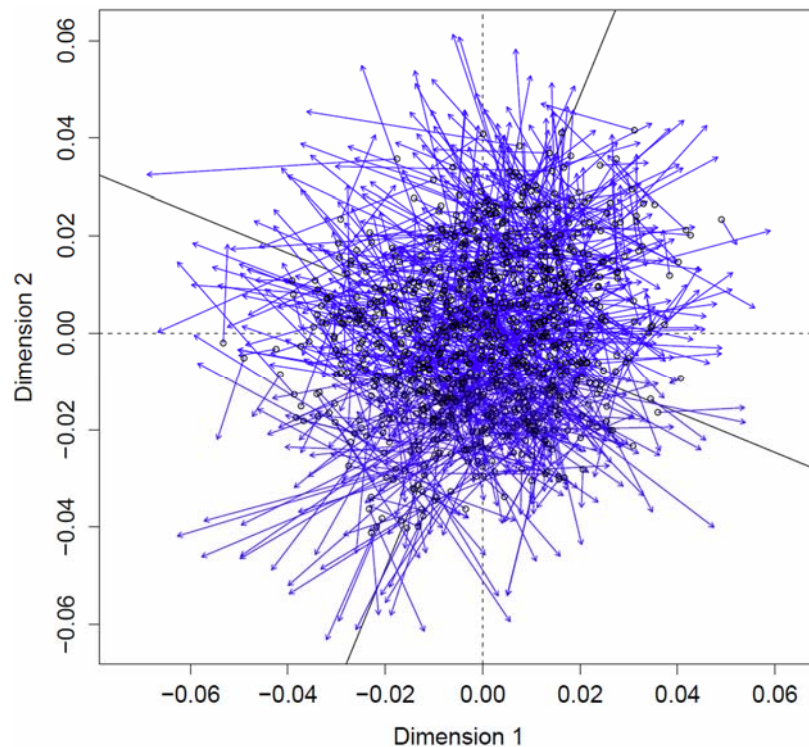
Procrustes Results

Fig. 1 Procrustes superimposition plot showing Procrustes errors, that is the differences between the PCA results obtained from original dataset (circles) and that obtained from a PCA using the validation dataset (ends of the arrows).

Procrustes Sum of Squares: 0.53

Correlation in a symmetric Procrustes rotation: 0.68

Significance: 0.001, Permutation: Free, Number of permutations: 999

Conclusion :

From Fig. 2 and Fig. 3 (see below) we see that the major modes of tree growth response to drought indices and the species patterns observed using station data from E-OBS was similar to that revelaed when using the CRU dataset (see paper, Fig. 3 and Fig. 4). Additionally, the results of the Procrustes test validate the findings in the paper.
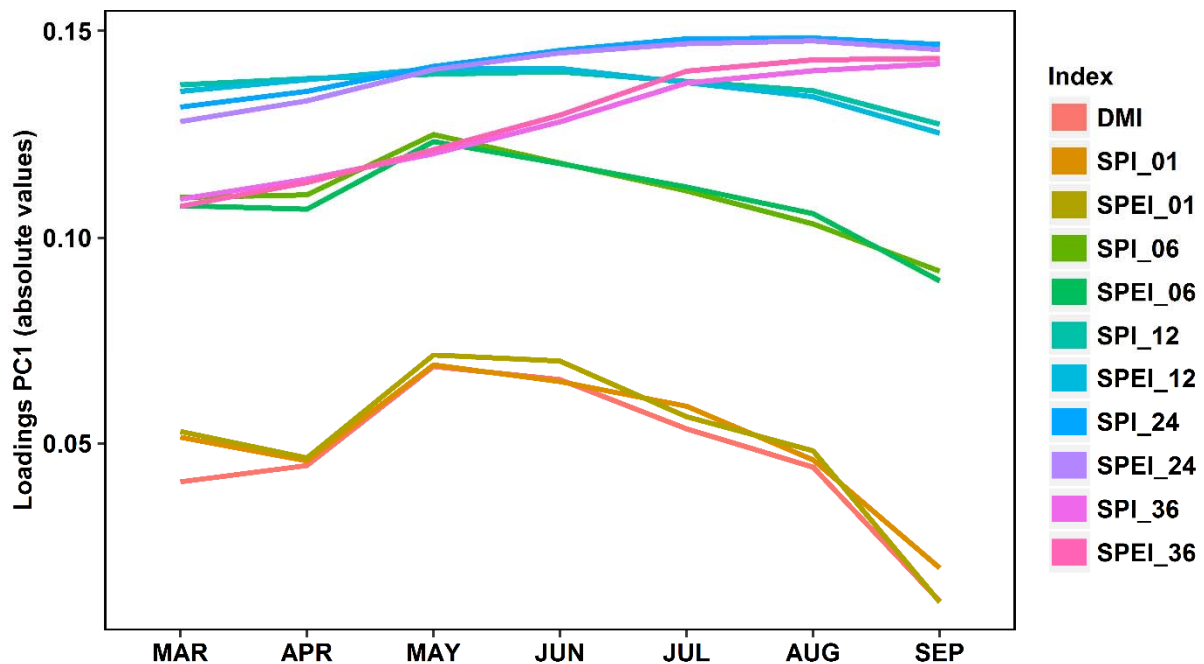

Fig. 2 Major modes of tree growth responses to 11 drought indices for the current year growing season based on the first principal component (PC1). PCA was performed on the correlation coefficients calculated between 850 RWI series and the monthly DMI, SPI/SPEI (time scales = 1, 6, 12, 24, 36) for the period of 1950-1975. DMI, SPI and SPEI stand for De Martonne Aridity Index, Standardized Precipitation, Index and Standardized Potential Evapotranspiration Index. The drought indices were calculated using E-OBS data.

Fig. 3 PCA score plot for nine studied species and elevation (m a.sl.) analyzed in the dataset. PCA was performed on the correlation coefficients calculated between 850 RWI series and the monthly DMI, SPI/SPEI (time scales = 1, 6, 12, 24, 36) for the period of 1950-1975. DMI, SPI and SPEI stand for De Martonne Aridity Index, Standardized Precipitation, Index and Standardized Potential Evapotranspiration Ind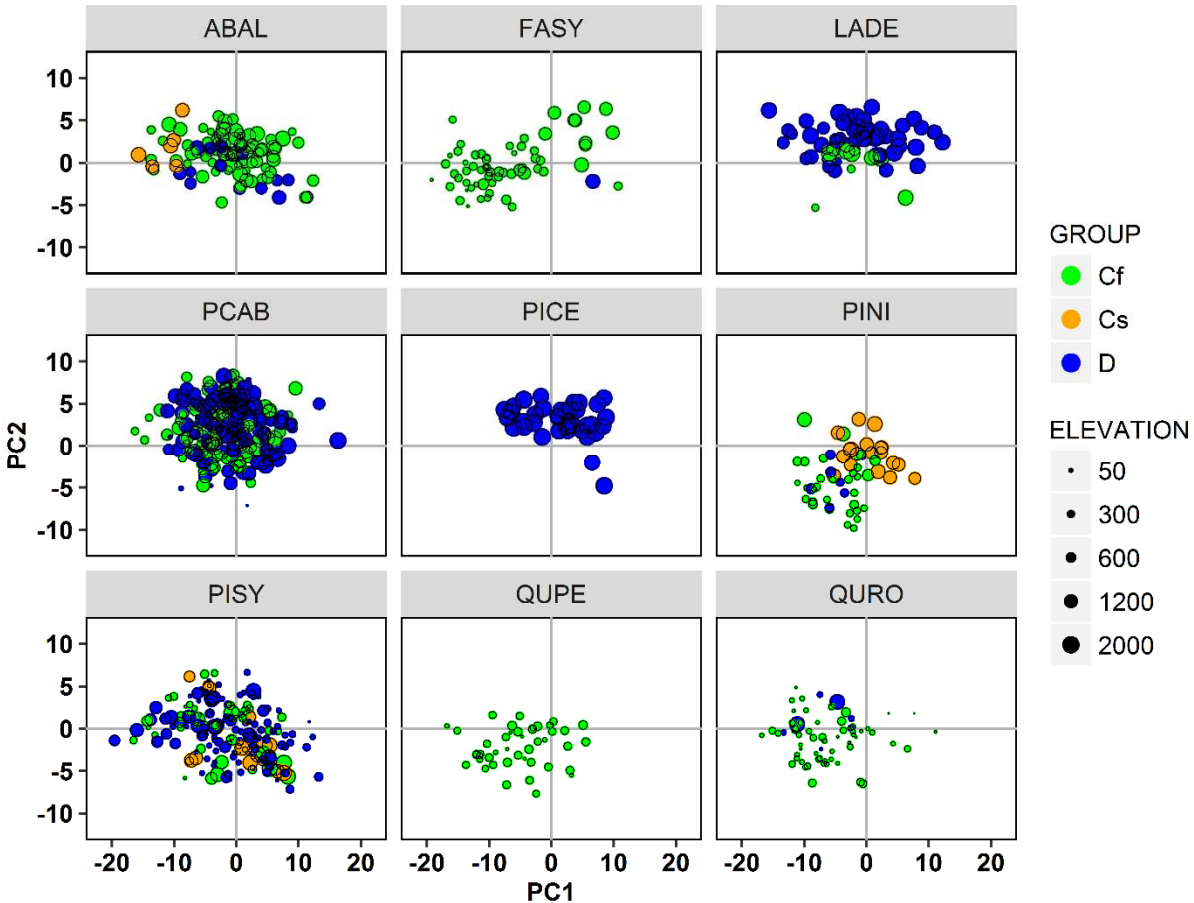ex. The drought indices were calculated using E-OBS data. Cf, Cs and D denote temperate climate without dry season, temperate climate with dry summer (Mediterranean) and continental climate respectively as per Köppen climate classification. The species analyzed are ABAL silver fir, FASY European beech, LADE European larch, PCAB Norway spruce, PICE stone pine, PINI black pine, PISY Scots pine, QUPE sessile oak, and QURO common oak.

References

Harris, I., Jones, P.D., Osborn, T.J., Lister, D.H. (2014). Updated high-resolution grids of monthly climatic observations - the CRU TS3.10 Dataset. *Int. J. Climatol*. 34, 623–642

Haylock, M. R., Hofstra, N., Klein Tank, A. M. G, Klok, E. J., Jones, P. D. and New, M. (2008). A European daily high-resolution gridded data set of surface temperature and precipitation for 1950–2006. *J. Geophys. Res*. 113. D20119. doi:10.1029/2008JD010201.

Legendre, P.,Legendre, L. (1998). *Numerical ecology.* Elsevier Ltd, Amsterdam

Peres-Neto, P.R., Jackson, D.A. (2001). How well do multivariate data sets match? The advantage of a procrustean superimposition approach over the mantel test. *Oecologia.* 129,169-178

Ramette, A. (2007). Multivariate analyses in microbial ecology. *FEMS Microbiol Ecol.* 62,142-160

Exploring Relationships among Tree-Ring Growth, Climate Variability, and Seasonal Leaf Activity on Varying Timescales and Spatial Resolutions

Upasana Bhuyan [1,*], Christian Zang [2], Sergio M. Vicente-Serrano [3] and Annette Menzel [1,4]

[1] Ecoclimatology, Department of Ecology and Ecosystem Management, Technische Universität München, Freising 85354, Germany; amenzel@wzw.tum.de

[2] Land Surface-Atmosphere Interactions, Department of Ecology and Ecosystem Management, Technische Universität München, Freising 85354, Germany; christian.zang@wzw.tum.de

[3] Instituto Pirenaico de Ecología, Consejo Superior de Investigaciones Científicas (IPE–CSIC), Zaragoza 50059, Spain; svicen@ipe.csic.es

[4] Institute for Advanced Study, Technische Universität München, Garching 85748, Germany

[*] Correspondence: bhuyan@wzw.tum.de; Tel.: +49(0)8161-714-746

Abstract: In the first section of this study, we explored the relationship between ring width index (RWI) and normalized difference vegetation index (NDVI) time series on varying timescales and spatial resolutions, hypothesizing positive associations between RWI and current and previous- year NDVI at 69 forest sites scattered in the Northern Hemisphere. We noted that the relationship between RWI and NDVI varies over space and between tree types (deciduous versus coniferous), bioclimatic zones, cumulative NDVI periods, and spatial resolutions. The high-spatial-resolution NDVI (MODIS) reflected stronger growth patterns than those with coarse-spatial-resolution NDVI (GIMMS3g). In the second section, we explore the link between RWI, climate and NDVI phenological metrics (in place of NDVI) for the same forest sites using random forest models to assess the complicated and nonlinear relationships among them. The results are as following (a) The model using high-spatial-resolution NDVI time series explained a higher proportion of the variance in RWI than that of the model using coarse-spatial-resolution NDVI time series. (b) Amongst all NDVI phenological metrics, summer NDVI sum could best explain RWI followed by the previous year's summer NDVI sum and the previous year's spring NDVI sum. (c) We demonstrated the potential of NDVI metrics derived from phenology to improve the existing RWI-climate relationships. However, further research is required to investigate the robustness of the relationship between NDVI and RWI, particularly when more tree-ring data and longer records of the high-spatial-resolution NDVI become available.

Keywords: radial growth; NDVI; MODIS; GIMMS3g; phenology; dendroecology; scPDSI

1. Introduction

Remote sensing and dendroecology are considered instrumental in monitoring net primary productivity [1,2]. Dendroecologists have successfully used samples of tree growth from radial increments to quantify long-term variability in forest productivity [3,4]. Tree-ring width or annual radial growth increment is a widely used proxy for tree vitality [5], and its connections to climate and extreme climatic events, such as drought, are well established [5,6]. However, preparing tree-ring chronologies involves time-consuming field and laboratory work, thereby undermining the technique's potential to be used for monitoring real-time forest growth over large spatial scales [7–9]. Real-time observations based on remote sensing are also not feasible; however, at the end of the growing season, a solid assessment of the past annual growth should be possible. The remotely

sensed normalized difference vegetation index (NDVI), which is based on red and near-infrared reflectances [10], is a good measure of photosynthetic activity at landscape-scales and can be used to estimate vegetation productivity [1,11–17]. Against the background of global climate warming and an associated lengthening of the growing season [18,19], studying how climatic factors and NDVI are related to ring width index (RWI) could lead to a better and more immediate understanding of forest growth.

The utility of remote sensing indices in observing and monitoring phenology over large scales and at regular intervals has been well documented [20], and a handful of studies have related NDVI directly to tree-rings [4,7,12–15,21,22]. Although these studies linked NDVI values with tree-ring growth data, the relationship of the latter with NDVI phenological metrics remains to be explored. From an ecological perspective, plant phenology plays a significant role in determining the carbon sequestration period of terrestrial ecosystems and is widely used to diagnose responses of ecosystems to global change [23–25]. Accurate information related to phenology is important in the study of regional-to-global carbon budgets [26]; hence, exploring its role in explaining tree-ring growth could be crucial.

Remote sensing of phenology using time series of vegetation indices is based on the intra-annual changes of canopy greenness [25]. We have extracted important phenological metrics from NDVI time series to examine their relationship with RWI because the spatio-temporal variations of vegetation phenology are known to serve as important indicators of photosynthetic activity [27]. We analyzed NDVI time series to extract key phenological metrics, such as the start of the growing season (SOS) and end of the growing season (EOS). These characteristics may not necessarily correspond directly to defined, ground-based phenological events, but they do provide indications of seasonal ecosystem dynamics [25]. They can reveal landscape-scale climate/tree-ring growth interactions. We compared RWI time-series from 69 forest sites with NDVI at fine (250 m, MODIS) and coarse (8 km, GIMMS3g) spatial resolutions for different timescales (cumulative NDVI values from one to 20 observations). Tree-ring width as a proxy for tree growth is known to correlate with several monthly values of temperature and precipitation during the year of growth and, in some cases, previous years (e.g., [5,28]). Intercomparison of corresponding data of tree-ring growth, climate, and NDVI may help deepen our understanding of the response of a forest to recent warming trends.

In the first section of this study, we evaluated whether NDVI correlates with the radial growth of trees scattered in the Northern Hemisphere. In the second section, we tried to fill the gap in literature that exists in exploring the relationship between RWI and various NDVI phenological metrics. Overall, we seek to resolve whether NDVI metrics can help to refine or improve the existing RWI-climate relationship, and whether such metrics could be used for explaining the RWI. If so, such knowledge could be useful in supporting forest management practices.

2. Materials and Methods

2.1. NDVI Data

We used two NDVI datasets with different spatial resolutions: (1) Moderate Resolution Imaging Spectroradiometer (MODIS) and (2) Global Inventory Modeling and Mapping Studies 3g (GIMMS3g). This allowed us to study the possible effects of spatial resolution on the RWI-NDVI relationship. For MODIS, we used MOD13Q1 [29], which is the MODIS/Terra vegetation index. It has a spatial resolution of 250 m and is provided as a 16-day composite, resulting in 23 observations per year. Quality information was used to discard possible snow and cloud values. The MODIS NDVI record begins in February 2000; however, we analyzed data from 2001 (the first complete year of NDVI data) until 2010, the last year of our assembled tree-ring dataset.

The third-generation Global Inventory Modeling and Mapping Studies, GIMMS3g [30] is based on the Advanced Very High Resolution Radiometer (AVHRR), has a spatial resolution of 8 km, and is provided at a temporal resolution of 15 days resulting in two maximum-value composites per month and 24 observations per year. The GIMMS3g NDVI record begins in July 1981; we analyzed data

from 1982 (the first complete year of NDVI data) to the end of 2010 to maximize the overlap with the assembled tree-ring dataset. The latitude and longitude of each of the tree-ring sites were used to select the corresponding pixel from the GIMMS3g and MODIS NDVI datasets. For each annual NDVI time series, cumulative values (1–20 observations) were calculated and then used in the Pearson correlation analysis. For instance, a cumulative NDVI value of five implies that the data from the current observation and of four previous observations (four observations equates to approximately two months) will be used to compute the cumulative NDVI value (sum) for a given time.

2.2. Tree-ring Data

Tree-ring data were downloaded from the International Tree-Ring Data Bank (ITRDB) [31] which is a repository containing tree-ring data [32]. All downloaded time series from the ITRDB were filtered for three requirements (1) tree-ring widths complete for the period 1982 to 2010, (2) no missing NDVI data in the time-series of each overlapping pixel, and (3) having forest cover in the corresponding remote sensing pixel. For the third requirement, we used the world forest-cover map GlobCover from the European Space Agency, which is based on Envisat Medium Resolution Imaging Spectrometer (MERIS) data between December 2004 and June 2006 [33]. We excluded tree-ring sites in remote sensing pixels covering bare areas, water bodies, areas with permanent snow and ice, or areas located in the Southern Hemisphere. In total, 69 sites were retained for the analysis (Figure 1). Each tree-ring series was detrended on a per-site basis using a cubic-smoothing spline with a frequency response of 50% at 32 years [34]. This was done to remove the trend present in the original raw tree-ring width measurements, while at the same time preserving the inter-annual to decadal variability. Prior to detrending, the series were power-transformed to remove temporal heteroscedasticity, and were then robustly averaged into dimensionless chronologies of RWIs. Readers unfamiliar with tree-ring detrending and chronology development can refer to Cook et al. [9]. Table S1 (Supplementary) gives all information on sites, species, climate zones (see Section 2.3), chronology coverage, and important tree-ring metrics.
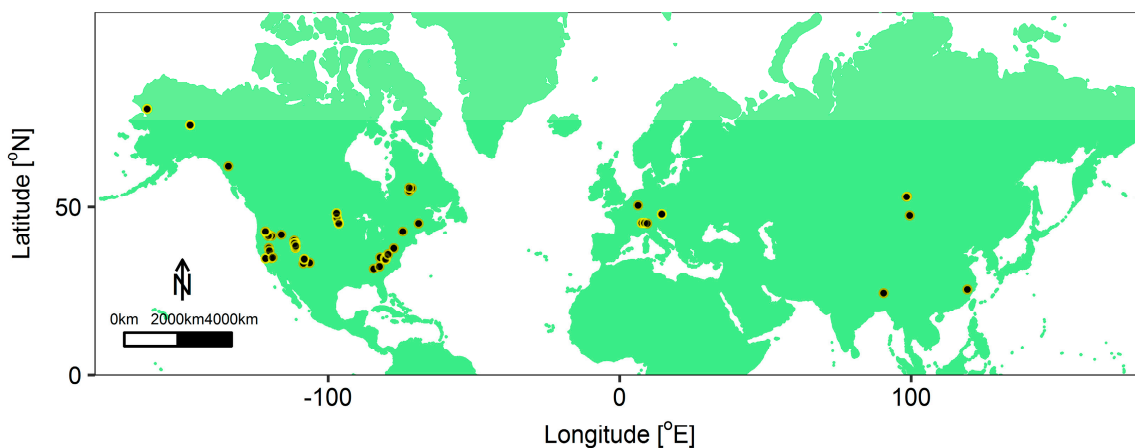

Figure 1. World map showing the location of the 69 study sites.

2.3. Climate Data

We used monthly mean temperature (TMP), mean monthly sums of precipitation (PRE), and potential evapotranspiration (PET) from the CRU TS 3.21 dataset [35] available on a 0.5° grid [36]. Monthly time series of the self-calibrating Palmer Drought Severity Index (scPDSI) [37] on a 0.5° grid were downloaded from the KNMI Climate Explorer web page [38]. The drought index Standardized Precipitation Evapotranspiration Index (SPEI) was calculated using the R package SPEI [39] based on input data from CRU. Climate was classified according to the world Köppen–Geiger climate-classification map [40], in which zone B indicates an arid/semiarid climate, C and D are temperate and continental climates, respectively. Conifer sites were analyzed separately for the three climate zones (B, C, and D) (4, 21, and 28 sites, respectively), whereas the 16 sites with broadleaf forests constituted the fourth group (see Table S1).

2.4. Extracting Phenological Metrics from the NDVI Time Series

Annual time series of NDVI allow the extraction of key phenological events such as the start (SOS) and end (EOS) of the growing season as well as of different NDVI metrics. However, prior to this, the NDVI time series had to be preprocessed to deal with perturbations due to atmospheric and geometric interferences and noise.

In the case of MODIS, individual NDVI observations that were marked in the corresponding pixel-reliability layer as either missing or as affected by snow or clouds were removed. Only those marked as good were retained in the NDVI time series that, despite containing gaps, constituted reliable and uncontaminated data; the gaps were then linearly interpolated. In the case of GIMMS3g, it was not necessary to discard data based on a quality layer because the GIMMS3g data had already been corrected for solar zenith and viewing angles, volcanic aerosols, atmospheric water vapor, and cloud cover [41], thus assuring the quality and consistency of the data.

To extract the seasonality of the NDVI time series, the series were filtered using a Gaussian filter [42] to remove noise. As mentioned in Misra et al. [43], the weights in the Gaussian filter were distributed symmetrically around the central value, and their fractional weights *Wi* were calculated as follows:

$$W_i = \frac{1}{0.5 * k * \sqrt{pi}} * \exp *(-\frac{w_i^2}{(0.5 * k)^2}),$$ (1)

where k is the size of the filter and w_i is the *i*th value in a sequence from −k to k; for this study, we used k = 6. To achieve values that summed to unity, W_i was normalized by the sum of itself. Deviations of the raw NDVI from the Gaussian-filtered data were z-transformed, and values beyond two standard deviations were considered outliers and removed from the raw data. After removing such outliers, the NDVI data were again smoothed using the weighted Gaussian filter and then linearly interpolated to daily values.

Based on these daily NDVI time series, a threshold of 50% of the seasonal amplitude was used to define the start (SOS) and end (EOS) of the growing season. An example of a processed NDVI time series with the phenological parameters SOS and EOS is given in Figure S1 (Supplementary). For subsequent use in the modelling approach, we calculated ten different NDVI phenological metrics (Table 1), that we then standardized using the site-specific mean and standard deviation. These NDVI metrics derived from phenology are subsequently referred to as NDVI phenological metrics.

Table 1. Phenological metrics calculated from normalized difference vegetation index (NDVI) time series.

Phenological Metric	Definition
NDVI_GS	sum of the NDVI values extracted from the start of season to the end of season
NDVI_GS_prv	sum of the NDVI values extracted from the start of season to the end of season of previous year
NDVI_Sum	sum of the NDVI values of the summer months June to August
NDVI_Sum_prv	sum of the NDVI values of the summer months of previous year
NDVI_Spr	sum of the NDVI values of the spring months March to May
NDVI_Spr_prv	sum of the NDVI values of the spring months of previous year
NDVI_SOS	NDVI extracted at the start of season
NDVI_SOS_prv	NDVI extracted at the start of season of the previous year
SOS_date	date of the start of season
EOS_date_prv	date of the end of season of the previous year

2.5. Statistical Analyses

In order to assess the relationships between tree growth and NDVI, Pearson correlations between RWI and cumulative NDVI (MODIS and GIMMS3g) for the 69 study sites were calculated for different timescales of NDVI integration. The resulting correlation coefficients were summarized for both MODIS and GIMMS3g, as well as for the four climate groups (deciduous of all climate zones, coniferous in climate zone B, in C, and in D) by calculating the mean and variance of each group.

2.6. Relationship of RWI with NDVI Metrics and Climate

To establish quantitative relationships between ground-based RWI, climate, and phenological metrics derived from NDVI time series, we performed random forest (RF) analysis as a multivariate non-parametric regression method [44–47]. The RF model, which is an ensemble learning technique developed by Breiman [45], was fitted using all tree-ring sites. We used 70% of the data randomly sampled to train the RF and the remaining were retained for RF prediction-error testing. The proportion of explained variance in the outcome of the training data and the normalized root mean square error (NRMSE) were used to quantify the association between RWI and NDVI / climate. The normalized root mean square error (NRMSE) is computed as $\text{NRMSE} = \text{sqrt}\,(n^{-1}\sum_{1}^{n}\{x_{obs} - x_{model}\}^2))/n^{-1}\sum_{1}^{n}x_{obs} = \text{RMSE}/\text{mean}(x_{obs})$, where x_{obs} and x_{model} refer to observed RWI values (of the test data) and predicted RWI values of the RF model respectively. The variance explained is computed as $(1 - \text{MSE}/\text{var}(x_{obs}))$ of the training data. To evaluate the importance of predictors, we used the Increased Mean Square Error which is a robust measure defined as the increase in the mean squared error of predictions as a result of the variable being permuted. Higher values indicate a variable that is more important [45]. A second measure for variable importance, the Increased Impurity Index, relates to the loss function by which best splits are chosen. More important variables achieve higher increases in node purities. RF analysis was performed in the R statistical environment [48] using the randomForest package [49].

To assess the importance of NDVI phenological metrics derived from two different remote sensing products, we fixed the period of analysis from 2001 to 2010 in order to have a fair comparison using the same time span for the models. In this way, we had an identical RWI-climate model, to which NDVI phenological metrics from both MODIS and GIMMS3g were added. In the RWI-climate model, RWI was explained by predictors: scPDSI (self-calibrating Palmer Drought Severity Index), PRE (monthly sums of precipitation), TMP (monthly mean temperature), latitude of the forest site, elevation of the forest site, tree type (coniferous or broadleaf), and climate zone (B, C, or D) as per Köppen–Geiger climate classification. To explain tree growth (RWI) by MODIS/GIMMS3g NDVI and climate, the number of regression trees in RF was fixed to 200, and the number of variables sampled at each node was set to seven after a preliminary analysis. For the RF climate-NDVI models, besides the predictors of the RWI-climate model, 10 standardized NDVI phenological metrics, namely NDVI_GS, NDVI_GS_prv, NDVI_Sum, NDVI_Sum_prv, NDVI_Spr, NDVI_Spr_prv, NDVI_SOS, NDVI_SOS_prv, SOS_date, and EOS_date_prv (see Table 1) were used. The same analysis was also performed with

drought index SPEI (Figure S5, Supplementary), however, it is not presented in the manuscript as it explained less variance of the RWI in comparison to drought index scPDSI. We performed a validation of the RF model (MODIS) using a test dataset corresponding to 30% of the original dataset randomly sampled. We report here the mean relative error (RE), ratio of root mean square error (RMSE), and ratio of mean absolute error (MAE) as validation statistics. The formulas used to calculate these metrics are given in Section S3 (Supplementary). Additionally, we provide the scatterplot between observed RWI values from the test dataset and predicted RWI values from the RF model (Figure S4, Supplementary).

3. Results

3.1. Relationships between RWI and NDVI/Climate

A typical pattern of Pearson correlation coefficients between annual RWI and cumulative NDVI (up to 20 observations) is given in Figure 2 for a site in Utah (UT531), United States of America, with a continental-type (D) climate and a RWI series for tree species *Juniperus scopulorum* Sarg. The correlation patterns based on GIMMS3g NDVI (8 km resolution, 29 years of data) and MODIS NDVI (250 m resolution, 10 years of data) for up to 20 cumulative observations are quite similar. The NDVI from May–June (observations 10+) until August–September (observations 15+) and integrating up to 15 cumulative time points show positive associations with the corresponding annual RWI. However, the correlation based on the MODIS resolution and time frame is stronger and sharper in time compared to the respective GIMMS3g ones, pointing to May–September (observations 15+) as the decisive months for forest growth.
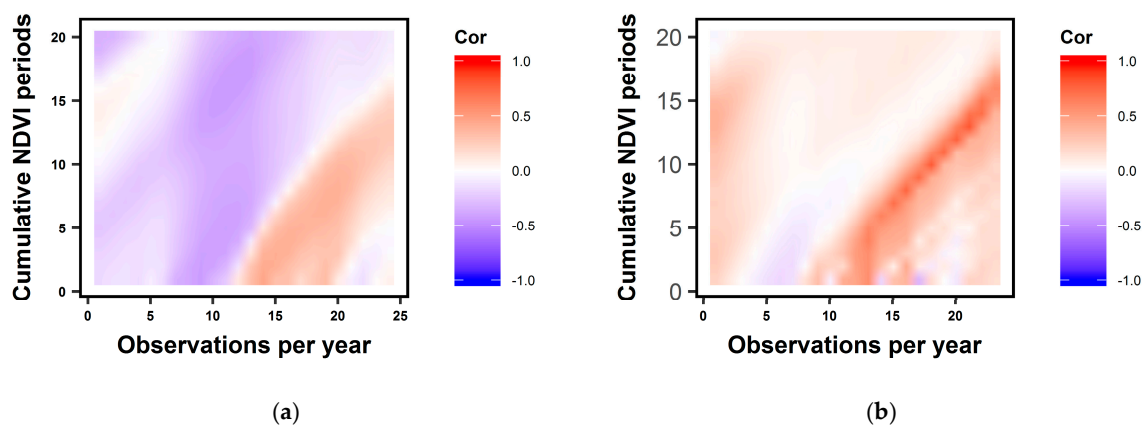

(**a**) (**b**)

Figure 2. Pearson correlation coefficients between time series of ring width index (RWI) and cumulative NDVI at different temporal scales (1–20, y-axis) at a continental D climate site with a coniferous forest in Utah, United States of America for (**a**) GIMMS3g, 8 km resolution (1982–2010) with 24 time points in a year (x-axis) and (**b**) MODIS, 250 m resolution (2001–2010) with 23 time points in a year (x-axis).

In general, the correlation patterns between RWI and NDVI show these positive inter-annual associations, yet strong variations with species type (deciduous versus coniferous), climatic zone (B, C, and D), spatial scale (GIMMS3g versus MODIS), and integration time (up to 20 observations of the NDVI time series) are observed. Figure 3 displays the correlation patterns for all sites summarized as mean correlations of the four groups. For broadleaf species, growth in terms of RWI is (if at all) represented by MODIS NDVI during spring and the optimal length of the cumulative time period is not well defined. The signal for GIMMS3g NDVI is even weaker, more spread-out, and does not display any pattern. For coniferous trees in the semiarid to arid climate zone B, tree growth is strongly associated with a wide-ranging MODIS NDVI signal, from the start of the year until early summer and for cumulative periods of up to 15–20 NDVI observations. For GIMMS3g NDVI, RWI is tightly linked to NDVI of summer months and up to 20 cumulative NDVI observations. For conifers in

climate zone C, the MODIS NDVI growth signal is stronger than the GIMMS3g NDVI signal. It is represented by summer months at a cumulative period of up to 7–10 NDVI observations, whereas the weaker GIMMS3g signal has cumulative periods of up to 15–20 NDVI observations. For conifers in climate zone D, the MODIS NDVI signal is strong and represents growth during the summer and up to 10–15 cumulative NDVI observations. In contrast, the GIMMS3g NDVI signal is almost nonexistent. The corresponding variances of the respective Pearson correlation coefficients are shown in Figure S2 (Supplementary).
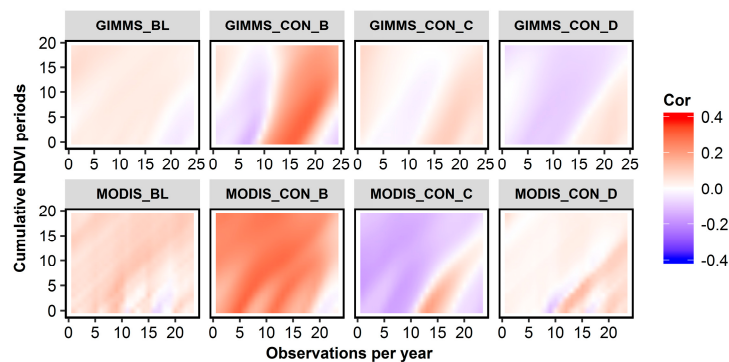

Figure 3. Mean Pearson correlation coefficients between time series of RWI and cumulative NDVI at different temporal scales (1–20, y-axis) for 69 tree-ring sites. Cumulative NDVI is either based on GIMMS3g (8 km resolution, 1982–2010) or MODIS (250 m resolution, 2000–2010). BL indicates 16 sites with broadleaf species, CON_B, CON_C, and CON_D refers to 4, 21, and 28 sites with coniferous tree species in climate zones B, C, and D, respectively. BL and CON refer to broadleaf and conifer species respectively. Zone B indicates arid/semiarid climate, C and D represent temperate and continental climates, respectively, as per the Köppen—Geiger climate classification [40].

3.2. Explaining RWI with NDVI Metrics and Climate

3.2.1. Variable Importance in RF based on MODIS NDVI/Climate

The RWI-climate model explained 28.2% of the variance of the RWI. When MODIS NDVI predictors were added to the model, the RWI-climate-NDVI model (Table 2) explained 37.2% of the variance of the RWI. The results of the RFs to describe the relationship between RWI and conditioning factors (MODIS NDVI /climate) in terms of the importance of the selected variables are shown in Figure 4. The Increased Mean Square Error lists the seven most important variables as scPDSI (9.30), NDVI_Sum (4.66), NDVI_Spr_prv (3.00), PRE (2.82), NDVI_Sum_prv (2.27), Latitude (2.24) and NDVI_GS (1.88). We notice similar results according to the Increased Impurity Index, which lists scPDSI (1.40), NDVI_Sum (0.61), PRE (0.42), NDVI_Sum_prv (0.27), NDVI_Spr_prv (0.24), Latitude (0.23), and NDVI_Spr (0.23) as the most important variables for the model.

Table 2. Results of RF models to explain RWI using two different datasets (GIMMS3g and MODIS). Here, NRMSE denotes the normalized root mean square error (in test data), and the explained variance is the explained-variation proportion in the outcome of the training data. The period of analysis for both the RF models is 2001 to 2010.

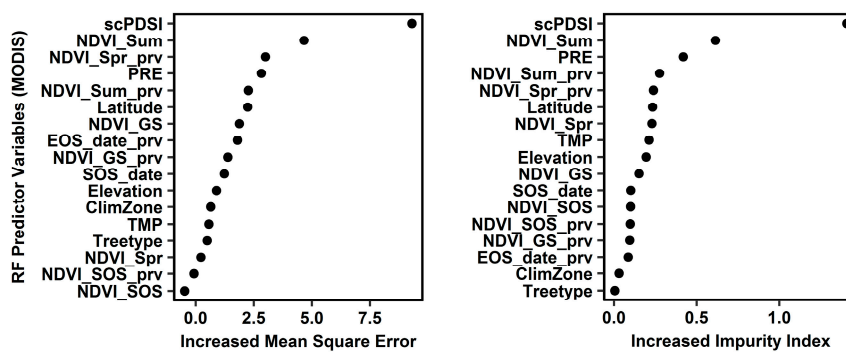| Model No.	Response Variable	Dataset	Explained Variance	Important Predictor Variables	NRMSE
1	RWI	Climate + MODIS NDVI	37.2%	scPDSI, NDVI_Sum, NDVI_Spr_prv, PRE, NDVI_Sum_prv, Latitude NDVI_GS	0.13
2	RWI	Climate + GIMMS3g NDVI	29.7%	scPDSI, NDVI_Sum, TMP, NDVI_Sum_prv, Elevation, NDVI_GS_prv, Latitude	0.26

Figure 4. Random-forest variable-importance plot for RF (MODIS) climate-NDVI model. Variables are ranked in terms of importance on the y-axis (with variables of highest importance for explaining RWI at the top). PRE, TMP, scPDSI, Latitude, Elevation, Tree type, and ClimZone represent precipitation, temperature, self-calibrating Palmer Drought Severity Index, latitude of the forest site, elevation of the forest site, tree type (coniferous or broadleaf), and climate zone (B, C or D) as per the Köppen–Geiger climate classification [40], respectively. For definitions of the NDVI phenological metrics: NDVI_GS, NDVI_GS_prv, NDVI_Sum, NDVI_Sum_prv, NDVI_Spr, NDVI_Spr_prv, NDVI_SOS, NDVI_SOS_prv, SOS_date, and EOS_date_prv, see Table 1.

3.2.2. Variable Importance in RF based on GIMMS3g NDVI/Climate

An analogous RF approach was used to model tree growth with climate and GIMMS3g NDVI. The RWI-climate model explained 28.2% of the variance of the RWI. When GIMMS3g NDVI predictors were added to the RWI-climate model, the RWI-climate-NDVI model (Table 2) explained 29.7% of the variance. In general, the importance of predictors was found to be similar to the case of MODIS NDVI, however, the model explained less variance compared to the model with MODIS data. The variable-importance measure, the Increased Mean Square Error lists scPDSI, NDVI_Sum, TMP, NDVI_Sum_prv, Elevation, NDVI_GS_prv and Latitude as the most important variables. The Increased Impurity Index lists NDVI_Spr, scPDSI, Latitude, NDVI_GS, PRE, NDVI_GS_prv, and NDVI_Sum as the important variables. As the increase in variance explained after adding NDVI metrics was approximately 1.5%, the results of the GIMMS3g NDVI are not discussed in detail.

3.3. Important NDVI Metrics and Validation of MODIS RF Model

We extracted several phenological parameters from the NDVI time series. However, it was shown that not all of the extracted parameters were equally important for the RF models. When added to climate, the following NDVI phenological metrics better explained tree-ring growth: Summer NDVI of the current and previous year followed by spring NDVI of the previous year and growing season NDVI of current and previous year. While validating the model, the following validation metrics were computed: the mean RE (0.03), the MAE ratio (0.66) and the RMSE ratio (0.53). The ratios which were calculated between the values of the RF model and the test dataset showed weak prediction skills of the validation model and in general performed approximately half as well as the RF model. A scatterplot between the observed RWI from the test dataset and predicted RWI from the RF model, (Figure S4, Supplementary) show that they are not very well correlated.

4. Discussion

4.1. Relationship between RWI-NDVI

In general, a positive relationship between NDVI in the growing season and RWI was seen for many forests in our study. Early work by Kaufmann et al. [50] based on GIMMS data equally showed a positive correlation between tree-rings and NDVI over the entire growing season and monthly values for April–July and October. Nevertheless, the positive and robust relationship observed between radial

growth and NDVI identified for 69 sites across the Northern Hemisphere at the local level cannot be considered a rule on the global scale [7]. For broadleaf species of different climate zones (B, C, D), we found that growth in terms of RWI was only weakly correlated by a weak MODIS NDVI signal during spring, with the optimal length of the cumulative time period not well defined and by an even weaker GIMMS3g signal that did not display any clear pattern. This is in line with findings of Brehaut et al. [51] for Northern Canada, where little or no correlation across the region for deciduous trees was observed. For conifers in a continental (D) climate, growth was linked to a MODIS NDVI signal during summer at cumulative NDVI periods of up to 10–15. This finding is supported by earlier studies based on GIMMS data, e.g. by Lopatin et al. [14] for continental Russia reporting a similar positive association between NDVI of June to August and conifer growth (Siberian spruce and Scots pine) as well as by Bunn et al. [4] for Siberia. Similarly, for North America, studies have reported positive associations between NDVI and conifer ring-widths for the interior of Alaska [52], for Siberia/Canada [22], and for Northern Canada [51]. However, this is contradictory to a study by Beck et al. [21], who found no significant correlation between ring-widths of Canadian spruce and NDVI at any point during the growing season. It should be pointed out here that the majority of the studies mentioned above used GIMMS/GIMMS3g NDVI for their analyses and not MODIS as in our study. For conifers in semiarid (B) climate, growth was represented by a wide-ranging MODIS NDVI signal but this was tightly linked to summer months at a cumulative period of up to 20 by GIMMS3g. For conifers in a temperate (C) climate, growth was strongly represented by MODIS NDVI of summer months at a cumulative period of up to 10. There are no comparable studies for these climate regions to support or contradict our findings. The variance of the Pearson correlation coefficients between NDVI and RWI was generally small (see Supplementary, Figure S2) except for conifer species in arid/semi-arid zone B, indicating that there is some confidence in the above interpretation. The comparably large variance in the correlation coefficient for the B climate zone is most likely due to the small number of sites (n = 4) included. In some forests in our study, a negative relationship between NDVI and RWI was observed. The reasons for such a mismatch could be varied growth-responses of trees depending on site-level factors [53], or the effects of changing environmental conditions.

4.2. Relationship between RWI, NDVI Phenological Metrics and Climate Parameters Based on RF Model

In general, when comparing the variables identified as important in the RF approach, it should be noted that the variable-importance score depends on the number of included variables. Removing or replacing predictors, for example, may change the importance scores because different inter-correlated variables could act as surrogates. RFs use bagging to build the many different decision trees on the same dataset. While each individual decision would fit the identical model to the exact same data, a different aggregate model is observed each run because it takes different bootstrap samples. Nevertheless, in the second part of this study (Section 3.2), we could demonstrate that NDVI phenological metrics have the potential to improve relationships between RWI and climate. In order to identify the most important NDVI metrics derived from phenology, we ran various random forest models to explain RWI of the period 2001–2010; firstly using climate data as predictors and secondly using both climate and NDVI metrics as predictors. Using MODIS NDVI metrics and climate data, 37.2% of the variance of RWI could be explained, increasing it from 28.2% if only climate was used as predictor for RWI (see Table 2). In contrast, for the GIMMS3g model, the increase was approximately 1.5 percent (28.2% versus 29.7%) after adding NDVI metrics. This clearly underlines that including MODIS NDVI based phenological information improved the RWI modelling noticeably. The difference in performance of the two NDVI based models could be because high-spatial-resolution of the MODIS data is able to capture local climatic or other information reflecting the changes in vegetation or RWI better than the coarse-spatial-resolution GIMMS data, since the latter with a spatial-resolution of 8 km is more likely to contain an integrated signal as well as noise. Our results indicate a relatively better performance of the MODIS NDVI model compared to the GIMMS3g NDVI model, and this is in line with the findings of Kern et al. [54]. In their comparative study of GIMMS3g and MODIS NDVI, a significant disagreement is reported and a limited

applicability of GIMMS3g is concluded for Central Europe. Moreover, GIMMS3g-based SOS and EOS detection showed poorer performance than MODIS with differences of up to 20–30 days in the majority of the cases without any systematic fashion. Amongst NDVI phenological metrics, we found that the RWI was best reflected by the summer NDVIs of current and previous years. This is in agreement with the findings of Kauffman et al. [15], who suggested that tree-rings are correlated with NDVI in the months of June–July. Other important NDVI parameters found in our study were the spring and growing season NDVIs of previous and current years. They had a higher score than precipitation in the RF model, which demonstrates the potential of NDVI metrics derived from phenology to improve RWI-climate relationships. Amongst the climatic parameters and auxiliary factors, it was precipitation, drought index scPDSI, and latitude that were highly ranked in the RF approach, whereas climate zone and tree type were the least important ones. It is worth noting that according to the variable score, summer and spring NDVIs of the previous year had a higher score than precipitation. Although scPDSI integrates the precipitation signal, the variable score reflects the potential of NDVI metrics to refine existing climate-RWI relationships. Similar results of the RF MODIS models were obtained using SPEI, a multiscalar index that takes into account the sensitivity to the evaporative demand of the atmosphere (Supplementary, Figure S5). However, the proportion of variance explained was lower (22.1% instead of 37.2%) and therefore the results were not presented in detail.

The results of our study were consistent across tree-ring chronologies set up with three different detrending methods (not shown in this paper). This clearly demonstrates that our obtained results are not an artifact of the detrending and standardization methods. Despite the considerable model improvement through the incorporation of MODIS phenological metrics, we have to stress that according to different validation metrics (Section S3, Supplementary), the RF model is still not very robust for prediction. However, with this study we aim to only compare the two NDVI datasets, to propose which NDVI phenological metrics have higher potential to explain RWI but not to reconstruct or predict RWI. One possible reason that the prediction skills are not robust could be that the present study is constrained by the assumption that the forests being analyzed lie within the NDVI pixel, which cannot be further investigated because of a lack of auxiliary information about the sites. There is no accurate information on whether species composition was homogeneous or heterogeneous across the landscape, or whether the proportions of multiple dominant species are comparable and responding similarly to climatic variables. Hence, the interpretation of NDVI and its relation to ring-widths becomes challenging. Also, tree-ring data collected originally for dendrochronological studies, if not spatially representative of a large area, can hamper correlations between the NDVI and the tree-ring data [55].

5. Conclusions

This paper presents the first comparison of RWI with several phenological parameters of satellite-derived proxies of vegetation activity at multiple sites in the Northern Hemisphere. We demonstrated positive associations between RWI and NDVI and between RWI and the NDVIs of preceding years, and noted that such relationships vary over space and between tree types (deciduous versus coniferous), bioclimatic zones, cumulative NDVI periods and the spatial resolution. Summer and spring NDVIs were found to be the most important NDVI metrics amongst those tested. There is strong potential for NDVI phenological metrics to improve RWI-climate relationships, especially for high-spatial-resolution NDVI, such as MODIS. However, further research is needed to investigate the robustness of the NDVI–RWI relationship. Therefore, it will be particularly interesting to see the results when more tree-ring data and longer temporal records of the high-spatial-resolution NDVI become available.

performed with drought index SPEI. Table S1: Information on sites analyzed: country, co-ordinates, species, climate zone (see climate data), elevation, important tree-ring metrics and chronology coverage.

Author Contributions: Upasana Bhuyan, Annette Menzel, Sergio M. Vicente-Serrano and Christian Zang conceptualized the design of the study. Upasana Bhuyan carried out the data processing. Upasana Bhuyan and Annette Menzel wrote the manuscript. All authors contributed to the interpretation of results and editing of the manuscript.

Conflicts of Interest: The authors declare no conflict of interest.

References

1. Pettorelli, N.; Vik, J.O.; Mysterud, A.; Gaillard, J.M.; Tucker, C.J.; Stenseth, N.C. Using the satellite-derived NDVI to assess ecological responses to environmental change. *Trends Ecol. Evol.* **2005**, *20*, 503–510. [CrossRef] [PubMed]

2. Danby, R.K. Monitoring forest-tundra ecotones at multiple scales. *Geogr. Compass* **2011**, *5*, 623–640. [CrossRef]

3. Biondi, F. Comparing tree-ring chronologies and repeated timber inventories as forest monitoring tools. *Ecol. Appl.* **1999**, *9*, 216–227. [CrossRef]

4. Bunn, A.G.; Hughes, M.K.; Kirdyanov, A.V.; Losleben, M.; Shishov, V.V.; Berner, L.T.; Oltchev, A.; Vaganov, E.A. Comparing forest measurements from tree rings and a space-based index of vegetation activity in Siberia. *Environ. Res. Lett.* **2013**, *8*. [CrossRef]

5. Fritts, H.C.; Blasing, T.J.; Hayden, B.P.; Kutzbach, J.E. Multivariate techniques for specifying tree-growth and climate relationships and for reconstructing anomalies in paleoclimate. *J. Appl. Meteorol.* **1971**, *10*, 845–864. [CrossRef]

6. Dobbertin, M. Tree growth as indicator of tree vitality and of tree reaction to environmental stress: A review. *Eur. J. For. Res.* **2005**, *24*, 319–333. [CrossRef]

7. Vicente-Serrano, S.M.; Camarero, J.J.; Olano, J.M.; Martín-Hernández, N.; Peña-Gallardo, M.; Tomás-Burguera, M.; Gazol, A.; Azorin-Molina, C.; Bhuyan, U.; Kenawy, A. Diverse relationships between forest growth and the Normalized Difference Vegetation Index at a global scale. *Remote Sens. Environ.* **2016**, *187*, 14–29. [CrossRef]

8. Camarero, J.J.; Franquesa, M.; Sangüesa-Barreda, G. Timing of drought triggers distinct growth responses in holm oak: implications to predict warming-induced forest defoliation and growth decline. *Forests* **2015**, *6*, 1576–1597. [CrossRef]

9. Cook, E.R.; Kairiukstis, L.A. *Methods of Dendrochronology: Applications in the Environmental Sciences*; Springer Netherlands: Dordrecht, The Netherlands, 1990.

10. Tucker, C.J. Red and photographic infrared linear combinations for monitoring vegetation. *Remote Sens. Environ.* **1979**, *8*, 127–150. [CrossRef]

11. Myneni, R.B.; Keeling, C.D.; Tucker, C.J.; Asrar, G.; Nemani, R.R. Increased plant growth in the northern high latitudes from 1981 to 1991. *Nature* **1997**, *386*, 698–702. [CrossRef]

12. Liang, E.Y.; Shao, X.M.; He, J.C. Relationships between tree growth and NDVI of grassland in the semi-arid grassland of north China. *Int. J. Remote Sens.* **2005**, *26*, 2901–2908. [CrossRef]

13. Wang, J.; Rich, P.M.; Price, K.P.; Kettle, W.D. Relations between NDVI, grassland production, and crop yield in the central Great Plains. *Geocarto Int.* **2005**, *20*, 5–11. [CrossRef]

14. Lopatin, E.; Kolström, T.; Spiecker, H. Determination of forest growth trends in Komi Republic (northwestern Russia): Combination of tree-ring analysis and remote sensing data. *Boreal Environ. Res.* **2006**, *11*, 341–353.

15. Kaufmann, R.K.; D'Arrigo, R.D.; Paletta, L.F.; Tian, H.Q.; Jolly, W.M.; Myneni, R.B. Identifying climatic controls on ring width: The timing of correlations between tree rings and NDVI. *Earth Interact.* **2008**, *12*, 1–14. [CrossRef]

16. Prince, S.D.; Tucker, C.J. Satellite remote sensing of rangelands in Botswana II. NOAA AVHRR and herbaceous vegetation. *Int. J. Remote Sens.* **1986**, *7*, 1555–1570. [CrossRef]

17. Sellers, P.J.; Randall, D.A.; Collatz, G.J.; Berry, J.A.; Field, C.B.; Dazlich, D.A.; Zhang, C.; Collelo, G.D.; Bounoua, L. A revised land surface parameterization (SiB2) for atmospheric GCMs. Part I: Model formulation. *J. Clim.* **1996**, *9*, 676–705. [CrossRef]

18. Menzel, A.; Fabian, P. Growing season extended in Europe. *Nature* **1999**, *397*. [CrossRef]

19. Menzel, A.; Sparks, T.H.; Estrella, N.; Koch, E.; Aasa, A.; Ahas, R.; Alm-Kübler, K.; Bissolli, P.; Braslavská, O.; Briede, A.; et al. European phenological response to climate change matches the warming pattern. *Glob. Chang. Biol.* **2006**, *12*, 1969–1976. [CrossRef]

20. Justice, C.O.; Townshend, J.R.G.; Holben, B.N.; Tucker, C.J. Analysis of the phenology of global vegetation using meteorological satellite data. *Int. J. Remote Sens.* **1985**, *6*, 1271–1318. [CrossRef]

21. Beck, P.S.A.; Andreu-Hayles, L.; D'Arrigo, R.D.; Anchukaitis, K.J.; Tucker, C.J.; Pinzón, J.E.; Goetz, S.J. A large-scale coherent signal of canopy status in maximum latewood density of tree rings at arctic treeline in North America. *Glob. Planet. Chang.* **2013**, *100*, 109–118. [CrossRef]

22. Berner, L.T.; Beck, P.S.A.; Bunn, A.G.; Goetz, S.J. Plant response to climate change along the forest-tundra ecotone in northeastern Siberia. *Glob. Chang. Biol.* **2013**, *19*, 3449–3462. [CrossRef] [PubMed]

23. Churkina, G.; Schimel, D.; Braswell, B.H.; Xiao, X. Spatial analysis of growing season length control over net ecosystem exchange. *Glob. Chang. Biol.* **2005**, *11*, 1777–1787. [CrossRef]

24. Richardson, A.D.; Raswell, B.H.; Hollinger, D.Y.; Jenkins, J.P. Near-surface remote sensing of spatial and temporal variation. *Ecol. Appl.* **2009**, *19*, 1417–1428. [CrossRef] [PubMed]

25. Liu, Y.; Wu, C.; Peng, D.; Xu, S.; Gonsamo, A.; Jassal, R.S.; Arain, M.A.; Lu, L.; Fang, B.; Chen, J.M. Improved modeling of land surface phenology using MODIS land surface reflectance and temperature at evergreen needleleaf forests of central North America. *Remote Sens. Environ.* **2016**, *176*, 152–162. [CrossRef]

26. Ganguly, S.; Friedl, M.A.; Tan, B.; Zhang, X.; Verma, M. Land surface phenology from MODIS: Characterization of the Collection 5 global land cover dynamics product. *Remote Sens. Environ.* **2010**, *114*, 1805–1816. [CrossRef]

27. Dong, T.; Liu, J.; Shang, J.; Qian, B.; Huffman, T.; Zhang, Y.; Champagne, C.; Daneshfar, B. Assessing the impact of climate variability on cropland productivity in the Canadian prairies using time series MODIS FAPAR. *Remote Sens.* **2016**, *8*. [CrossRef]

28. Briffa, K.R.; Osborn, T.J.; Schweingruber, F.H.; Jones, P.D.; Shiyatov, S.G.; Vaganov, E. Tree-ring width and density data around the Northern Hemisphere: Part 1, local and regional climate signals. *Holocene* **2002**, *12*, 737–757. [CrossRef]

29. MOD13Q1: MODIS/Terra Vegetation Indices 16-Day L3 Global 250m Grid SIN V006. Available online: https://lpdaac.usgs.gov/dataset_discovery/modis/modis_products_table/mod13q1_v006 (accessed on 18 February 2016).

30. GIMMS NDVI3g Dataset. ECOCAST. Available online: https://ecocast.arc.nasa.gov/data/pub/gimms/ (accessed on 26 February 2016).

31. Tree Ring. National Centers for Environmental Information, NOAA. Available online: https://www.ncdc.noaa.gov/data-access/paleoclimatology-data/datasets/tree-ring (accessed on 4 February 2016).

32. Grissino-Mayer, H.D.; Fritts, H.C. The international tree-ring data bank: An enhanced global database serving the global scientific community. *Holocene* **1997**, *7*, 235–238. [CrossRef]

33. Olivier, A.; Jose Julio, R.P.; Vasileios, K.; Bontemps, S.; Defourny, P.; Van Bogaert, E. Global Land Cover Map for 2009 (GlobCover 2009). Available online: https://doi.pangaea.de/10.1594/PANGAEA.787668 (accessed on 30 May 2016).

34. Cook, E.R.; Peters, K. Calculating unbiased tree-ring indices for the study of climatic and environmental change. *Holocene* **1997**, *7*, 361–370. [CrossRef]

35. Harris, I.; Jones, P.D.; Osborn, T.J.; Lister, D.H. Updated high-resolution grids of monthly climatic observations—The CRU TS3.10 Dataset. *Int. J. Climatol.* **2014**, *34*, 623–642. [CrossRef]

36. Jones, P. D.; Harris, I. CRU TS3.21: Climatic Research Unit (CRU) Time-Series (TS) Version 3.21 of High Resolution Gridded Data of Month-by-Month Variation in Climate (January 1901–December 2012). 2013. Available online: http://catalogue.ceda.ac.uk/uuid/ac4ecbd554d0dd52a9b575d9666dc42d (accessed on 10 Jan 2016).

37. Wells, N.; Goddard, S.; Hayes, M.J. A self-calibrating palmer drought severity index. *J. Clim.* **2004**, *17*, 2335–2351. [CrossRef]

38.　CRU scPDSI 3.25. KNMI Climate Explorer. Available online: https://climexp.knmi.nl/select.cgi?id= someone@somewhere&field=scpdsi (accessed on 10 January 2016).

39.　Vicente-Serrano, S.M.; Beguería, S.; López-Moreno, J.I. A multiscalar drought index sensitive to global warming: The standardized precipitation evapotranspiration index. *J. Clim.* **2010**, *23*, 1696–1718. [CrossRef]

40.　Kottek, M.; Grieser, J.; Beck, C.; Rudolf, B.; Rubel, F. World map of the Köppen-Geiger climate classification updated. *Meteorol. Z.* **2006**, *15*, 259–263. [CrossRef]

41.　Pinzon, J.E.; Tucker, C.J. A non-stationary 1981–2012 AVHRR NDVI3g time series. *Remote Sens.* **2014**, *6*, 6929–6960. [CrossRef]

42.　Haddad, R.A.; Akansu, A.N. A class of fast Gaussian binomial filters for speech and image processing. *IEEE Trans. Signal Process.* **1991**, *39*, 723–727. [CrossRef]

43.　Misra, G.; Buras, A.; Menzel, A. Effects of different methods on the comparison between land surface and ground phenology—A methodological case study from south-western Germany. *Remote Sens.* **2016**, *8*. [CrossRef]

44.　Wohlfart, C.; Liu, G.; Huang, C.; Kuenzer, C. A river basin over the course of time: multi-temporal analyses of land surface dynamics in the yellow river basin (China) based on medium resolution remote sensing data. *Remote Sens.* **2016**, *8*. [CrossRef]

45.　Breiman, L. Random forests. *Mach. Learn.* **2001**, *45*, 5–32. [CrossRef]

46.　Rodriguez-Galiano, V.F.; Dash, J.; Atkinson, P.M. Intercomparison of satellite sensor land surface phenology and ground phenology in Europe. *Geophys. Res. Lett.* **2015**, *42*, 2253–2260. [CrossRef]

47.　Pourtaghi, Z.S.; Pourghasemi, H.R.; Aretano, R.; Semeraro, T. Investigation of general indicators influencing on forest fire and its susceptibility modeling using different data mining techniques. *Ecol. Indic.* **2016**, *64*, 72–84. [CrossRef]

48.　R Core Team. R: A Language and Environment for Statistical Computing. Available online: http://www. gbif.org/resource/81287 (accessed on 22 February 2017).

49.　Liaw, A.; Wiener, M. Classification and regression by randomForest. *R News* **2002**, *3*, 18–22.

50.　Kaufmann, R.K.; D'Arrigo, R.D.; Laskowski, C.; Myneni, R.B.; Zhou, L.; Davi, N.K. The effect of growing season and summer greenness on northern forests. *Geophys. Res. Lett.* **2004**, *31*, 3–6. [CrossRef]

51.　Brehaut, L.D. 2015. The Use of NDVI and Tree Ring-Widths to Evaluate Changes in Vegetation Production in a Mountainous Boreal Landscape. Master's Thesis, Queen's University, Kingston, ON, Canada, 2015.

52.　Beck, P.S.A.; Goetz, S.J. Satellite observations of high northern latitude vegetation productivity changes between 1982 and 2008: Ecological variability and regional differences. *Environ. Res. Lett.* **2011**, *6*. [CrossRef]

53.　Wilmking, M.; D'Arrigo, R.D.; Jacoby, G.C.; Juday, G.P. Increased temperature sensitivity and divergent growth trends in circumpolar boreal forests. *Geophys. Res. Lett.* **2005**, *32*, 2–5. [CrossRef]

54.　Kern, A.; Marjanović, H.; Barcza, Z. Evaluation of the quality of NDVI3g dataset against collection 6 MODIS NDVI in central Europe between 2000 and 2013. *Remote Sens.* **2016**, *8*. [CrossRef]

55.　D'Arrigo, R.D.; Malmstrom, C.M.; Jacoby, G.C.; Los, S.O.; Bunker, D.E. Correlation between maximum latewood density of annual tree rings and NDVI based estimates of forest productivity. *Int. J. Remote Sens.* **2000**, *21*, 2329–2336. [CrossRef]

Supplementary material

Upasana Bhuyan, Christian Zang, Sergio M. Vicente−Serrano, Annette Menzel
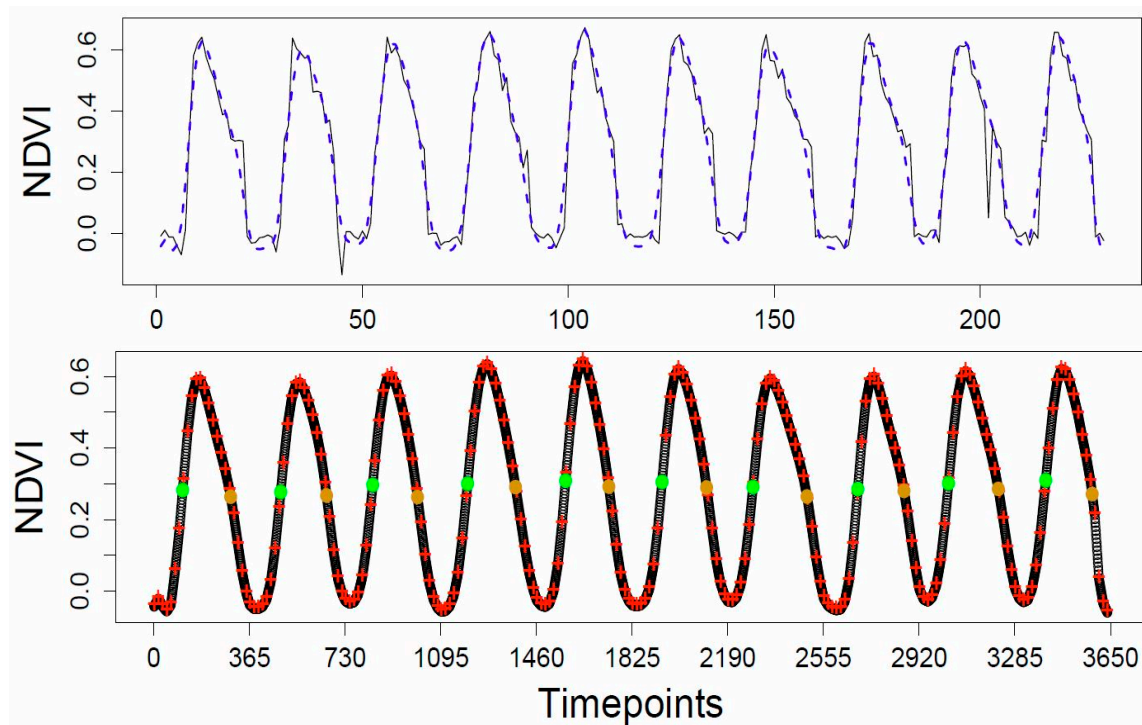

Figure S1. Figure showing preprocessing and phenology extraction from NDVI time series. Raw (black) and corrected and smoothed (dotted blue) time series of bi−weekly NDVI (upper panel) are interpolated to daily values for phenology extraction (lower panel). Red crosses represent the corrected bi−weekly NDVI values and the black points are interpolated ones. Start (SOS) and end (EOS) of the growing season (green and brown dots) are determined as time points when 50% of the annual amplitude are reached.
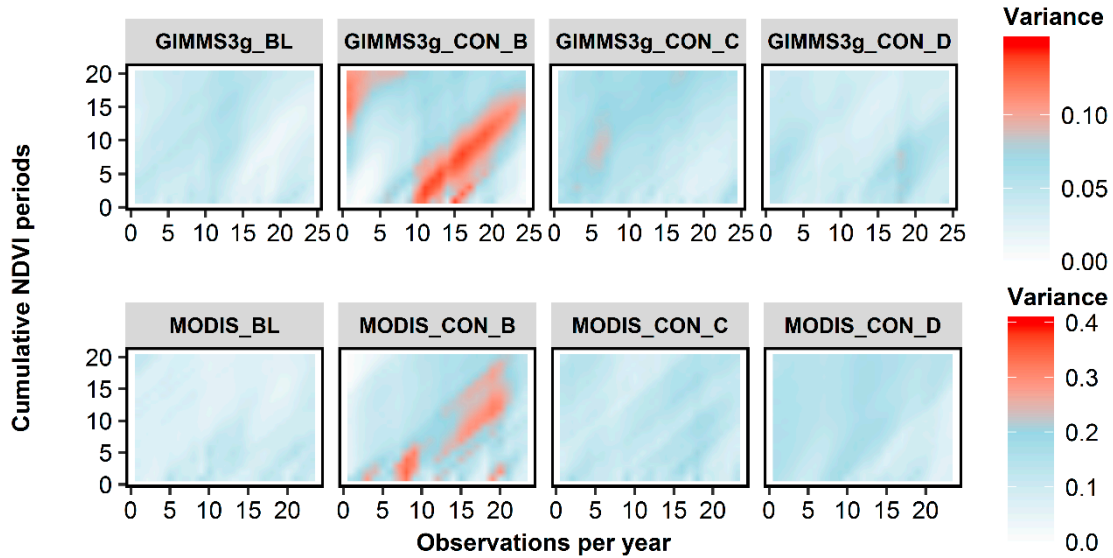
Figure S2 Variance of Pearson correlation coefficients between time series of RWI and cumulative NDVI at different temporal scales (1–20, y−axis) for 69 tree-ring sites. Cumulative NDVI is either based on GIMMS3g (8 km resolution) or MODIS (250 m resolution). BL indicates 16 sites with broadleaf species, CON_B, CON_C, and CON_D refers to 4, 21, and 28 sites with coniferous tree species in climate zones B, C, and D, respectively. Zone B indicates arid/semiarid climate, C and D represent temperate and continental climates, respectively, as per the Köppen–Geiger climate classification [1].

Section S3: Validation Statistics to Assess Performance of RF Model

In order to access the performance of the Climate−NDVI MODIS RF model, we list some validation statistics. Observed refers to observed RWI and predicted to the corresponding predictions of the Climate−MODIS NDVI Random Forest Model. In the formulae of the validation metric ratios, model refers to the training and validation to the test data.

- The mean relative error (RE) is given by mean of {(predicted − observed) / observed} = 0.03
- The mean absolute error (MAE) error ratio is given by mean ((abs (predicted − observed))), The MAE ratio is calculated as Model MAE/Validation MAE = 0.66.
- The root mean square error (RMSE) is given by sqrt(mean((predicted − observed)^2)), The RMSE ratio is calculated as Model RMSE/Validation RMSE = 0.53.

From the above we see that the mean Relative Error, the MAE ratio and RMSE ratio were calculated to be 0.03, 0.66 and 0.53, respectively. The results show that the model is not very robust for prediction. However, with this study we aim to only make a comparison of the different spatial−resolution NDVI datasets and propose which phenological metrics have the potential to best explain RWI. RWI reconstruction or prediction is not intended or suggested.
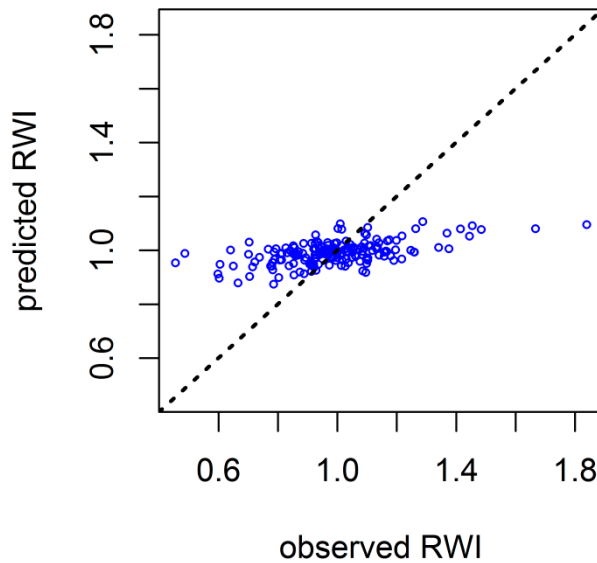
Figure S4. Scatter plot of observed and predicted RWI. The predicted values are from the Climate−MODIS NDVI Random Forest Model and observed values are from the test dataset. The black dashed line represents the line when intercept and slope is fixed at 0 and 1 respectively.
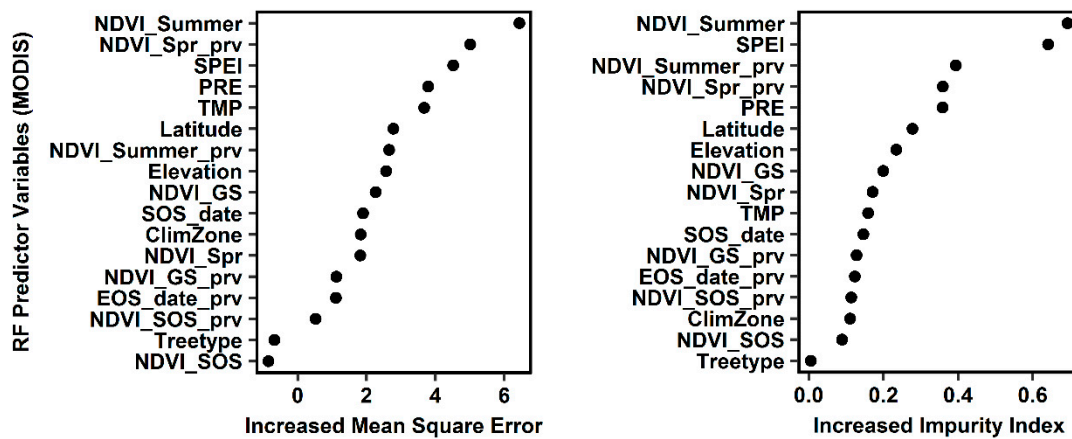

Figure S5. Random−forest variable−importance plot for RF (MODIS) climate−NDVI model performed with drought index SPEI. Variables are ranked in terms of importance on the y−axis (with variables of highest importance for predicting RWI at the top). PRE, TMP, SPEI, Latitude, Elevation, Tree type and ClimZone represent precipitation, temperature, Standardized Precipitation Evapotranspiration Index , latitude of the forest site, elevation of the forest site, tree type (coniferous or broadleaf) and climate zone (B, C or D) as per the Köppen–Geiger climate classification [1], respectively. For definitions of NDVI phenological metrics: NDVI_GS, NDVI_GS_prv, NDVI_Sum, NDVI_Sum_prv, NDVI_Spr, NDVI_Spr_prv, NDVI_SOS, NDVI_SOS_prv, SOS_date and EOS_date_prv, see Table 1. The variance of RWI of all forests explained by the RF model was 22.1%.

Table S1. Information on sites analyzed: Co−ordinates, species, climate zone (see climate data important tree−ring metrics and chronology coverage. Latitude (Lat) and Longitude (Lon) are the geographic coordinates (WGS84 datum) of each site. Country names are coded according to ISO3. For Type, "CON" and "BL" denotes conifers and broadleaves respectively. Zone B, C and D denote arid/semiarid, temperate and continental climates, respectively as per Köppen−Geiger climate classification [1]. Elevation is given in m a.s.l. The tree ring metrics shown are the mean inter−series correlation (RBAR) and mean sensitivity (MS). RBAR is the average correlation coefficient between tree−ring series and MS is a within−series statistic that measures the relative change in ring width from one year to the next.

ID	Country	Lat (°)	Lon (°)	Species	Type	Zone	Elevation	RBAR	MS	Start	End
UT531	USA	41.23	−111.26	*Juniperus scopulorum* Sarg.	CON	D	1980	0.62	0.24	1173	2010
UT538	USA	41.91	−111.65	*Pseudotsuga menziesii* (Mirb.) Franco	CON	D	2730	0.55	0.17	1274	2010
CA680	USA	37.46	−119.49	*Calocedrus decurrens* (Torr.) Florin	CON	C	1843	0.57	0.19	1581	2011
UT534	USA	40.15	−111.25	*Pinus edulis* Engelm.	CON	D	2130	0.65	0.28	1428	2011
UT533	USA	40.08	−111.2	*Pinus edulis* Engelm.	CON	D	1960	0.71	0.27	1313	2011
swit280	CHE	46.35	7.58	*Pinus cembra* L.	CON	D	1900	0.51	0.21	1546	2011
swit279	CHE	46.35	7.59	*Picea abies (L.)* Karst.	CON	D	1850	0.65	0.17	1670	2011
swit281	CHE	46.32	8.5	*Pinus cembra* L.	CON	D	1850	0.52	0.19	1707	2012
swit282	CHE	46.32	8.5	*Pinus mugo* Turra	CON	D	1920	0.5	0.18	1761	2012
swit274	ITA	46.26	9.47	*Larix decidua* Mill.	BL	D	1850	0.71	0.27	1691	2011
RUSS240	RUS	52.29	98.58	*Larix decidua* Mill.	BL	D	2170	0.65	0.3	1603	2013
VA036	USA	37.16	−80.26	*Quercus alba* L.	BL	C	800	0.53	0.24	1918	2010
UT532	USA	41.3	−111.23	*Juniperus scopulorum* Sarg.	CON	D	2100	0.58	0.2	1227	2010
UT536	USA	41.21	−111.58	*Pseudotsuga menziesii* (Mirb.) Franco	CON	D	2133	0.66	0.24	1370	2012
UT537	USA	41.22	−111.57	*Pseudotsuga menziesii* (Mirb.) Franco	CON	D	2750	0.54	0.21	1133	2011

ME036	USA	46.24	−69	*Picea rubens* Sarg.	CON	D	310	0.6	0.21	1879	2013
CANA458	CAN	53.52	−72.25	*Picea mariana* (Mill.) Britt.	CON	D	481	0.49	0.17	642	2011
CANA460	CAN	54.06	−71.38	*Picea mariana* (Mill.) Britt.	CON	D	451	0.49	0.16	774	2011
CANA461	CAN	54.15	−72.23	*Picea mariana* (Mill.) Britt.	CON	D	436	0.52	0.16	596	2011
NM588	USA	36.17	−106.38	*Pinus ponderosa* Dougl. ex Laws.	CON	D	2525	0.75	0.41	620	2011
NM589	USA	36.05	−108.52	*Pinus ponderosa* Dougl. ex Laws.	CON	B	2650	0.66	0.31	842	2010
MONG039	MNG	48.1	99.52	*Pinus sibirica* Du Tour	CON	D	2077	0.8	0.39	−106	2010
CA687	USA	37.33	−121.51	*Quercus lobata* Nee	BL	C	89	0.54	0.29	1697	2010
CA686	USA	37.33	−121.51	*Platanus racemosa* Nutt.	BL	C	89	0.54	0.38	1700	2010
BT021	BTN	27.25	90.58	*Picea* spp. A. Dietr.	CON	C	3268	0.42	0.16	1280	2013
CA674	USA	40.06	−120.38	*Pinus ponderosa* Dougl. ex Laws.	CON	C	1385	0.56	0.27	1450	2010
OR093	USA	43.42	−120.28	*Juniperus occidentalis* Hook.	CON	B	1475	0.82	0.42	870	2010
OR094	USA	43.57	−121.03	*Juniperus occidentalis* Hook.	CON	C	1146	0.79	0.46	830	2010
CA677	USA	39.34	−120.17	*Pinus Jeffreyi* Grev. & Balf. in A. Murr.	CON	C	1688	0.61	0.26	1415	2010
OR095	USA	43.09	−119.48	*Juniperus occidentalis* Hook	CON	B	1514	0.78	0.36	1337	2010
CA678	USA	37.57	−119.09	*Pinus Jeffreyi* Grev. & Balf. in A. Murr.	CON	C	2499	0.58	0.24	1304	2010
OR092	USA	43.1	−120.53	*Juniperus occidentalis* Hook	CON	C	1428	0.78	0.49	530	2010
GERM188	BEL	50.36	6.29	*Pinus sylvestris* L.	CON	C	415	0.66	0.24	1854	2011
OR097	USA	44.13	−121.52	*Tsuga mertensiana* (Bong.) Carr.	CON	C	1454	0.57	0.21	1837	2013

OR096	USA	44.26	−121.57	*Pseudotsuga menziesii* (Mirb.) Franco	CON	C	1139	0.5	0.17	1838	2013
WV009	USA	37.58	−80.56	*Pinus rigida* Mill.	CON	C	700	0.53	0.31	1828	2014
WV007	USA	37.59	−82.22	*Tsuga canadensis* (L.) Carr.	CON	C	250	0.55	0.24	1756	2012
WV006	USA	37.31	−80.59	*Tsuga canadensis* (L.) Carr.	CON	C	670	0.66	0.25	1858	2012
CZEC003	AUT	48.4	14.42	*Abies alba* Mill.	CON	C	785	0.51	0.2	1587	2010
CZEC004	AUT	48.4	14.42	*Fagus sylvatica* L.	BL	C	785	0.45	0.26	1603	2010
CZEC005	AUT	48.4	14.42	*Picea abies* (L.) Karst.	CON	C	785	0.49	0.21	1569	2010
CHIN073	CHN	28.36	119.27	*Pinus massoniana* Lamb.	CON	C	435	0.54	0.27	1846	2013
CO652	USA	37.14	−108.25	*Pseudotsuga menziesii* (Mirb.) Franco	CON	D	2226	0.78	0.42	480	2014
CO651	USA	37.16	−108.21	*Pseudotsuga menziesii* (Mirb.) Franco	CON	D	2226	0.82	0.4	722	2011
NY043	USA	44.21	−74.44	*Pinus strobus* L.	CON	D	455	0.58	0.2	1916	2012
AK149	USA	67.29	−162.13	*Picea glauca* (Moench) Voss	CON	D	120	0.57	0.24	1814	2012
AK148	USA	67.29	−162.13	*Picea glauca* (Moench) Voss	CON	D	125	0.5	0.26	1855	2012
RUSS241	RUS	52.24	98.41	*Larix sibirica* Ledeb.	BL	D	2020	0.44	0.29	1523	2013
GA023	USA	34.53	−84.39	*Tsuga canadensis* (L.) Carr.	CON	C	600	0.44	0.2	1947	2011
NC024	USA	35.17	−82.43	*Tsuga canadensis* (L.) Carr.	CON	C	670	0.46	0.22	1910	2010
PA016	USA	40	−77.48	*Tsuga canadensis* (L.) Carr.	CON	C	500	0.49	0.19	1896	2010
VA032	USA	37.11	−80.29	*Tsuga canadensis* (L.) Carr.	CON	C	570	0.57	0.25	1869	2010
WV008	USA	38.37	−79.47	*Tsuga canadensis* (L.) Carr.	CON	C	900	0.55	0.21	1770	2010

MN029	USA	46.17	−96.36	*Quercus macrocarpa* Michx.	BL	D	293	0.56	0.26	1877	2010
ND009	USA	47.54	−97.01	*Quercus macrocarpa* Michx.	BL	D	254	0.65	0.28	1854	2010
ND012	USA	46.51	−96.47	*Quercus macrocarpa* Michx.	BL	D	268	0.66	0.27	1870	2010
ND010	USA	46.53	−96.46	*Quercus macrocarpa* Michx.	BL	D	268	0.65	0.28	1878	2010
ND007	USA	48.58	−97.14	*Quercus macrocarpa* Michx.	BL	D	236	0.68	0.28	1856	2010
ND011	USA	46.52	−96.47	*Quercus macrocarpa* Michx.	BL	D	275	0.57	0.26	1886	2010
ND008	USA	47.56	−97.02	*Quercus macrocarpa* Michx.	BL	D	254	0.73	0.27	1865	2010
MN028	USA	48.58	−97.14	*Quercus macrocarpa* Michx.	BL	D	236	0.76	0.27	1890	2010
MN030	USA	46.17	−96.36	*Quercus macrocarpa* Michx.	BL	D	290	0.6	0.24	1868	2010
ak131	NA	58.23	−134.26	*Tsuga mertensiana* (Bong.) Carr.	CON	D	220	0.5	0.24	1454	2010
id015	USA	43.45	−116.06	*Pinus ponderosa* Dougl. ex Laws	CON	B	1825	0.62	0.25	1488	2011
ak134	USA	65	−147.39	*Picea mariana* (Mill.) Britt.	CON	D	431	0.41	0.23	1875	2010
ak133	USA	65	−147.39	*Picea mariana* (Mill.) Britt.	CON	D	465	0.54	0.23	1908	2010
ak135	USA	65	−147.4	*Picea mariana* (Mill.) Britt.	CON	D	317	0.5	0.23	1895	2010
ak136	USA	65	−147.4	*Picea mariana* (Mill.) Britt.	CON	D	300	0.43	0.21	1857	2012
UT541	USA	40.55	−111.13	*Juniperus osteosperma* (Torr.) Little	CON	D	2130	0.79	0.37	736	2013

References:

1. Kottek, M.; Grieser, J.; Beck, C.; Rudolf, B.; Rubel, F. World map of the Köppen−Geiger climate classification updated. *Meteorol. Z.* **2006**, *15*, 259–263.

Validation of drought indices using environmental indicators: streamflow and carbon flux data

Upasana Bhuyan-Erhardt[1*], Tobias M. Erhardt[2], Gregor Laaha[3], Christian Zang[4], Juraj Parajka[5], Annette Menzel[1, 6]

[1]Ecoclimatology, Department of Ecology and Ecosystem Management, Technische Universität München, Hans-Carl-von-Carlowitz-Platz 2, 85354 Freising, Germany

[2]Mathematical Statistics, Department of Mathematics, Technische Universität München, Boltzmannstraße 3, 85748 Garching b. München, Germany

[3]Institute of Applied Statistics and Computing, University of Natural Resources and Life Sciences, Peter-Jordan-Straße 82/I, 1190 Vienna, Austria

[4]Land Surface-Atmosphere Interactions, Department of Ecology and Ecosystem Management, Technische Universität München, Hans-Carl-von-Carlowitz-Platz 2, 85354 Freising, Germany

[5]Institute for Hydraulic and Water Resources Engineering, TU Wien, Karlsplatz 13/222, A-1040, Vienna, Austria

[6]Institute for Advanced Study, Technische Universität München, Lichtenbergstraße 2 a, 85748 Garching, Germany

* Correspondence:

E-mail: bhuyan@wzw.tum.de, Tel: +49 (0) 8161-714746, Fax: +49 (0) 8161-714753

Abstract

In several scientific disciplines, quantitative indices are the most popular approach for drought quantification. Aiming for refined drought characterization, the validation of such drought indices is of vital importance. It allows assessing the indices' accuracy in detecting drought. In this study, we compared the performance of established drought indices – the SPI (Standardized Precipitation Index) and the SPEI (Standardized Precipitation Evapotranspiration Index) – with standardized drought indices computed using a recently developed, vine copula based method for the computation of multivariate drought indices (here addressed as VC-Index or VCI). For our validation study, we used several environmental drought indicators: streamflow time series from a network of 332 catchments across Europe, as well as gross primary production (GPP) and net ecosystem exchange (NEE) for Germany. The novel multivariate VC-Indices can combine two or more user-selected, drought relevant variables to model different drought types, depending on the user-application. This approach utilizes the flexibility of vine copulas in modeling multivariate non-Gaussian dependencies and allows for stable indices using much shorter observation periods. The results of the validation showed that the VC-Indices outperform the established drought indices SPI and SPEI. For the streamflow data, the VCI was found to have advantageous attributes such as higher probability of drought detection and lower false alarm ratio compared to SPEI and SPI. Regression of the drought indices against NEE and GPP showed that the VCI captured the drought-impact relationship on carbon flux data best. Overall, our results emphasize that the major key to improving our understanding of drought impacts on ecosystem conditions could be a user-defined, application-based drought monitoring on a high spatial resolution, using a method such as vine copulas. We recommend using the VCI as an additional source of information, in order to allow better understanding of drought characterization.

1 Introduction

Drought is a complex, multidimensional climatic phenomenon and a major cause of economic and environmental damage (Wilhite & Glantz, 1985; Obasi, 1994; Mishra & Singh, 2010). The mean global air temperature has increased by 0.85°C during the period 1880–2012 (IPCC, 2013) which has led to an increasing rise in water demand entailing drought aggravation in the recent years (Kogan et al., 2013). Droughts are rare events of water deficit that propagate through the hydrological cycle and may manifest themselves as meteorological, soil moisture, streamflow and ground water drought (Tallaksen & Van Lanen, 2004; Laaha et al, 2017). As such, a universal definition of drought does not exist and it is difficult to determine its start, termination and extent, making it fundamentally different from other climate extremes (Tate & Gustard, 2000; Wilhite & Glantz, 1985). Therefore, it becomes challenging to quantify the characteristics of drought episodes with objectivity in terms of their intensity, magnitude, duration and spatial extent (Vicente-Serrano et al., 2010).

Quantitative indices are – for many scientific disciplines – among the most popular approaches for drought quantification. Such indices integrate drought related variables such as precipitation into a single number that is more useful for decision making compared to the raw data (Hayes et al., 2007). Most studies on drought in scientific disciplines such as dendroecology, ecology, remote sensing and agricultural sciences that use drought indices, primarily employ either the Standardized Precipitation Evapotranspiration Index (SPEI, Vicente-Serrano et al., 2010) or Standardized Precipitation Index (SPI, Mckee et al., 1993). These standardized indices account only for one or two climatic variables promoting drought conditions and neglect their dependence (Erhardt & Czado, 2017). Several studies have argued that a single variable is inadequate for describing a complex, stochastic phenomenon like drought and that combining multiple variables/indicators is essential for reliable risk assessment (Hao & AghaKouchak, 2013). In the recent years, an array of drought indices that combine at least two variables have been developed (Keyantash & Dracup, 2004; Kao & Govindaraju, 2010; Hao & AghaKouchak, 2013; Farahmand & AghaKouchak, 2015). Erhardt & Czado (2017) discuss and compare the properties and disadvantages of these recent approaches with other established drought indices such as SPI and SPEI, and provide a list of desirable properties for drought indices. Based on this list, they develop a flexible approach for the computation of standardized drought indices that allows the end-users to decide which type(s) of drought to investigate and to select drought relevant variables for their specific application. Their multivariate

approach models inter-variable dependencies using vine copulas (Aas et al., 2009) allowing for flexible modeling of the full multivariate distribution of interest. This is important to account for the joint occurrence of extremes of different drivers of drought and to capture the diverse range of vegetation responses across different ecosystems. In this study, the performance of the novel, vine copula based indices (subsequently addressed as VC-Index or VCI) are compared to the established indices SPEI and SPI.

An important step in the process towards refined drought characterization, is the validation of drought indices. So far, only a few studies have compared the performance of different drought indices in identifying drought impacts using different ecosystem indicators (Vicente-Serrano et al., 2012) and there is no general opinion on the most apt technique for the validation of drought indices (Hao & Singh, 2015). Validation through temporal and spatial comparison with well-established drought indices is the most commonly used technique. In this study, we assess the performance of the different drought indices in terms of an analysis of past drought events, both in the temporal and spatial domain, using hydrological and carbon flux variables. We characterize hydrological drought by anomalies (dry spells) of monthly streamflow, a concept that has been frequently used for hydrologic drought analysis (e.g. Dracup et al., 1980; Mohan & Rangacharya, 1991; Clausen & Pearson, 1995) and for exploring spatio-temporal characteristics of drought events (Lorenzo-Lacruz et al., 2010; Zhai et al., 2010; Van Lanen et al., 2016, Haslinger et al, 2014). Similarly, the carbon flux variables gross primary production (GPP) and net ecosystem exchange (NEE) are known to serve as proxies for drought promoted decline in productivity in forest ecosystems (Ciais et al., 2005; Luyssaert et al., 2007; Pereira et al., 2007). We assess the performance of the drought indices based on the following criteria: (i) their skill to detect streamflow anomalies in the low-flow season, (ii) their ability to detect past drought signals captured in the carbon flux data. The aim of the paper is to investigate if the novel multivariate indices (VCI) accounting for several drought relevant variables and their dependencies at the same time, can provide more accurate information about the magnitude of different drought events. Additionally, we discuss major challenges in using such indices.

2   Material and methods

2.1   Data

Drought Indices All standardized drought indices, SPEI, SPI and VCI, were calculated based on input data from the ECMWF Atmospheric Reanalysis of the

74   20th Century (ERA-20C) (European Centre for Medium-Range Weather Forecasts,
75   2014) for the period 1980 till 2010. The drought indices SPEI and SPI were
76   calculated using the R package SPEI (Vicente-Serrano et al., 2010). For the
77   calculation of the SPI, monthly precipitation time series were converted to
78   probabilities which were then transformed further to standardized series (Mckee et
79   al., 1993). The SPEI uses the multi-timescales attribute of the SPI and combines
80   information about both precipitation and evapotranspiration, making it more
81   suitable for studies related to climate change (Vicente-Serrano et al., 2010). Using
82   the method proposed by Thornthwaite (1948), the variable potential
83   evapotranspiration was computed based on temperature and latitude information.
84   For the calculation of the VC-Indices (two different variants for validation against
85   streamflow data and carbon flux data) we followed the method described in
86   Erhardt & Czado (2017), which can be used flexibly in different applications to
87   model different drought types based on user-selected (time series of) drought
88   related variables. In several modeling steps, their method first eliminates
89   seasonality and temporal dependence observed in the time series. Using vine
90   copulas it models the dependencies among these pre-processed time series, which
91   then allows to combine the drought information captured in the different variables
92   into a single time series of a standardized multivariate drought index. Note, that for
93   this last step, we used the aggregation method (Method A) as described in Erhardt
94   & Czado (2017). As the order of the variables matters for the aggregation, we
95   subsequently state them in the order which was used.

96   For our validation against streamflow data, a hydro-meteorological VC-Index was
97   developed using a three-variate data set consisting of monthly mean precipitation,
98   volumetric soil water content and potential evapotranspiration (variables in that
99   order). For our validation against carbon flux variables, an eco-meteorological VC-
100   Index was developed using a different three-variate data set consisting of monthly
101   means of climatic water balance, volumetric soil water content and air temperature
102   (variables in that order). We computed the so-called climatic water balance (see
103   e.g. Vicente-Serrano et al., 2010) as difference between mean monthly precipitation
104   and potential evapotranspiration. The monthly mean potential evapotranspiration
105   was calculated using the method proposed by Thornthwaite (1948) based on air
106   temperature and latitude information. For the validation with streamflow and
107   carbon flux data, all drought indices were computed on a 0.25°×0.25° grid and a
108   0.50°×0.50° grid (matching the resolution of the flux data), respectively.

109   **Streamflow** The Global Runoff Data Centre in Koblenz (GRDC, 2016) is a
110   repository for daily and monthly streamflow data. In the archive, there are
111   streamflow time series from 1315 European catchments. In this study, we selected

112   332 catchments for the period 1980-2010, which have a size less than 500 km², as
113   smaller catchments are more likely to contain drought signals less affected by
114   external processes. For each catchment, we derived the catchment boundary using
115   data from Catchment Characterisation and Modelling database (de Jager and Vogt,
116   2010). The coordinates of the centroid of each catchment were used to extract data
117   from the gridded climate products to calculate the corresponding drought indices.
118   The location of the catchments is presented in Fig. 1.

119   **Carbon fluxes** Monthly carbon flux data for Germany was obtained from the
120   RS+METEO product of FLUXCOM (FLUXCOM, 2017; Jung et al., 2017;
121   Tramontana et al., 2016) at 0.50° spatial resolution for the period 1980-2013. Time
122   series of two carbon flux variables namely GPP and NEE were generated from the
123   monthly ensemble means of six variants (three machine learning algorithms and
124   two observed flux variants from two partitioning methods) (Reichstein et al., 2005;
125   Lasslop et al., 2010). For details about the data product see Tramontana et al.
126   (2016) and Jung et al. (2017). For our validation of the drought indices against the
127   carbon flux data, Germany was taken as a case study. For both types of
128   environmental impact variables the common period 1980-2010 and the drought
129   year 2003 were studied.
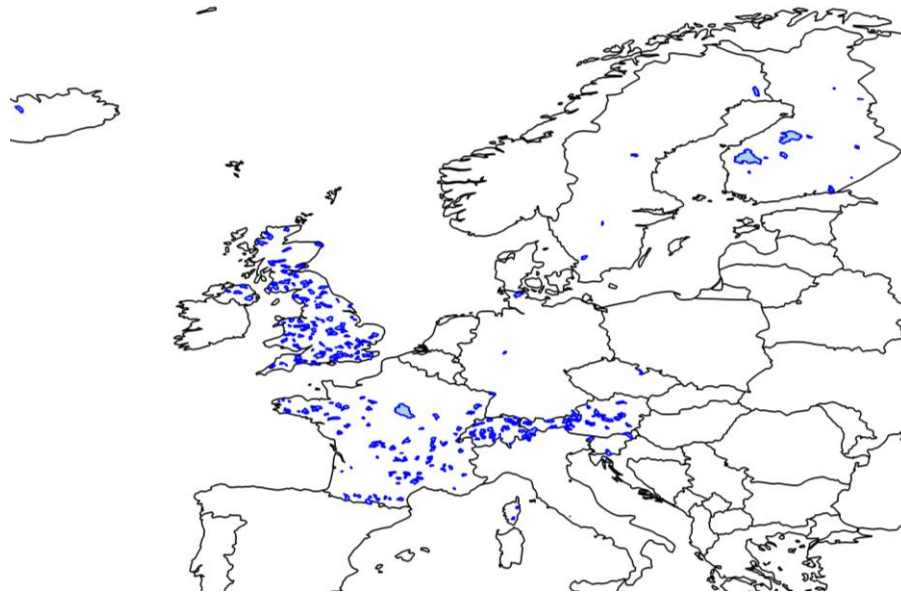
130

131

132   **Fig. 1.** Locations of the 332 catchments used in the validation of the drought indices.
133   Streamflow data of these catchments was analyzed for the period 1980 to 2010.

2.2 Methods

Validation against streamflow data

For comparison of the drought indices with the streamflow time series, daily streamflow data for 1980-2010 were aggregated into monthly mean values, and subsequently standardized using long-term monthly mean and standard deviation. This was done to bring the streamflow data to the same (temporal) scale as the drought indices. In the first part of our validation, we investigated seasonal differences in the month-wise correlation of the streamflow time series with the drought indices using Spearman's rank correlation. In the second part of the analysis, we aimed to assess the performance of the drought indices to predict low-flow events focusing on the summer/autumn low-flow season (August to November). We computed various verification skill scores, which are generally used to compare event forecasts to corresponding event observations and hence enable validation of the quality of different forecasts. Verification skill scores help in identifying and rectifying model shortcomings and to improve forecasting. In this study, we followed the approach shown in Haslinger et al. (2014) where the streamflow represents the "observation" and the "forecast" is given by the drought indices. A low-flow event was flagged as "1" when the streamflow was below the 20th percentile of the monthly hydrograph; otherwise it was flagged as "0". An analogous flagging rule was applied for the drought indices. Then, the binary coded streamflow and drought time series were used to determine the entries A, B, C, and D of a contingency table (see Table 1) which is used to calculate different skill scores (Wilks, 2011; WWRP/WGNE Joint Working Group on Forecast Verification Research, 2015). In this study, we focused on two metrics, namely probability of detection (POD), also known as hit rate, and false alarm ratio (FAR). POD is a verification measure of categorical forecast performance that measures the total number of correct event forecasts (hits) divided by the total number of events observed. FAR is the number of false alarms divided by the total number of event forecasts. While POD is only sensitive to hits and ignores false alarms, the opposite holds for the FAR. Hence, it is always recommended to use these two verification skills together (WWRP/WGNE Joint Working Group on Forecast Verification Research, 2015). Therefore, to visualize the skill of the different indices, POD and FAR were used in conjunction. Mathematical formulas for the calculation of these skill scores are provided in Table 2; we used the R package Verification (Pocernich, 2012) for their computation. Besides POD and FAR, additional verification measures such as Critical Success Index (CSI), Extremal Dependency Index (EDI), Symmetric EDI (SEDI), Extreme Dependency Score (EDS) and Symmetric EDS (SEDS) were determined (see Table 2 for their formulas).

Validation against carbon flux data

For comparison of the drought indices with the carbon flux time series, we standardized the carbon flux data using the long-term monthly mean and standard deviation. Based on growing season (March to October) data for the period from 1980 to 2010, we performed pixel-wise linear regressions between each carbon flux indicator and each drought index (VCI, SPEI and SPI). R^2 and p-values of the regression analyses are reported. Furthermore, we analyzed the drought conditions year-wise for the years 2001 to 2005, again using regression. Consequently, we could assess the relationship between the different carbon flux variables and drought indices for each pixel, where a high positive correlation indicates good performance of the respective drought index in reproducing the drought signal captured in the carbon flux data. The R package rasterVis was used to visualize our results on maps (Lamigueiro & Hijmans, 2016). All statistical computations were performed using R version 3.3.1 (R Core Team, 2016).

Table 1. Contingency table illustrating the counts used for the calculation of verification skill scores for binary forecasts and observations. A denotes the number of event forecasts that correspond to event observations (hits), B denotes the number of event forecasts that do not correspond to observed events, C denotes the number of no-event forecasts corresponding to observed events, and D denotes the number of no-event forecasts corresponding to observations of no event.

2x2 Contingency table		Event Observed	
		Yes	No
Event Forecast	Yes	A	B
	No	C	D

## 3 Results

3.1 Validation against streamflow data

Seasonal varying correlation with drought indices

In this section, the results of validation of SPEI, SPI and VCI against streamflow data are discussed, where the VCI was calculated based on the variables monthly mean precipitation, volumetric soil water content and potential evapotranspiration. The locations of the 332 considered catchments are shown in Fig. 1. While a high concentration of catchments was present in Great Britain, France and Austria, also a few catchments scattered across Scandinavia were included. To examine the

201 seasonal variability in correlations, Spearman rank correlations were computed
202 separately for each month. Fig. 2 compares the seasonal differences in month-wise
203 correlations of the drought indices VCI, SPEI and SPI with the streamflow time
204 series for the period from 1980 to 2010 using boxplots and corresponding mean
205 values. It can be observed that for all months (except January), the VCI had the
206 highest average correlation with streamflow (ranging between 0.4 and 0.6),
207 compared to the indices SPEI and SPI (ranging between 0.2 and 0.55), with highest
208 peaks for all indices either in October or November. On the other hand, the lowest
209 correlations with SPI and SPEI are observed between March and June.
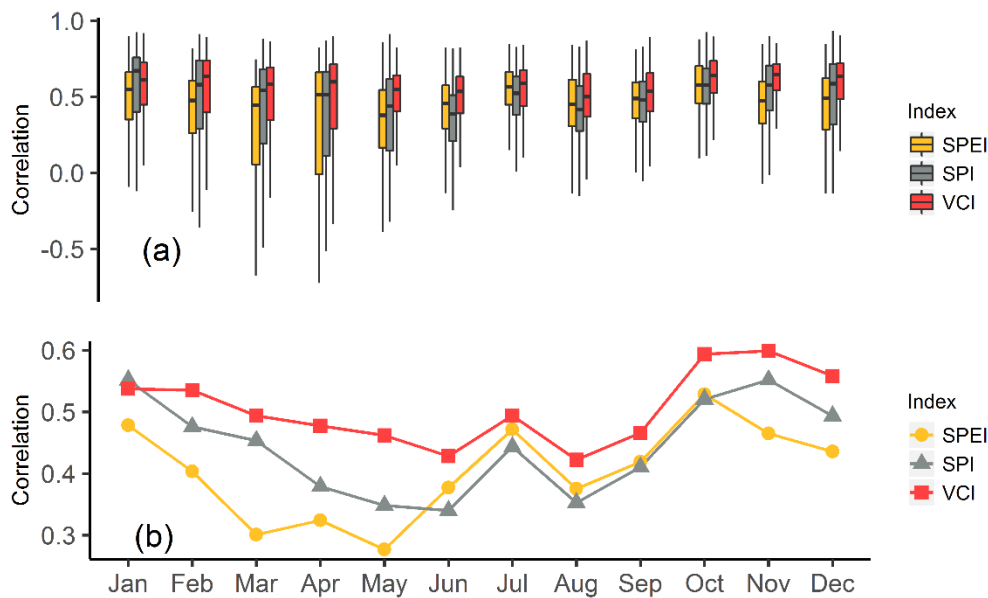
210

211 **Fig. 2.** Monthly Spearman correlation coefficients of SPEI, SPI and VCI with mean
212 monthly streamflow data from 332 catchments for the period 1980 to 2010 visualized as
213 (a) boxplots and (b) mean values. SPEI and SPI stand for Standardized Precipitation
214 Evapotranspiration Index and Standardized Precipitation Index, respectively. VCI is a
215 standardized, multivariate index based on variables: monthly mean precipitation,
216 volumetric soil water content and potential evapotranspiration, computed using the vine
217 copula based approach proposed by Erhardt & Czado (2017).

218

Ability of drought indices to detect low-flow events

220 We are now interested in assessing if the drought indices can predict low-flow
221 events. The 20th percentiles of the monthly streamflow and drought index
222 distributions were chosen as a threshold to define extreme low-flows and drought
223 events, respectively. Given this setup, forecast verification scores such as POD and
224 FAR were calculated as described in the methods section and reported in Table 2.

225 From Table 2 we see that – amongst the three drought indices – VCI has the
226 highest value for both Spearman's correlation and POD, and the lowest FAR value.
227 Results of the other verification scores, CSI, EDI, SEDI, EDS and SEDS, are
228 reported in Table 2, where a higher value of these scores mean better drought
229 detection ability. For all these scores, VCI had higher values than SPEI and SPI.

230 The best performing drought index for each catchment based on maximum POD
231 value is shown in Fig. 3a. According to POD, drought was best detected by VCI for
232 62% of the catchments, followed by 25.9% and 12% of the catchments for SPI and
233 SPEI, respectively (see Table 1, Supplementary). For the five countries where data
234 for more than ten catchments was available (i.e., Great Britain, France, Austria,
235 Switzerland and Finland), the largest percentage of the catchments was best
236 represented by the VCI, with Austria being the only exception. It is worth noting
237 that for Switzerland the performance of the VCI was closely followed by the SPI and
238 vice-versa for Austria. When the catchments were divided into three groups based
239 on gauge or mean catchment elevation (m.a.s.l.), i.e., low (0-100), medium (100-
240 500) and high (>500), 15.5%, 13.2% and 71.3% of the low elevation catchments
241 were best represented by SPEI, SPI and VCI, respectively. 12.8%, 27.8% and 59.4%
242 of the medium elevation catchments were best represented by SPEI, SPI and VCI,
243 respectively. The high elevation catchments were best represented by SPEI, SPI
244 and VCI for 4.3%, 45.7% and 50%, respectively. In general, it was observed that for
245 low and medium elevations, VCI was the best index for a substantial majority of the
246 catchments. In case of high elevation catchments, SPI performed similar to VCI. An
247 analysis of the effect of catchment size showed that the performance of the
248 individual indices was not related to catchment size: The mean area of the
249 catchments where the indices SPEI, SPI and VCI best detected drought according
250 to POD were quite similar with 164, 171 and 172 km², respectively.

251 The best performing drought index for each catchment based on minimum FAR
252 value is shown in Fig. 3b. The minimum FAR value was observed for SPEI, SPI and
253 VCI for 20.5%, 33.4% and 46.1% of the catchments, respectively, showing that
254 based on FAR, VCI was the best performing index. Again, we did not observe
255 differences in performance related to catchment area. For all three elevation
256 classes, low, medium and high, VCI had the relatively larger share of catchments
257 with minimum FAR, i.e., 42.6, 42.1 and 60.0%, respectively (see Table 1,
258 Supplementary). For all countries excluding France, VCI had the largest share of
259 catchments with minimum FAR. Overall, both skills POD and FAR indicated a
260 better performance of VCI compared to SPEI and SPI.
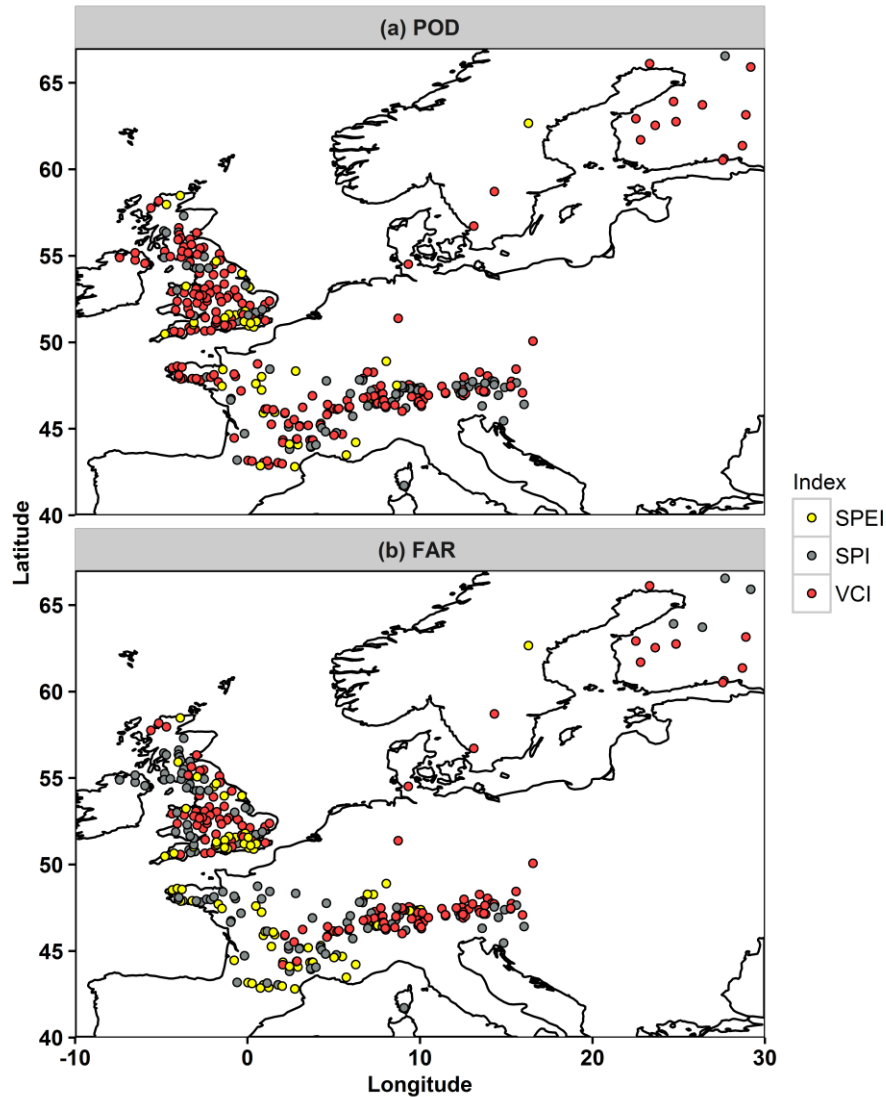
Fig. 3. Plot showing for all 332 catchments used in the validation of the drought indices, which index has (a) the maximum Probability of Detection (POD) and (b) minimum False Alarm Ratio (FAR) values. Values of POD and FAR scores of the drought indices were calculated based on monthly streamflow data for the low-flow season (August to November) during the period 1980 to 2010. The highest POD for SPEI, SPI and VCI was observed for 12%, 25.9% and 62% of the catchments, respectively. The lowest FAR for SPEI, SPI and VCI was observed for 20.5%, 33.4% and 46.1% of the catchments, respectively. SPEI and SPI stand for Standardized Precipitation Evapotranspiration Index and Standardized Precipitation Index, respectively. VCI is a standardized, multivariate index based on variables: monthly mean precipitation, volumetric soil water content and potential evapotranspiration, computed using the vine copula based approach proposed by Erhardt & Czado (2017).

Table 2. Skill scores (and their definitions) used for validation of the drought indices SPEI, SPI and VCI. The values of the scores for the different drought indices are based on streamflow data for 332 catchments during the low-flow season (August to November) of the period 1980 to 2010. SPEI and SPI stand for Standardized Precipitation Evapotranspiration Index and Standardized Precipitation Index, respectively. VCI is a standardized, multivariate index computed using the vine copula based approach proposed by Erhardt & Czado (2017). For definitions of A, B, C and D, see the contingency table provided in Table 1.

Skill Score	Definition	SPEI	SPI	VCI
Correlation	Spearman's rank correlation coefficient	0.41	0.46	0.53
Probability of Detection (POD)	POD=A/(A+C)	0.35	0.37	0.42
False Alarm Ratio (FAR)	FAR=(B)/(A+B)	0.64	0.63	0.59
Critical Success Index (CSI)	CSI=(A)/(A+B+C)	0.22	0.23	0.26
Extremal Dependency Index (EDI)	EDI=(logF-logH)/(logF+ logH), where H=A/(A+C) and F=B/(B+D)	0.28	0.31	0.38
Symmetric EDI (SEDI)	SEDI= logF-logH-log(1-F)+log(1-H)/ logF+logH+log(1-F)+log(1-H), where H = A/A+C and F=B/B+D	0.30	0.33	0.41
Extreme Dependency Score (EDS)	EDI=logp-logH/logp+logH, where p=(A+C)/(A+B+C+D , H=A/A+C	0.21	0.24	0.31
Symmetric EDS (SEDS)	SEDS=logq-logH/logq+logH, where q= (A+B)/(A+B+C+D) and H=A/A+C	0.22	0.25	0.30

3.2 Validation against carbon flux data

In this section, the results of validation of SPEI, SPI and VCI against carbon flux data are discussed, where the VCI was calculated based on variables: monthly means of climatic water balance, volumetric soil water content and air temperature. Maps of the drought indices (SPEI, SPI and VCI) for Germany for the single years 2001 to 2005 are shown in Fig. 4. The drought of 2003 was generally

more severe in the eastern and south-eastern part of Germany. Box plots of the seasonal means of the drought indices for 2003 are provided in Fig. 5, which – for the different indices SPEI, SPI and VCI – showed obvious differences in the severity of the detected drought conditions, especially during spring. Overall, we found that in average the multivariate drought index VCI indicated more severe drought conditions for 2003 than SPEI and SPI. Equally, annual sums of standardized NEE and GPP for 2001 to 2005 (Fig. 1 and Fig. 2, Supplementary) indicate drought during the year 2003.
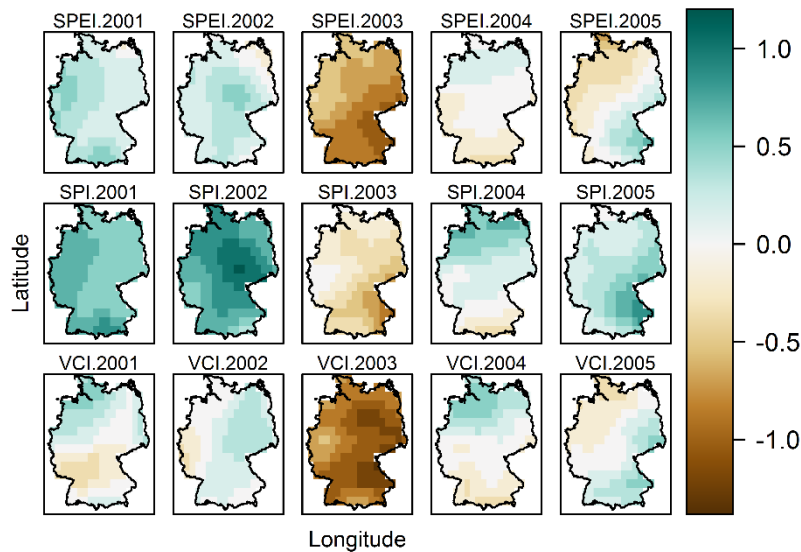
Fig. 4. Annual mean of drought indices (SPEI, SPI and VCI) for Germany for the years 2001 to 2005, including the drought year 2003. SPEI and SPI stand for Standardized Precipitation Evapotranspiration Index and Standardized Precipitation Index, respectively. VCI is a standardized, multivariate index based on variables: monthly means of climatic water balance, volumetric soil water content and air temperature, computed using the vine copula based approach proposed by Erhardt & Czado (2017). Negative values of all indices indicate dry conditions.

Further, we analyzed the performance of the different drought indices for the long-term period 1980 to 2010. The results of a pixel-wise linear regression between the drought indices and NEE for the growing season (April to September) for the years 1980 to 2010 are given in in Fig. 6a. For the growing season NEE, VCI had the highest R^2 values (0.5) followed by SPEI. SPI did not mirror strong drought impacts, with maximum R^2 values below 0.3. The average R^2 values for SPEI, SPI and VCI with
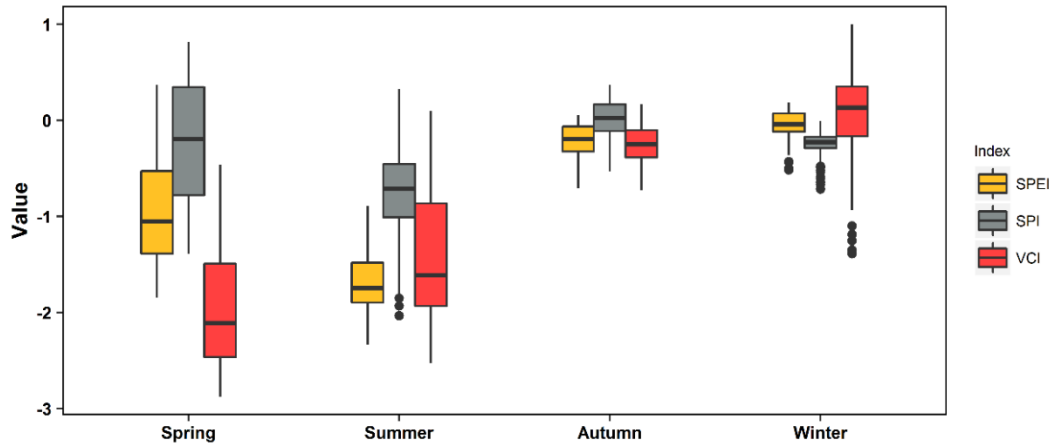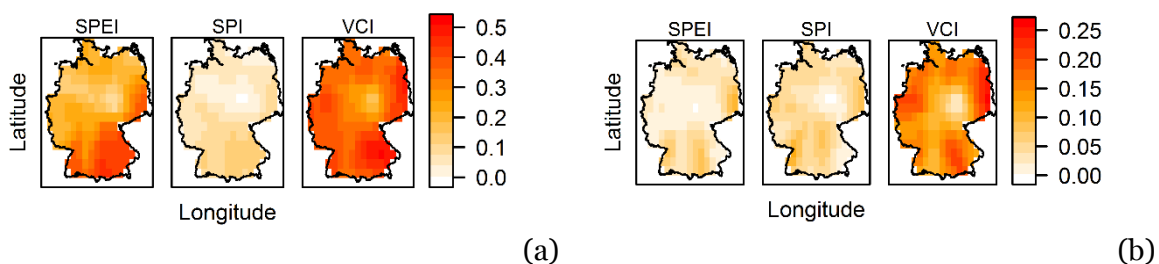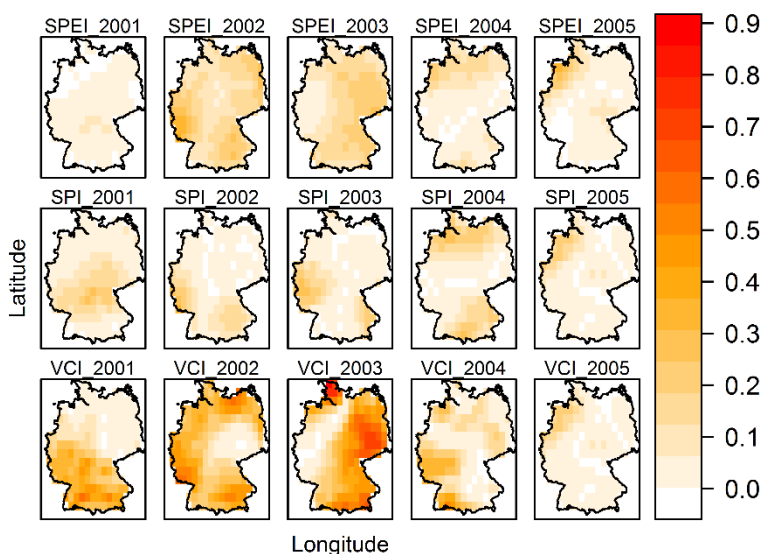
Fig. 5. Box plots of seasonal means of drought indices (SPEI, SPI and VCI) for Germany for the drought year 2003. SPEI and SPI stand for Standardized Precipitation Evapotranspiration Index and Standardized Precipitation Index, respectively. VCI is a standardized, multivariate index based on variables: monthly means of climatic water balance, volumetric soil water content and air temperature, computed using the vine copula based approach proposed by Erhardt & Czado (2017). Negative values of the indices indicate dry conditions.

NEE were 0.26, 0.07 and 0.37, respectively. According to the p-values of the regression (Fig. 3a, Supplementary) all R^2 values for VCI and SPEI, and 88% of those for the SPI were statistically significant at a confidence level of 0.05. Similarly, for the growing season GPP, R^2 values were highest for VCI with values up to 0.3 whereas SPEI and SPI showed only weak signals with R^2 values below 0.15 (Fig. 6b). The average R^2 values for SPEI, SPI and VCI with GPP were 0.03, 0.04 and 0.14, respectively. All R^2 values for VCI were statistically significant at the 0.05 confidence level, followed by 85% and 54% statistically significant values for SPI and SPEI (see p-values in Fig. 3b, Supplementary).

Similarly, the results of year- and pixel-wise linear regressions for the drought indices SPEI, SPI and VCI against NEE for the years 2001 to 2005 are mapped in Fig. 7. During the drought year 2003, VCI had the strongest correlations with NEE with R^2 values reaching up to 0.86, whereas in case of SPEI and SPI, the R^2 values reached only maxima of 0.39 and 0.33, respectively. The average R^2 values of SPEI, SPI and VCI, were 0.13, 0.06 and 0.31, respectively. Analogous maps of the results of pixel-wise linear regressions with GPP are given in Fig. 8. During the drought year 2003 VCI had comparatively higher correlations with GPP, with R^2 values reaching maxima of 0.31, 0.24 and 0.87 for SPEI, SPI and VCI, respectively. The

average R² values corresponding to SPEI, SPI and VCI for 2003 were 0.15, 0.05 and 0.29, respectively. The corresponding p-value maps for NEE and GPP (Fig. 4 and Fig. 5, Supplementary) show that for the drought year 2003, at the 0.05 confidence level, the percentage of statistically significant R² values for VCI are 48% and 21%, respectively. For both carbon flux variables (NEE and GPP), SPI and SPEI did not show any significant correlations.
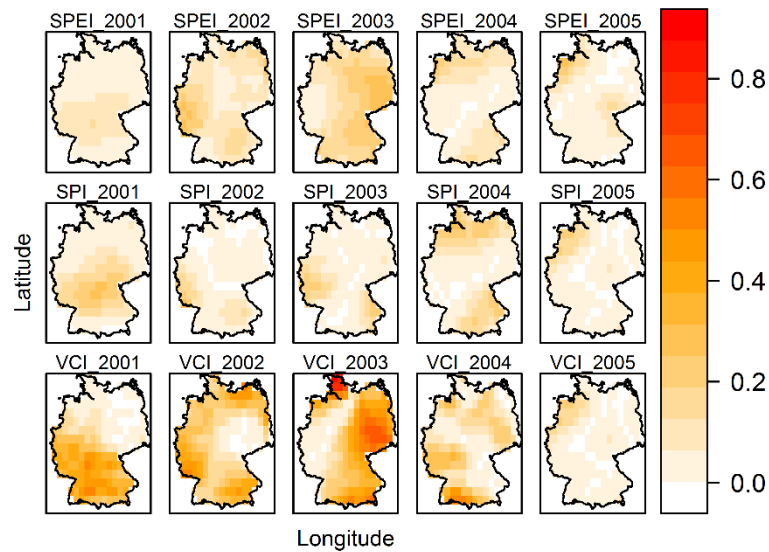

(a)   (b)

Fig. 6. R² values of a pixel-wise linear regression of the drought indices SPEI, SPI and VCI against (a) standardized net ecosystem exchange (NEE) and (b) standardized gross primary production (GPP), on a 0.5x0.5 degree spatial grid for Germany, for the growing season (April to September) during the period 1980 to 2010. SPEI and SPI stand for Standardized Precipitation Evapotranspiration Index and Standardized Precipitation Index, respectively. VCI is a standardized, multivariate index based on variables: monthly means of climatic water balance, volumetric soil water content and air temperature, computed using the vine copula based approach proposed by Erhardt & Czado (2017).

Fig. 7. R² values of year- and pixel-wise linear regressions of the drought indices SPEI, SPI and VCI against standardized net ecosystem exchange (NEE) on a 0.5x0.5 degree spatial grid for Germany for the period 2001 to 2005, including the drought year 2003. SPEI and

SPI stand for Standardized Precipitation Evapotranspiration Index and Standardized Precipitation Index, respectively. VCI is a standardized, multivariate index based on variables: monthly means of climatic water balance, volumetric soil water content and air temperature, computed using the vine copula based approach proposed by Erhardt & Czado (2017).

Fig. 8. R^2 values of year- and pixel-wise linear regressions of the drought indices VCI, SPEI and SPI against standardized gross primary production (GPP) on a 0.5x0.5 degree spatial grid for Germany for the period 2001 to 2005, including the drought year 2003. SPEI and SPI stand for Standardized Precipitation Evapotranspiration Index and Standardized Precipitation Index, respectively. VCI is a standardized, multivariate index based on variables: monthly means of climatic water balance, volumetric soil water content and air temperature, computed using the vine copula based approach proposed by Erhardt & Czado (2017).

4 Discussion

In our study we analyzed and compared the performance of the drought indices SPEI, SPI and VCI based on streamflow and carbon flux data over a period of three decades. The results of the validation of the exemplary multivariate hydro-meteorological drought index with streamflow data and the multivariate eco-meteorological drought index against carbon flux data confirmed the superiority of the multivariate, vine copula based drought indices (VCI) calculated using the flexible methodology proposed by Erhardt & Czado (2017). All in all, our validation has once more established the benefits of a multivariate approach, similar to many recent studies which show that combining multiple data sets improves drought characterization (Keyantash & Dracup, 2004; Kao & Govindaraju, 2010; Hao &

382 AghaKouchak, 2013, 2014; AghaKouchak, 2015; AghaKouchak et al., 2015;
383 Farahmand & AghaKouchak, 2015).

4.1 Validation against streamflow data

385 The correlation analysis of the drought indices with the streamflow data showed
386 varying magnitudes of correlation depending on the drought index under
387 consideration. Overall, the correlations are not greater than 0.6, and false alarm
388 rates are of same order of magnitude as success rates. As shown in Van Lanen et al.
389 (2016) and Laaha et al. (2017), hydrological events can substantially differ from the
390 meteorological ones because of the catchments' ability to store and release water,
391 which may dampen or even amplify atmospheric drought signals. However, the
392 streamflow-drought relationship was found to be most pronounced for VCI, since
393 for almost all months we observed higher average correlations, with maximum
394 values in fall. For SPI and SPEI we observed low correlations during the period
395 from March to June. This could be due to the fact that the considered drought
396 indices do not account for rainfall deficits and snow melt, which effectively
397 influence streamflow (Haslinger et al., 2014; Staudinger et al., 2014) and our study
398 considers a substantial number of catchments in the alpine region (see Fig. 1).
399 During this period of the year, snow accumulation and snowmelt processes overlap
400 the variations of the streamflow year, driven by rainfall (Haslinger et al., 2014),
401 resulting in the low correlations during the months March to June. This effect due
402 to snowmelt processes is however less pronounced in case of the VCI compared to
403 SPEI and SPI, which could be due to the fact that with VCI we consider a hydro-
404 metorological drought index, by including soil moisture, and not a purely
405 meteorological one. In case of the latter, a time lag is foreseen with streamflow
406 drought (Shukla & Wood, 2008; Haslinger et al., 2014). In general, our results
407 confirm the hypothesis discussed in Haslinger et al. (2014) that the link between
408 streamflow anomalies and drought indices is more evident for sophisticated
409 drought indices.

410 Amongst the studied indices, VCI can be considered superior in terms of
411 probability of drought detection, showing the highest POD values for 62% of the
412 catchments. For most of the catchments, the false alarm rate was the lowest and
413 hence best for VCI, whereas the minimum FAR for VCI was observed for 46.1% of
414 the catchments. These results show that considering both measures, the VCI
415 outperformed the other indices in terms of highest POD and lowest FAR scores.
416 This is in line with studies of Hao & AghaKouchak (2014) where a multivariate
417 drought index (Hao & AghaKouchak, 2013) based on precipitation and soil
418 moisture lead to a higher probability of drought detection compared to the

corresponding univariate standardized indices (AghaKouchak, 2014). Erhardt & Czado (2017) validated an exemplary, vine copula based, agro-meteorological drought index (VCI) using a soybean yield dataset and showed its superiority over other uni- and multivariate drought indices. The better performance of the VCI for streamflow data in our study could be a consequence of including volumetric soil water content into the multivariate drought index – which is indeed more closely related to catchment storage than meteorological indices and, hence, beneficial for predicting streamflow droughts. A second reason might be the fact that VCI accounts for inter-variable dependencies in a flexible fashion using vine copulas (Aas et al., 2009). While the climate-based indices (SPI and SPEI) describe only the climate anomalies in isolation from their hydrological context (Shukla & Wood, 2008), the VCI offers a skillful method for jointly characterizing the effects of climate anomalies and hydrologic conditions.

Upto 500 km² , the catchment area had no effect on the response of the drought indices, while the performance of the indices varied with the catchment elevation. For low elevations, the probability of drought detection was mostly best for VCI (71.3%). For high elevations, POD score was similar for VCI and SPI. This could be due to the fact that in alpine catchments the low-flows tend to occur in winter, which were outside the studied season (August to November). Subsequently, this is reflected from the minimum FAR score, where VCI has the largest share of catchments VCI (60%) and SPI (27.7%) had the lowest, making VCI the better choice for high elevation studies as well (see Table 1, Supplementary). The lower skill of the VCI for high altitude could also point to lower accuracy of the volumetric soil water content data for alpine areas where soil structure is notably complex. Moreover, evapotranspiration is a less dominant process in the alpine areas. For hydrological drought, the seasonality of a regime (which depends on the elevation) plays an important role (Jung et al., 2013; Van Loon & Laaha, 2015) since in higher elevations lower temperatures lead to more streamflow drought. All in all, for all elevations, VCI was the preferred index when considering POD and FAR in conjunction (Table 1, Supplementary).

4.2 Validation against carbon flux data

A summary of the drought conditions in Germany for the drought year 2003 based on the different drought indices revealed that VCI indicated comparatively worse drought conditions in average (see maps in Fig. 4) – where the results of SPEI were more similar to VCI than those for SPI – and especially during spring and summer (see Fig. 5). In general, for the year 2003, all three different indices detected more severe drought conditions in the eastern half of Germany (Ciais et al., 2005;

112

456 Thomas et al., 2013). The pixel-wise regression analysis of the drought indices
457 versus the carbon fluxes showed a varying magnitude of their correlation
458 depending on the drought index, the period of analysis (1980-2010 versus 2003)
459 and the carbon flux indicator under consideration. However, the NEE-drought and
460 GPP-drought relationship became most obvious for VCI, in case of a validation
461 with both NEE and GPP, for both the long-term consideration (1980 to 2010) and
462 the single drought year 2003, with more statistically significant correlations for the
463 long period. Overall, NEE showed stronger associations with the drought indices
464 compared to GPP.

465 When considering the period from 1980 to 2010, the average R^2 values of linear
466 regressions of NEE and GPP against the drought indices were highest for VCI,
467 followed by SPEI and SPI. In general, the indices successfully established the
468 drought-NEE relationship (Ciais et al., 2005; Reichstein et al., 2005; Pereira et al.,
469 2007) and the drought-GPP relationship (Ciais et al., 2005; Pereira et al., 2007;
470 Vicca et al., 2016), most strongly reflected in both cases by VCI, with all R^2 values
471 being statistically significant. Based on these results, we conclude superiority of
472 VCI in detecting past drought events in an ecological context. In addition to the
473 period from 1980 to 2010, year-wise linear regressions were performed to examine
474 the performance of the drought indices, with focus on the drought year 2003.
475 Similar to the results for the three decade period, the R^2 values of linear regressions
476 of NEE and GPP against the drought indices were highest on average for VCI. It is
477 worth noting here that for our year-wise analysis (for instance for the drought year
478 2003), we considered only twelve observations, and the percentage of statistically
479 significant values at the confidence level of 0.05 were much less compared to the
480 analysis of the longer period.

481 *Challenges associated with using multivariate indices*

482 It is acknowledged that, similar to other methods, there are many challenges
483 associated with using/developing multivariate drought indices such as the vine
484 copula based indices discussed in this paper. Firstly, the availability of ground-
485 based observations of many drought-related variables (e.g., soil moisture,
486 snowmelt, water vapor) is very much limited or sparse in certain regions across the
487 world. This restricts the usage/development of multivariate indicators in regions
488 where no such data is available. Secondly, to ensure that data records with large
489 volumes are easily managed and made available to users is another challenge. For
490 many satellite data products, the length of the data records is not more than a
491 decade or they have only a very coarse spatial resolution which limits the
492 methodology of drought indices to be used to their maximum potential. The
493 methodology behind most multivariate indices requires long-term observations (30

years or more) to derive the joint distribution of the variables, and a short record of observations could lead to biased estimates (Hao & AghaKouchak, 2014). However, Erhardt & Czado (2017), showed that stable results can be obtained with their method for much shorter observation periods like 10 years, which is an advantage over other (multivariate) drought indices (see Erhardt and Czado, 2017).

5   Conclusion

In the case of our two applications, the VC-Indices yield the best performance compared to the other established indices, by reaching the best scores in all investigations. Our study emphasizes that the investigation of drought impacts should be based on multiple variables/indicators (Bhuyan et al., 2017) and, for this reason, the novel vine copula based indices are not meant to replace any established index. Instead, we propose that this approach should be used as an added source of information taking into account the joint probability of drought-relevant variables chosen by the user to investigate a specific drought type. Thus, the major key to improving our understanding of drought impacts on ecosystems could be high spatial resolution, user-defined, drought monitoring based on the method proposed by Erhardt & Czado (2017).

6   Acknowledgements

7   References

Aas K, Czado C, Frigessi A, Bakken H (2009) Pair-copula constructions of multiple dependence. *Insurance: Mathematics and Economics*, **44**, 182–198.

AghaKouchak A (2014) A baseline probabilistic drought forecasting framework using standardized soil moisture index: Application to the 2012 United States drought. *Hydrology and Earth System Sciences*, **18**, 2485–2492.

AghaKouchak A (2015) A multivariate approach for persistence-based drought prediction: Application to the 2010-2011 East Africa drought. *Journal of Hydrology*, **526**, 127–135.

AghaKouchak A, Farahmand A, Melton FS, Teixeira J, Anderson MC, Wardlow BD, Hain CR (2015) Remote sensing of drought: Progress, challenges and opportunities. *Reviews of Geophysics*, **53**, 1–29.

Bhuyan U, Zang C, Menzel A (2017) Different responses of multispecies tree ring growth to various drought indices across Europe. *Dendrochronologia*, 44, 1–8.

Ciais P, Reichstein M, Viovy N et al. (2005) Europe-wide reduction in primary productivity caused by the heat and drought in 2003. *Nature*, **437**, 529–533.

Clausen B, Pearson CP (1995) Regional frequency analysis of annual maximum streamflow drought. *Journal of Hydrology*, **173**, 111–130.

Dracup JA, Lee KS, Paulson Jr EG (1980) On the statistical characteristics of drought events. *Water Resources Research*, **16**, 289–296.

Erhardt TM, Czado C (2017) Standardized drought indices: A novel uni- and multivariate approach. *Journal of the Royal Statistical Society: Series C (Applied Statistics)*.DOI:10.1111/rssc.12242. Accepted manuscript

European Centre for Medium-Range Weather Forecasts (2014) ERA-20C Project (ECMWF Atmospheric Reanalysis of the 20th Century).

Farahmand A, AghaKouchak A (2015) A generalized framework for deriving nonparametric standardized drought indicators. *Advances in Water Resources*, **76**, 140–145.

FLUXCOM (2017) FLUXCOM Global Energy and Carbon Fluxes, Max Planck Institute for Biogeochemistry, Jena, Germany.

GRDC (2016) Global Runoff Data Centre-Dataset of river discharge time series. *Koblenz, Germany*.

Hao Z, AghaKouchak A (2013) Multivariate Standardized Drought Index: A parametric multi-index model. *Advances in Water Resources*, **57**, 12–18.

Hao Z, AghaKouchak A (2014) A Nonparametric Multivariate Multi-Index Drought Monitoring Framework. *Journal of Hydrometeorology*, **15**, 89–101.

Hao Z, Singh VP (2015) Drought characterization from a multivariate perspective: A review. *Journal of Hydrology*, **527**, 668–678.

Haslinger K, Koffler D, Schöner W, Laaha G (2014) Exploring the link between meteorological drought and streamflow: Effects of climate-catchment interaction. *Water Resources Research*, **50**, 2468–2487.

Hayes MJ, Alvord C, Lowrey J (2007) Drought indices. *Intermountain West Climate Summary*, **3**, 2-6.

IPCC (2013) *Summary for policymakers. Climate Change 2013: The Physical Science Basis. Contribution of Working Group I to the Fifth Assessment Report of the Intergovernmental Panel on Climate Change.* Cambridge University Press, Cambridge, UK and New York, NY, 3–39.

de Jager, A.L., Vogt, J.V. (2010). Development and demonstration of a structured hydrological feature coding system for Europe. *Hydrological Sciences Journal*, **55**, 5, 661-675.

Jung IW, Chang H, Risley J (2013) Effects of runoff sensitivity and catchment characteristics on regional actual evapotranspiration trends in the conterminous US. *Environmental Research Letters*, **8**, 44002.

Jung M, Reichstein M, Schwalm CR et al. (2017) Compensatory water effects link yearly global land CO_2 sink changes to temperature. *Nature*, **541**, 516–520.

Kao SC, Govindaraju RS (2010) A copula-based joint deficit index for droughts. *Journal of Hydrology*, **380**, 121–134.

Keyantash JA, Dracup JA (2004) An aggregate drought index: Assessing drought severity based on fluctuations in the hydrologic cycle and surface water storage. *Water Resources Research*, **40**, 1–14.

Kogan F, Adamenko T, Guo W (2013) Global and regional drought dynamics in the climate warming era. *Remote Sensing Letters*, **4**, 364–372.

Laaha G, Gauster T, Tallaksen LM et al. (2017) The European 2015 drought from a hydrological perspective. *Hydrology and Earth System Sciences*, **21**, 3001–3024.

Lamigueiro PO, Hijmans R (2016) meteoForecast. R package version 0.40. Available from http://oscarperpinan.github.io/rastervis/.

Van Lanen HAJ, Laaha G, Kingston DG et al. (2016) Hydrology needed to manage droughts: the 2015 European case. *Hydrological Processes*, **30**, 3097–3104.

Lasslop G, Reichstein M, Papale D et al. (2010) Separation of net ecosystem exchange into assimilation and respiration using a light response curve approach: Critical issues and global evaluation. *Global Change Biology*, **16**, 187–208.

Van Loon AF, Laaha G (2015) Hydrological drought severity explained by climate and catchment characteristics. *Journal of Hydrology*, **526**, 3–14.

Lorenzo-Lacruz J, Vicente-Serrano SM, López-Moreno JI, Beguería S, García-Ruiz JM, Cuadrat JM (2010) The impact of droughts and water management on

various hydrological systems in the headwaters of the Tagus River (central Spain). *Journal of Hydrology*, **386**, 13–26.

Luyssaert S, Inglima I, Jung M et al. (2007) CO2 balance of boreal, temperate, and tropical forests derived from a global database. *Global Change Biology*, **13**, 2509–2537.

Mckee TB, Doesken NJ, Kleist J (1993) The relationship of drought frequency and duration to time scales. *Water*, **179**, 17–22.

Mishra AK, Singh VP (2010) A review of drought concepts. *Journal of Hydrology*, **391**, 202–216.

Mohan S, Rangacharya NCV (1991) A modified method for drought identification. *Hydrological Sciences Journal*, **36**, 11–21.

Obasi GOP (1994) WMO's Role in the International Decade for Natural Disaster Reduction. *Bulletin of the American Meteorological Society*, **75**, 1655–1661.

Pereira JS, Mateus JA, Aires LM et al. (2007) Effects of drought - altered seasonality and low rainfall - in net ecosystem carbon exchange of three contrasting Mediterranean ecosystems. *Biogeosciences Discussions*, **4**, 1703–1736.

Pocernich M (2012) Verification Package : examples using weather forecasts. *Forecast*, 1–9.

R Core Team (2016) R: A Language and Environment for Statistical Computing. R Foundation for Statistical Computing, Vienna Austria https://www.R-project.org/.

Reichstein M, Falge E, Baldocchi D et al. (2005) On the separation of net ecosystem exchange into assimilation and ecosystem respiration: Review and improved algorithm. *Global Change Biology*, **11**, 1424–1439.

Shukla S, Wood AW (2008) Use of a standardized runoff index for characterizing hydrologic drought. *Geophysical Research Letters*, **35**, 1–7.

Staudinger M, Stahl K, Seibert J (2014) A drought index accounting for snow. *Water Resources Research*, **50**, 7861–7872.

Tallaksen LM, Van Lanen HAJ (2004) Hydrological drought: processes and estimation methods for streamflow and groundwater, Elsevier.

Tate EL, Gustard A (2000) Drought definition: a hydrological perspective. *Drought and Drought Mitigation in Europe* (ed. by J. V. Vogt and F. Somma), Kluwer Academic Publishers, the Netherlands, 23-48.

629 Thomas DSK, Wilhelmi OV, Finnessey TN, Deheza V (2013) A comprehensive
630   framework for tourism and recreation drought vulnerability reduction.
631   *Environmental Research Letters*, **8**, 44004.

632 Thornthwaite CW (1948) An approach toward a rational classification of climate.
633   *Geographical Review*, **38**, 55–94.

634 Tramontana G, Jung M, Schwalm CR et al. (2016) Predicting carbon dioxide and
635   energy fluxes across global FLUXNET sites with regression algorithms.
636   *Biogeosciences*, **13**, 4291–4313.

637 Vicca S, Balzarolo M, Filella I et al. (2016) Remotely-sensed detection of effects of
638   extreme droughts on gross primary production. *Scientific Reports*, **6**, 28269.

639 Vicente-Serrano SM, Beguería S, López-Moreno JI (2010) A multiscalar drought
640   index sensitive to global warming: The standardized precipitation
641   evapotranspiration index. *Journal of Climate*, **23**, 1696–1718.

642 Vicente-Serrano SM, Beguería S, Lorenzo-Lacruz J et al. (2012) Performance of
643   drought indices for ecological, agricultural, and hydrological applications.
644   *Earth Interactions*, **16**.

645 Wilhite DA, Glantz MH (1985) Understanding: the Drought Phenomenon: The
646   Role of Definitions. *Water International*, **10**, 111–120.

647 Wilks DS (2011) *Statistical Methods in the Atmospheric Sciences*. Academic Press,
648   676 pp.

649 WWRP/WGNE Joint Working Group on Forecast Verification Research (2015)
650   WWRP/WGNE Joint Working Group on Forecast Verification Research.

651 Zhai J, Su B, Krysanova V, Vetter T, Gao C, Jiang T (2010) Spatial variation and
652 trends in PDSI and SPI indices and their relation to streamflow in 10 large regions
653 of China. *Journal of Climate*, **23**, 649–663.

654

8 Supplementary

Table I. Percentage of catchments having maximal POD and FAR values for the different drought indices (VCI, SPEI and SPI) distinguishing between different groups of catchments. The catchments are grouped according to elevation (low, medium and high) and country (countries with more than ten catchments, i.e., N>10). POD and FAR refer to the verification skill scores probability of detection and false alarm ratio, respectively. SPEI and SPI stand for Standardized Precipitation Evapotranspiration Index and Standardized Precipitation Index, respectively. VCI is a standardized, multivariate index based on variables: monthly mean precipitation, volumetric soil water content and potential evapotranspiration, computed using the vine copula based approach proposed by Erhardt & Czado (2017).

| Index	N	% of catchments with maximum POD			% of catchments with minimum FAR		
		SPEI	SPI	VCI	SPEI	SPI	VCI
Low Elevation	129	15.5	13.2	71.3	24.8	32.6	42.6
Medium Elevation	133	12.8	27.8	59.4	20.3	37.6	42.1
High Elevation	70	4.3	45.7	50.0	12.9	27.1	60.0
Great Britain	118	16.9	14.4	68.6	21.2	33.9	44.9
France	96	16.7	21.9	61.5	38.5	44.8	16.7
Austria	48	0	54.2	45.8	2.1	14.6	83.3
Switzerland	45	6.7	40.0	53.3	8.9	31.1	60
Finland	12	0	8.3	91.7	0	33.3	66.7
Overall	332	12.0	25.9	62.0	20.5	33.4	46.1

667
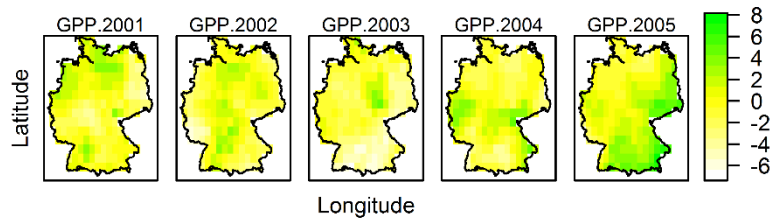
668

669 **Fig. 1.** Annual sum of standardized gross primary production (GPP) for Germany for the
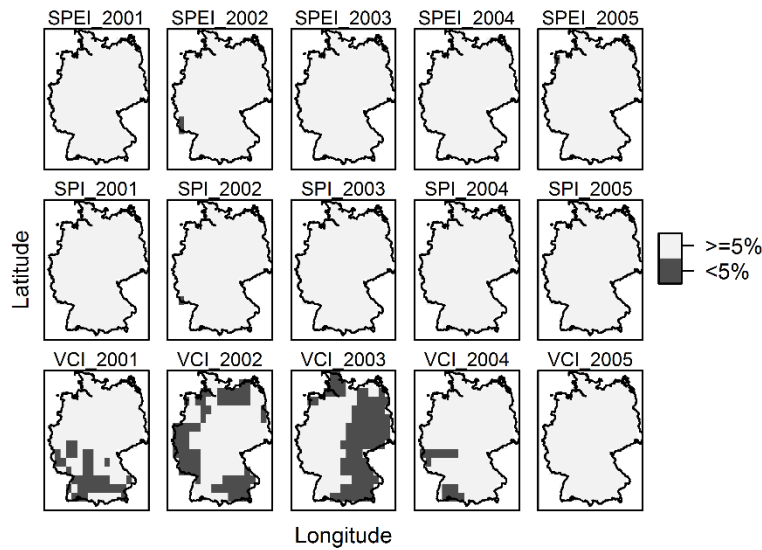670 years 2001 to 2005.
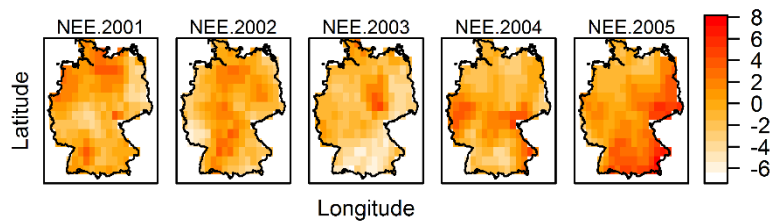
671

672 **Fig. 2.** Annual sum of standardized net ecosystem exchange (NEE) for Germany for the
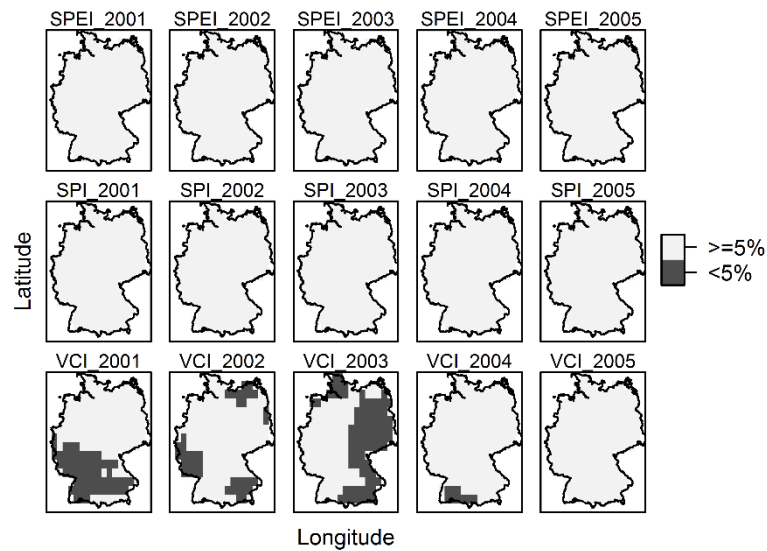673 years 2001 to 2005.

(a) (b)
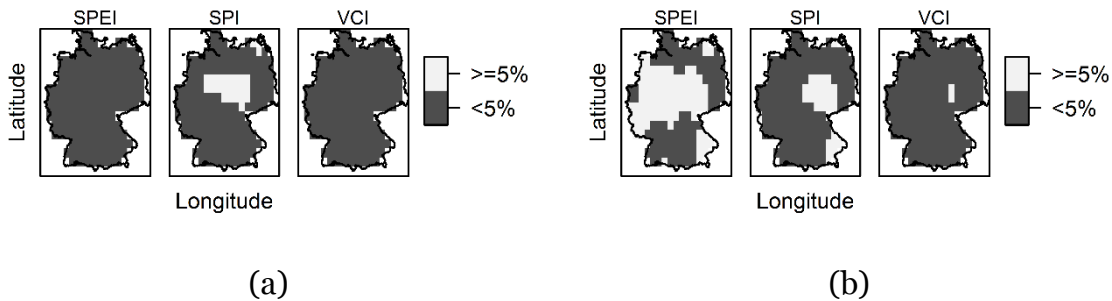
674 **Fig. 3.** P-values of a pixel-wise linear regression of the drought indices SPEI, SPI and VCI
675 against (a) standardized net ecosystem exchange (NEE) and (b) standardized gross
676 primary production (GPP), on a 0.5x0.5 degree spatial grid for Germany, for the growing
677 seasons (April to September) during the period 1980 to 2010. The darker shaded part
678 shows the statistically significant correlations at the confidence level of 0.05. SPEI and SPI
679 stand for Standardized Precipitation Evapotranspiration Index and Standardized
680 Precipitation Index, respectively. VCI is a standardized, multivariate index based on
681 variables: monthly means of climatic water balance, volumetric soil water content and air
682 temperature, computed using the vine copula based approach proposed by Erhardt &
683 Czado (2017).

684

685

686
687 **Fig. 4.** P-values of year- and pixel-wise linear regressions of the drought indices VCI, SPEI
688 and SPI against standardized net ecosystem exchange (NEE) on a 0.5x0.5 degree spatial
689 grid for Germany for the period 2001 to 2005, including the drought year 2003. The
690 darker shaded part shows the statistically significant correlations at the confidence level of
691 0.05. SPEI and SPI stand for Standardized Precipitation Evapotranspiration Index and
692 Standardized Precipitation Index, respectively. VCI is a standardized, multivariate
693 index based on variables: monthly means of climatic water balance, volumetric soil
694 water content and air temperature, computed using the vine copula based
695 approach proposed by Erhardt & Czado (2017).

696

Fig. 5. P-values of year- and pixel-wise linear regressions of the drought indices VCI, SPEI and SPI against standardized gross primary production (GPP) on a 0.5x0.5 degree spatial grid for Germany for the period 2001 to 2005, including the drought year 2003. The darker shaded part shows the statistically significant correlations at the confidence level of 0.05. SPEI and SPI stand for Standardized Precipitation Evapotranspiration Index and Standardized Precipitation Index, respectively. VCI is a standardized, multivariate index based on variables: monthly means of climatic water balance, volumetric soil water content and air temperature, computed using the vine copula based approach proposed by Erhardt & Czado (2017).